CENOZOIC SEISMIC STRATIGRAPHIC ANALYSIS OF THE SURINAME MARGIN, SOUTH AMERICA

by

Shawn J. Goss

Submitted in partial fulfilment of the requirements
for the degree of Master of Science

at

Dalhousie University
Halifax, Nova Scotia
December 2009

DALHOUSIE UNIVERSITY

DEPARTMENT OF EARTH SCIENCES

The undersigned hereby certify that they have read and recommend to the Faculty of Graduate Studies for acceptance a thesis entitled "CENOZOIC SEISMIC STRATIGRAPHIC ANALYSIS OF THE SURINAME MARGIN, SOUTH AMERICA" by Shawn J. Goss in partial fulfilment of the requirements for the degree of Master of Science.

Dated: December 18. 2009

Supervisors:

Readers:

Departmental Representative:

DALHOUSIE UNIVERSITY

DATE: December 18, 2009

AUTHOR: Shawn J. Goss

TITLE: CENOZOIC SEISMIC STRATIGRAPHIC ANALYSIS OF THE SURINAME MARGIN, SOUTH AMERICA

DEPARTMENT OR SCHOOL: Department of Earth Sciences

DEGREE: M.Sc. CONVOCATION: May YEAR: 2010

TABLE OF CONTENTS

LIST OF TABLES

LIST OF FIGURES

ABSTRACT

Latest understanding has shown that application of conventional seismic sequence stratigraphic methods on shelf-to-slope transition environments is difficult. The Suriname margin of the equatorial Atlantic is the youngest post-rift margin of the Atlantic, so should be the least complex. Cenozoic strata from offshore Suriname were placed into a sequence stratigraphic framework using the method of accommodation succession, proposed by Neal and Abreu (2009). This framework consists of seven reflection horizons correlated throughout a 3D seismic volume; each horizon defining the base of a seismic sequence. Within these sequences, seismic reflection stacking geometries indicate that sea level cycles and sediment supply are the primary controls on the margin's evolution, occasionally fitting eustatic sea level records. Mass transport deposits in deep water and erosional unconformities in shallow water result during sea level low stands. Periods of transgression and sea level high stands are marked by shelf margin aggradation, with minimal sedimentation on the slope. The Suriname margin provides a model for application of modern sequence stratigraphic concepts. It must be recognized, however, that each margin has various and unique external forcing mechanism controlling sediment distribution and that as a margin evolves, it becomes increasing complex.

LIST OF ABBREVIATIONS AND SYMBOLS USED

AP	Aggradation-to-Progradation
APD	Aggradation-to-Progradation, Degradation
AP(D)SS	Aggradational-Progradational-Degradational Sequence Set
AP(D)ST	Aggradational-Progradational-Degradational Systems Tract ("Highstand")
APSS	Aggradational-to-Progradational Sequence Set
CMFS	Composite Maximum Flooding Surface
CSB	Composite Sequence Boundary
DR	Demerara Rise
DSDP	Deep Sea Drilling Program
HST	High Stand Systems Tract
km	Kilometres
LST	Low Stand Systems Tract
MD	Measured Depth (Below Kelly Bushing)
mbfs	Metres Below Sea floor
ms	Milliseconds
m/s	Metres Per-Second
ODP	Ocean Drilling Program
PA	Progradation-to-Aggradation
PASS	Progradational-Aggradational Sequence Set
PAST	Progradational-Aggradational Systems Tract ("Lowstand")
PSI	Pounds Per Square Inch
R	Retrogradation
RMS	Root Mean Squared
RSS	Retrogradational Sequence Set
RST	Retrogradational Systems Tract ("Transgressive")
S	Seconds
SB	Sequence Boundary
SM	Suriname Margin
T-R	Transgressive-Regressive Sequence
TS	Transgressive Surface
TST	Transgressive System Tract
TWTT	Two-Way Travel Time

Wells

A2-1	Demerara A2-1
CO-1	Coronie Offshore-1
GLO-1	Galili Offshore-1
MO-1	Maroni Offshore-1
NCO-1	North Coronie Offshore-1
SON-1	Suriname Offshore-1

GLOSSARY OF TERMS USED

Accommodation: The space made available for potential sediment accumulation (Jervey, 1988).

Aggradation: Vertical build up of a sedimentary sequence (Posamentier and Allan, 1999).

AP (aggradation-to-progradation) stacking ("Highstand"): As the rate of sea level rise is decreasing, sediment fills coastal accommodation and clinoforms aggrade with slow then rapid progradation into the basin while still onlapping the inherited depositional profile (Neal and Abreu, 2009) (Figures 2.10 to 2.12 and 3.1).

Base Level: Base level delineates a dynamic surface of balance between erosion and deposition. The amount of space that is available for sediments to fill up to the base level defines the concept of "accommodation" (Jervey, 1988). A rise in base level creates accommodation, whereas a fall in base level destroys accommodation. Base level is commonly approximated as sea level (Jervey, 1988; Schumm, 1993; Posamentier and Allan, 1999). When base level is approximated as sea level, the concept of "base-level change" becomes equivalent with the concept of "relative sea level change" (Posamentier et al. 1988).

Chronostratigraphy: The establishment of the time significance of sedimentary units using biostratigraphy, radiometric methodologies and other time significant schemes.

Coastal Accommodation: The space available for sediment fill on the coastal plain (Jervey, 1988).

Costal Onlap: Is the progressive landward advance of coastal (marine or nonmarine) deposits in a given stratigraphic unit (Vail et al. 1977). The magnitude of coastal onlap is subdivided into horizontal and vertical components, known as encroachment and aggradation, respectively.

A) Rise in Relative sea Level: Indicated by coastal onlap, a landward advance of coastal (littoral or costal nonmarine) deposits in a given stratigraphic unit.

B) Fall in Relative Sea Level: Indicated by basinward shifts in coastal onlap position from the most shoreward point in the depositional sequence to the most basinward point in the overlying depositional sequence.

Composite Sequence: A relatively conformable succession of genetically related sequence-set elements (lowstand (PA), transgressive (R), and highstand AP (D) stacking patterns) and is bounded by surfaces of erosion or their correlative conformities (Figure 2.11) (Mitchum and Van Wagoner, 1991).

Composite Sequence Boundary: Significant erosional unconformities and their correlative conformities that envelope composite sequences (Mitchum and Van Wagoner, 1991) (Figures 2.10 to 2.12).

Composite Sequence Sets: Analogous to system tracts (see below) within a sequence.

Condensed Section: A thin marine stratigraphic interval characterized by very slow depositional rates (<1-10 mm/yr) (Vail et al. 1984).

D (degradational) stacking (forced regression- "Highstand"): Strong clinoform progradation with offlap breaks that step down into the basin without topsets onlapping the inherited depositional profile (Neal and Abreu, 2009) (Figures 2.10 to 2.12 and 3.1).

Depositional Sequence: A relatively conformable succession of genetically related strata bounded at base and top by unconformities and their correlative conformities. The basic stratigraphic unit of sequence stratigraphy (Mitchum and Van Wagoner, 1991).

Eustatic Sea Level: Global sea level, which changes in response to changes in the volume of ocean water and the volume of ocean basins.

Highstand Systems Tract: Systems tract overlying a maximum flooding surface, overlain by a sequence boundary, and characterized by an aggradational to progradational parasequence set.

High-Frequency Cycle: A term applied to a cycle of fourth order or higher, that is, having a period of less than 1 million years. Parasequences and sequences can be each considered high-frequency cycles when their period is less than 1 million years.

Lithostratigraphy: The correlation of sedimentary rocks based on lithology.

Lowstand Systems Tract: The lowstand systems tract is the set of depositional systems active during the time of relatively low sea level following the formation of the sequence boundary.

PA (progradational-to-aggradational) stacking ("Lowstand"): The rate of sea level rise is increasing but all coastal accommodation is filled with sediment, thus clinoforms rapidly prograde then aggrade while the topsets onlap the inherited depositional profile (Neal and Abreu, 2009) (Figures 2.10 to 2.12, and 3.1).

Progradation: Lateral outbuilding, or progradation, of strata in a sea-ward direction (Posamentier and Allan, 1999)

Marine Flooding Surface: A timeline separating younger from older strata across which, there is evidence for an abrupt increase in water depth.

Maximum Flooding Surface (MFS): A surface representing the maximum landward extent of marine facies. Constitutes the top of the transgressive systems tract.

Mega Sequence: Sets of depositional sequences that are related to particular phases of basin development (Allen and Allen 1990).

Parasequence: A relatively conformable succession of genetically related beds or bed sets bounded above and below by marine flooding surfaces or their correlative surfaces (Mitchum and Van Wagoner, 1991).

R (retrogradation) stacking ("Transgressive"): When rapid rise in sea level creates coastal accommodation faster then sediment can fill, units backstep, shorelines transgress, and deposition onlaps the inherited depositional profile (Neal and Abreu, 2009) (Figures 2.10 to 2.12, and 3.1).

Regression: A seaward movement of the shoreline indicated by a seaward migration of littoral facies (Mitchum, 1977).

Retrogradation: The movement of coastline landward in response to a transgression (Posamentier and Vail, 1988).

Relative Sea Level: The local sum of global sea level and tectonic subsidence. Locally, a rise in eustatic sea level and an increase in subsidence rates will have the same effect on accommodation. Likewise, a fall in eustatic sea level and tectonic uplift will have the same effect on accommodation. Because of the extreme difficulty in teasing apart the effects of tectonic subsidence and eustatic sea level in regional or local studies, sequence stratigraphy now generally emphasizes relative changes in sea level, as opposed to its earlier emphasis on eustatic sea level (Mitchum, 1977).

Seismic Facies Analysis: a mapable three-dimensional seismic unit composed of groups of reflections whose parameters, such as reflection configuration, continuity, amplitude, frequency or interval velocity, differ from those of adjacent facies units. Once the interval reflection parameters, the external form, and the three-dimensional associations of the seismic faces unit are delineated, then the unit can be then interpreted in terms of environmental setting, depositional process, and estimates of lithology.

Sequence: Relatively conformable (that is, containing no major unconformities), succession of genetically related strata bounded by unconformities or their correlative conformities (Vail et al. 1977).

Sequence Boundary: A laterally continuous (regional) unconformity and its relative conformity over which there is an abrupt basinward shift in facies.

Sequence Set: A set of depositional sequences arranged in a distinctive progradational, aggradational or retrogradational stacking pattern. Bounded at its base and top by regional surfaces of erosion or their correlative conformities (Mitchum and Van Wagoner, 1991) (Figure 2.11).

Sequence Stratigraphy: The study of genetically related facies within a framework of chronostratigraphically significant surfaces.

Systems Tracts: Genetically associated stratigraphic units deposited during specific phases of the relative sea level cycle. Defined on the basis of bounding surfaces, position within the sequence and parasequence stacking pattern (Van Wagoner et al, 1988).

Transgression: A landward movement of the shoreline indicated by landward migration of littoral facies in a given stratigraphic unit (Mitchum, 1977).

Transgressive Surface: The first major flooding surface across the shelf in a depositional sequence. Constitutes the top of a lowstand systems tract. Separates retrogradationally stacked parasequences from underlying progradational to aggradational parasequences.

Transgressive Systems Tract: Systems tract overlying a transgressive surface, overlain by a maximum flooding surface, and characterized by a retrogradational parasequence set.

Unconformity: A surface separating younger from older strata.

ACKNOWLEDGEMENTS

I would like extend my greatest thanks to my supervisors Dr. David Mosher (Geological Survey of Canada-Atlantic) and Dr. Grant Wach (Dalhousie University) for presenting me with such a intriguing project, allowing me to explore new ideas and develop this thesis while testing my critical thought.

I have great appreciation for Dr. David Mosher who has been an excellent mentor, friend and colleague. For the better part of 4 yrs, I have studied under Dr. Mosher completing an undergraduate honours thesis and this study. I will be leaving with a lifetime of gratitude.

Thanks are also extended to my friends who kept the ball rolling. Calvin Campbell who always had the time for questions/debates and was good for a much needed coffee from time to time, Ginny Brake; my so called symbiotic twin. Together we were often referred to as "Shinny", and Mike Giles who suffered the last of the late nights at B.I.O. with me while wrapping up this project. I wish him luck in his thesis and upcoming defense.

To my family, I could not have accomplished this project without you. My wife Meghan has been amazing, and has provided me with support and motivation to keep focus, allowing me to achieve any goal to which I set my mind.

Acknowledgement is owed to Allan Kean and Julio Eduardo Colmenares Bernal at RepsolYPF for providing me with this extraordinary opportunity, data for this project, and fielding all my last minute inquiries.

Research for this thesis was funded by RepsolYPF and the Nova Scotian Offshore Energy Technical Research Association grant No. 51834 to Drs. David Mosher and Grant Wach. The three-dimensional, two-dimensional seismic and well data were donated by RepsolYPF to the Geological Survey of Canada, and workstation facilities were available through the GSC-A with SMT Kingdom Suite educational licenses for seismic interpretation supplied by Seismic Micro Technologies Inc.
.

CHAPTER 1: INTRODUCTION

Understanding passive continental margin development requires a detailed knowledge of sedimentary processes and external forcing mechanisms such as sediment supply, tectonics, sea level excursions and ocean current circulation. These factors contribute to the deposition of sedimentary sequences along continental margins. The Suriname margin represents the last vestige of the proto-Atlantic, before West Africa's final rifting from South America (Gouyet et al. 1994) to join the South and North Atlantic Oceans into a single body of water. As a result of its young age, the margin offers an excellent opportunity to study post-rift Atlantic margin geology. This thesis investigates Cenozoic to Recent strata on the western portion of the Suriname continental margin. The upper-slope stratigraphy appears to represent a textbook example of sequence stratigraphy. In part, this appearance is because of the margin's short history relative to its northern counterparts. Additionally, it has been unaffected directly by Pleistocene glacial processes, which dominate Neogene successions in northern and southern hemisphere regions. Its sedimentary sequence is relatively complete, therefore, with external forcing mechanisms on the margin's evolution principally restricted to sea-level variations.

1.1 Objectives

This study aims to improve understanding of the geologic development of the Cenozoic section of the Suriname continental margin, with particular focus on shelf-to-slope sedimentation patterns and the role of sea level fluctuations. This objective will be accomplished by testing the recent sequence stratigraphic method presented by Neal and Abreu (2009) "The Accommodation Succession Method", with developed seismic facies, and seismic stratigraphic concepts to observed depositional, stratigraphic and morphological characteristics of data within a 3D seismic volume on a portion of the Suriname margin.

1.2 Study Location

The Suriname margin of South America lies in the equatorial Atlantic between 8° and 10°N latitude and 52° to 56°W longitude (Figure 1.1). The study location lies on the critical shelf to slope transition zone on the Suriname margin in water depths ranging from 100 m to > 2000 m, just northwest of the Demerara Rise. The shelf break is indicated by a change in slope gradient from essentially zero (<0.5°) to almost 5°.

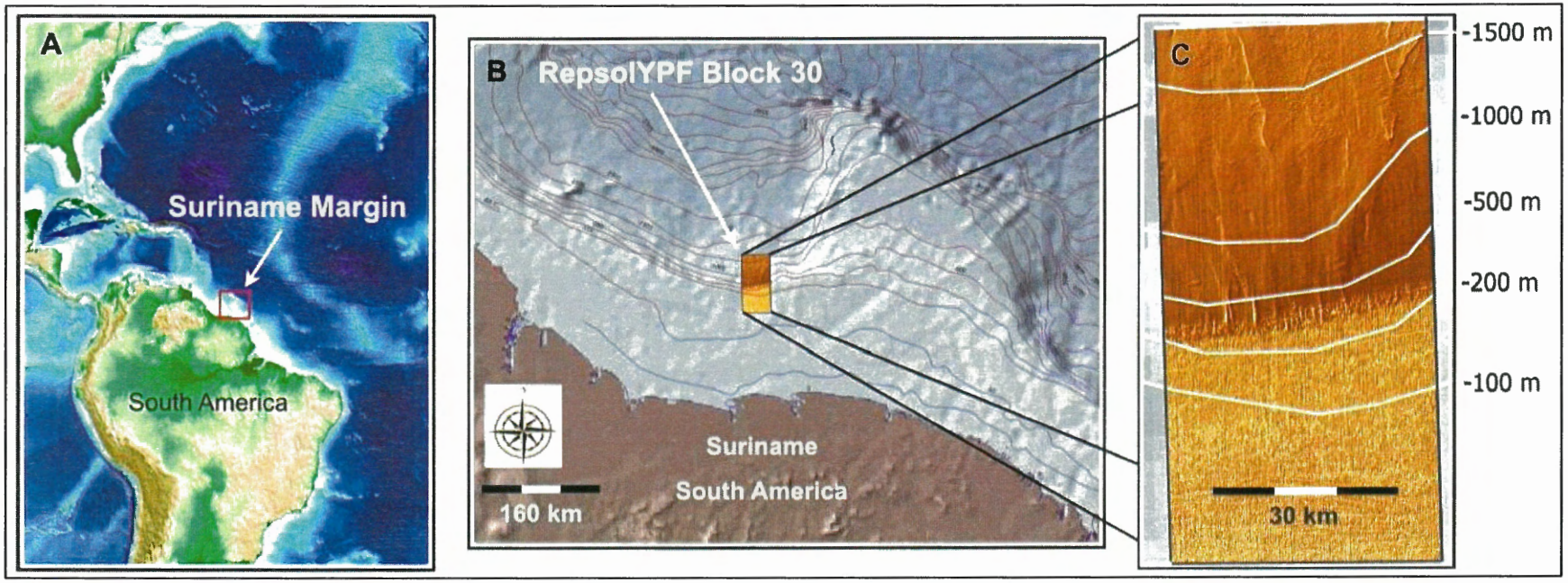

Figure 1.1 (A) Location of the Suriname margin with respect to South America, (B) Projection of the RepsolYPF Block30 on modern ETOPO bathymetry map. (C) Present day seafloor morphology of Block30 derived from rendered seafloor surface with associated depth contours.

1.3 Geologic Setting

The Suriname continental margin is underlain by Precambrian to early Mesozoic-aged continental crust (Benkhelil et al. 1995). It is conjugate to West Africa at about the position of Guinea (Figure 1.2). It formed the southern border of the central Atlantic margin during the Jurassic prior to rifting and opening of the Atlantic gateway (Figure 1.3A) (Benkhelil et al. 1995; Erbacher et al. 2004a). Geographically at that time, the Suriname margin would have been located somewhat south of the present day location of Dakar, Senegal (Erbacher et al. 2004b). In this area of the central Atlantic, north-south rifting initiated about 180 Ma resulting from east-west extension with a large component of dextral shearing (Figure 1.3B) (Mascle et al. 1986; Gouyet et al. 1994). Complexities caused by plate rotation resulted in a late compressional phase before final rifting in the Late Albian (Figure 1.3C). This compression resulted in en echelon folding and flower structures within the Suriname margin (Gouyet et al. 1994). Subsidence of the margin followed rapidly, initially due to thermal cooling of the crust (Figure 1.3D) (Benkhelil et al., 1995; Pindell and Kennan 2005).

Beneath the Suriname margin, Late Aptian and Late Albian unconformities are reported within the sedimentary section (Gouyet et al. 1994). The earlier unconformity may be correlated with the formation of the en echelon folds, while the late Albian event resulted from the main compressional phase (Benkhelil et al. 1995; Erbacher et al. 2004a; Mosher et al. 2005).

Following the minor recurrence of compressive tectonics, an extensional regime ensued during the Late Cretaceous. Extension was characterized by a general collapse of the

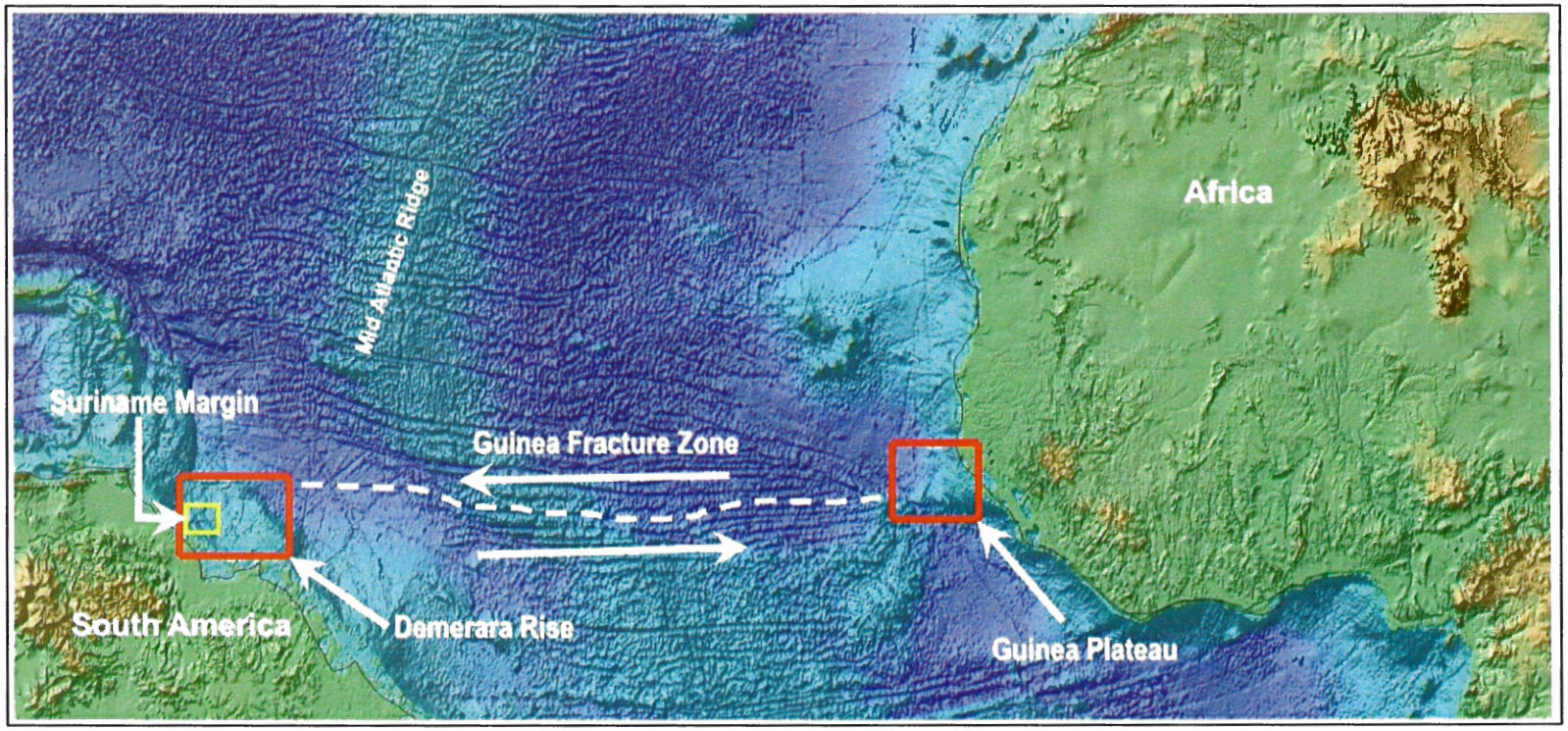

Figure 1.2 Equatorial Atlantic showing the location of the Suriname margin and its conjugate Guinea Plateau.

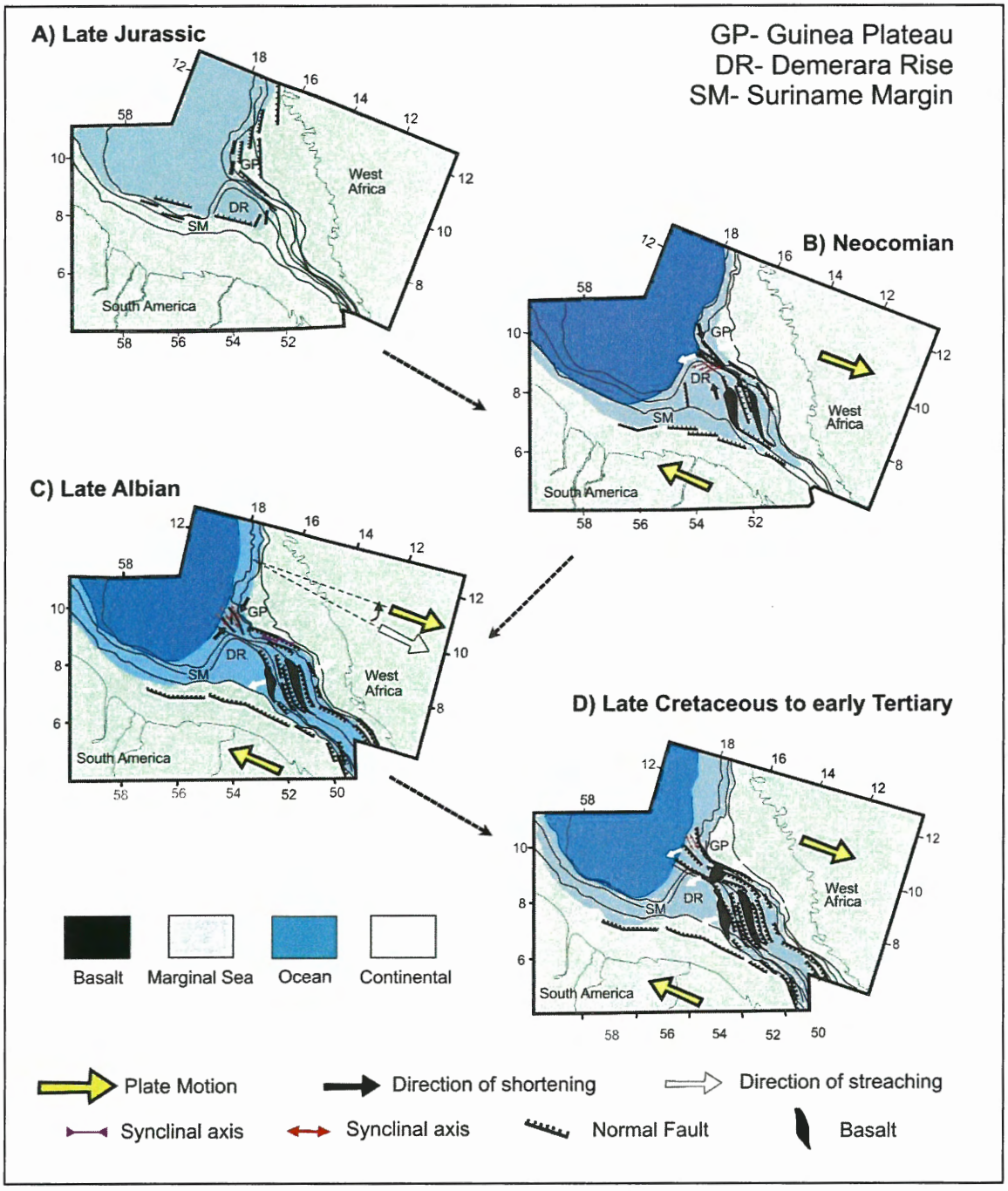

Figure 1.3 Schematic stages of Mesozoic evolution of the Equatorial Atlantic (modified after Gouyet et al. 1994, Benkhelil et al. 1995).

margin resulting in the final parting of the African and South American continental plates and the creation of oceanic crust (Benkhelil et al. 1995). Subsidence was presumably rapid, along with continental synrift sedimentation filling accommodation space provided by this subsidence (Figure 1.4) (Flicotaux et al. 1988; Erbacher et al. 2004a). Global sea-level continued to rise throughout this period, and reached its highest levels in the Turonian (Haq et al. 1988). Tectonic deformation ceased in the Late Cretaceous followed by normal cooling subsidence as a largely siliciclastic cover was deposited over the previous rift graben on the Suriname margin (Figures 1.5 and 1.6) (Gouyet et al. 1994). Largely east-west separation of the West African and central South American margins continued. A feature of this extension is the Guinea fracture zone; a transform fault that forms the eastern outer margin of Suriname (Figure 1.2).

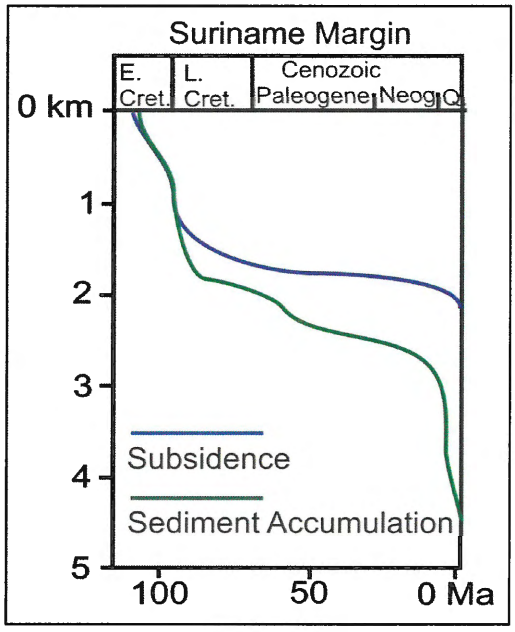

Figure 1.4 Schematic diagram illustrating rapid subsidence following the final parting between the African and South American continental plates. Tectonic deformation largely ceased in the Late Cretaceous followed by normal cooling, and clastic deposition (Modified after Flicotaux et al. 1988).

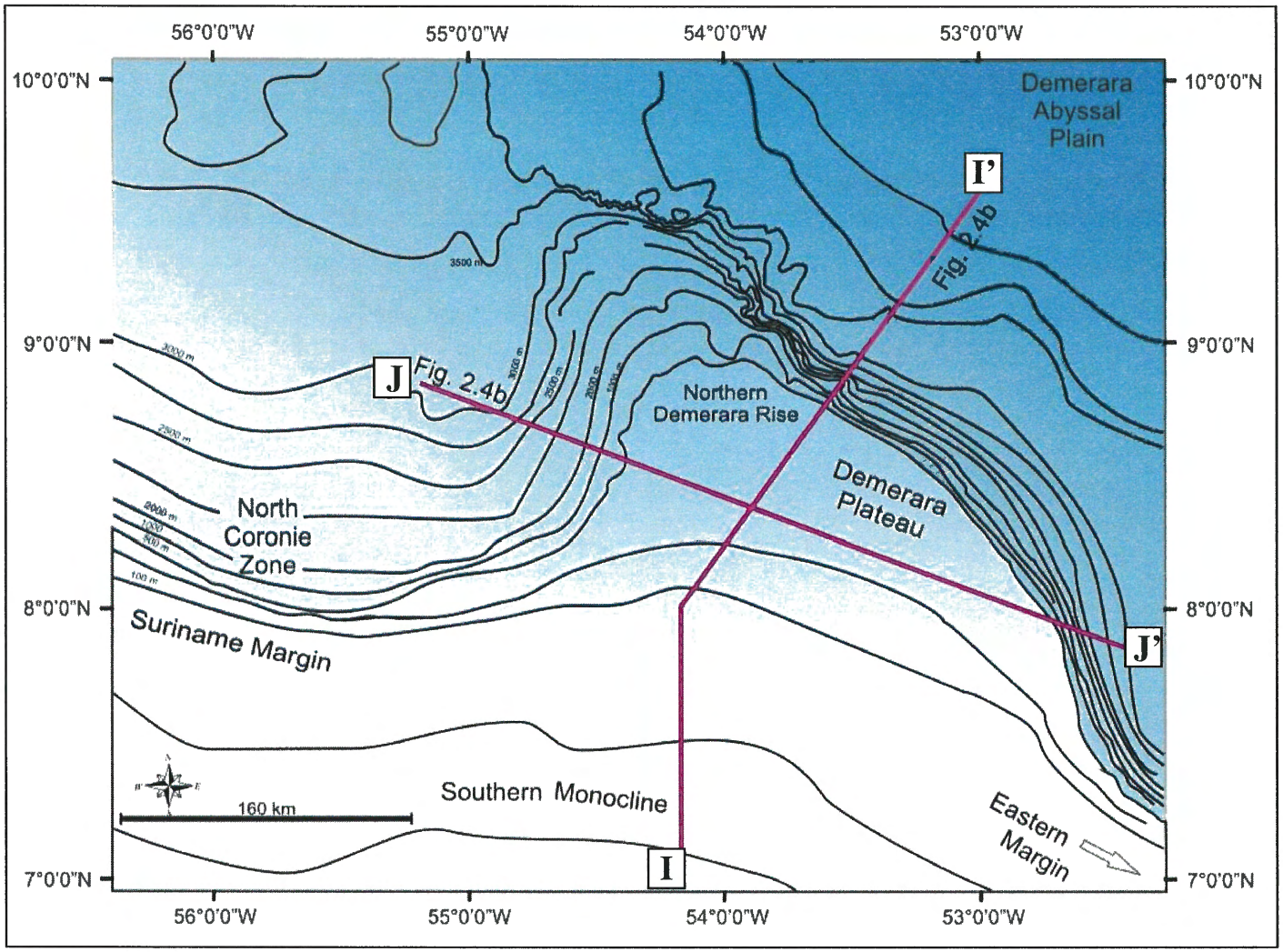

Figure 1.5 Main physiographic features of the Suriname margin and adjacent Demerara Rise with location lines for synthetic sections across the Demerara Plateau. Water depths in metres.

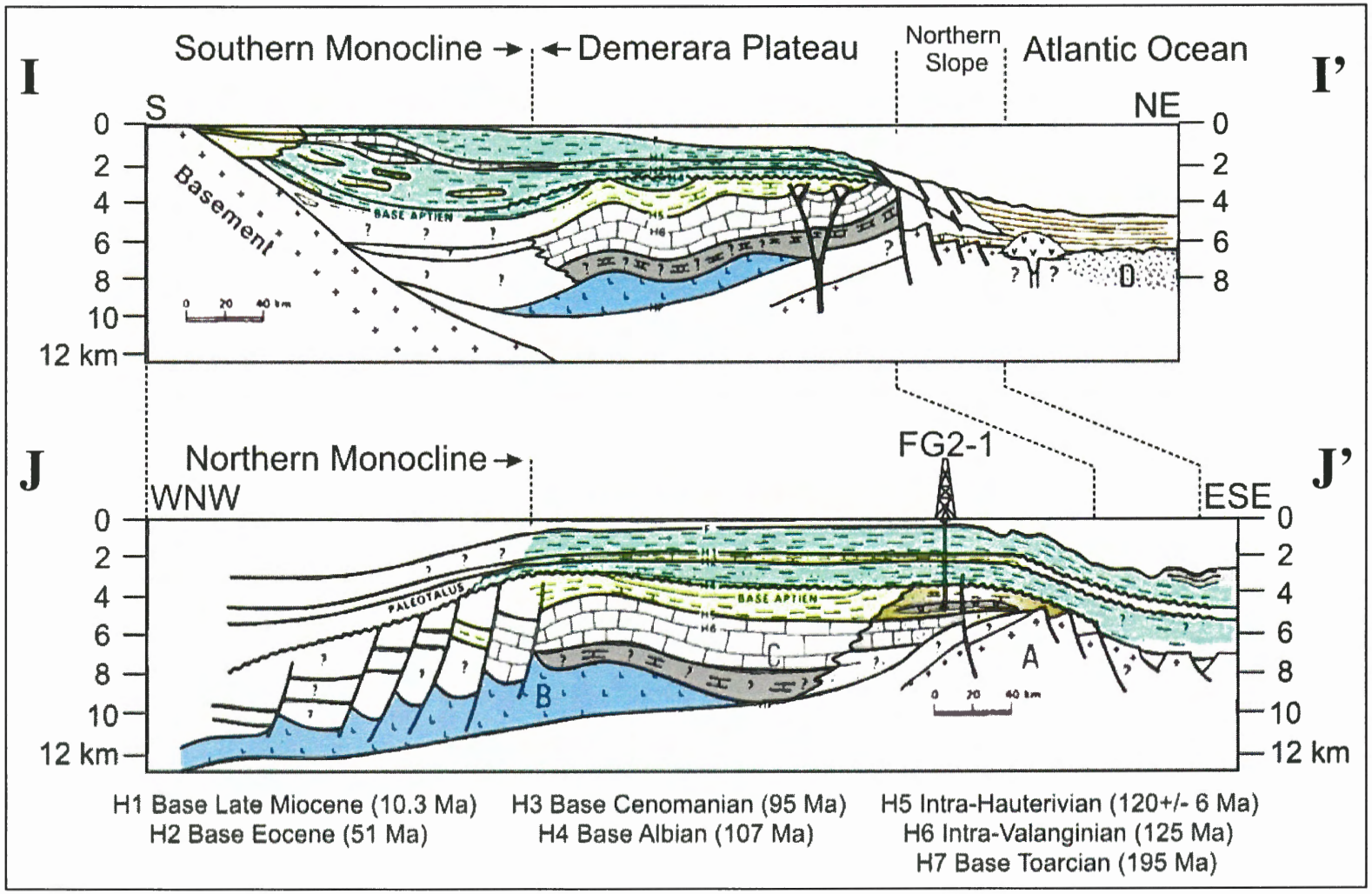

Figure 1.6 Schematic cross sections across the Suriname margin and adjacent Demerara Rise. Location of lines in Figure 1.5. *A*: Pre-Mesozoic continental basement; *B*: Inferred Jurassic salt; *C*: Predominantly carbonate series of Jurassic (?) Neocomian age (inferred *below H6*); *D*: Late Cretaceous oceanic crust (modified after Gouyet et al. 1994).

1.4 General Stratigraphy

The general stratigraphic succession of the Suriname margin is best described where the section thins and was sampled on the Demerara Rise by the Sinna Mary 1 exploration well and DSDP and ODP drilling. The entire sedimentary succession of the Suriname margin can be separated into two major depositional episodes; 1)Pre Albian and 2) Albian to Present (Figure 1.7).

1.4.1 Pre-Albian Sediments

The Sinna Mary 1 and DSDP Site 144 wells drilled on the Suriname margin penetrated the upper unit of the Pre-Albian succession (Staatsolie, 1976). Late Jurassic volcanic extrusion created an excessively thick oceanic crust, resulting in a shallow oceanic basin. The resulting continental margin slope is characterized by relatively gentle, low relief slopes. Neocomian shelf sedimentation involved deposition of carbonate and mixed carbonate-siliclastic sediments onlapping Jurassic volcanics. A thick argillaceous limestone of Berriasian to Aptian age was drilled on top of the plateau, followed by Berriasian to Aptian sediments becoming gradually more shaly upward, a possible result of deepening of the sea-floor at that time (Staatsolie, 1976).

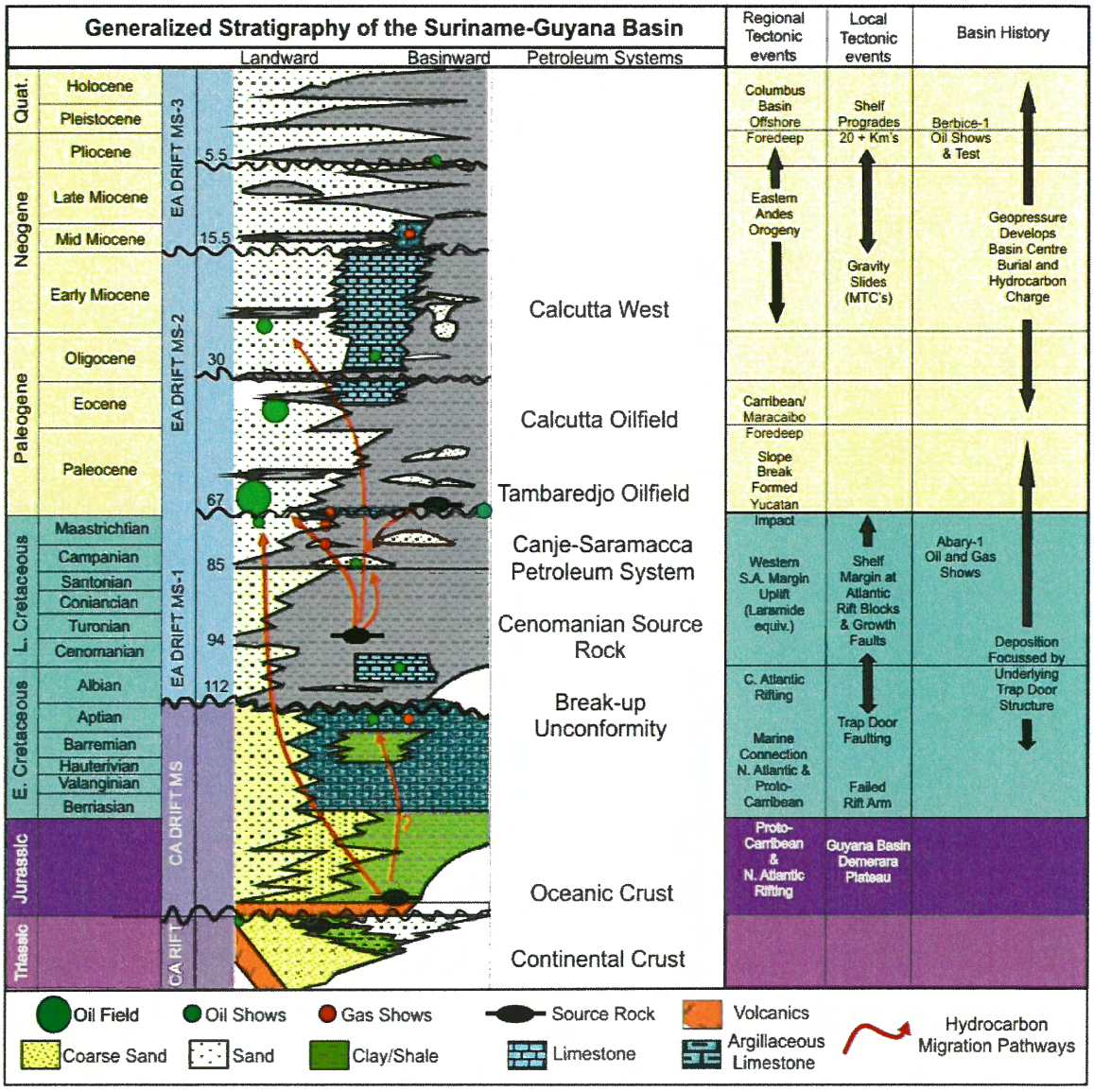

Figure 1.7 Generalized stratigraphic chart of the Suriname-Guyana basin showing major tectono-stratigraphic events, unconformities and petroleum system elements (modified after Staatsolie, 2005).

1.4.2 Albian-Present Sediments

The regional Aptian/Albian unconformity is overlain by a progradational succession of clastic sediments with short periods of carbonate deposition. The Albian to Present succession is reported at depths of 4000-6000 mbsf, and is divided into three intervals (Staatsolie, 1976).

1) The Albian to Late Cretaceous interval contains terrigenous marine sediments. Shallow organic-rich Cretaceous marine sediments are found principally unaltered from their original depositional state (Staatsolie, 1976; Forester et al. 2004).

2) Early Paleocene strata are absent from interval 2 corresponding to a regional erosional unconformity (Gouyet et al. 1994). From the Paleocene to late Early Miocene, a high energy carbonate platform developed, corresponding to a period of moderate subsidence of the margin.

3) The third interval, Middle Miocene to Present, is related to rejuvenation of the relief on the Guyana Shield and rapid Andean uplift along the western margin of South America, leading to deposition of thick terrigenous packages transported by drainage systems similar to the present. Sediments supplied by the Amazon River were entrained within strong coastal currents flowing northwest along the margin. This fact, together with relative fluctuations of eustatic sea-level, probably controlled the deposition of Neogene sediments (Gouyet et al. 1994).

1.5 Basin Evolution- Industry Prospective History

Suriname's continental margin exploration began in 1960 with a seismic survey conducted by the Colmar Company (Wong et al. 1998). The first offshore well SON-1 (*See list of abbreviations for complete well names) was spudded in 1963 by the Colmar Company and reached Oligocene sediments at a depth of 1350 m. Although the well contained good porosities and oil shows, including several gas intervals, it was not commercial (Table 1.1). A decade later, an additional 12415 km of seismic data were collected and three wells (MO-1, CO-1, and GLO-1) were drilled still without commercial show (Figure 1.8). In 1975, Elf/Esso drilled NCO-1 in the study area reaching a depth of 5406 m in Aptian sediments, with no commercial show. The next two years, an additional 2497 km of seismic data were shot in the deep, northern part of the Guiana basin. In 1978, Esso acted as operator and drilled A2-1 in a water depth of 1200 m. At 3700 m sub-seafloor, the well was terminated in Early Cretaceous strata with no commercial hydrocarbon abundences (Figure 1.8) (Table 1.1). Upon completion of A2-1, a 4 year moratorium ensued covering the entire offshore acreage. By 1983, six more wells were drilled off the Suriname coast with sparse oil shows, none of which were of commercial interest. From 1983 to 1986, another 5 wells were drilled under the operator Austra-Tex to evaluate the Lower Paleocene oil finds by Gulf in more detail. Although the presence of oil was confirmed in this interval, the quantities were considered non-commercial and the lease area was relinquished. Since then, a number of oil companies studied the offshore database and although numerous targets were identified, no further action was taken. In 2005, RepsolYPF acquired Block30, with operating partner Occidental. RepsolYPF acquired 8000 km of 2-D and 3200 km^2 of 3D seismic reflection

data. The West Tapir well was drilled in 2008 by operators RepsolYPF and Noble gas. The total depth of the well reached 3870 m sub-seafloor in an Oligocene/Eocene target. Although the well reported no commercial discovery, this was the first well drilled on the margin in over 20 years (Figure 1.8) (Table 1.1).

Table 1.1 Wells drilled offshore Suriname.

Well Name	Operator	Year Completed	T.D. (m)	Status
Suriname Offshore-1	Colmar	1964	1350	P & A
Suriname Offshore-2	Petrosur	1965	1925	P & A
Maroni Offshore-1	Petrosur	1965	1866	P & A dry
Coronie Offshore-1	Petrosur	1967	3294	Suspended
DSDP Site 144	DSDP	1970	327	Scientific
Galibi Offshore-1	Elf	1971	4663	P & A dry
North Coronie-1	Elf	1975	5406	P & A dry
Demerara A2-1	Esso	1978	3700	P & A dry
B/34-1x	Gulf	1982	1648	P & A dry
I/23-1x	Gulf	1982	4248	P & A dry
L/10-1x	Gulf	1982	1545	P & A dry
ODP Site 1257	ODP	2003	285	Scientific
ODP Site 1258	ODP	2003	461	Scientific
ODP Site 1259	ODP	2003	554	Scientific
ODP Site 1260	ODP	2003	509	Scientific
ODP Site 1261	ODP	2003	674	Scientific
West Tapir	RepsolYPF	2008	3870	Dry

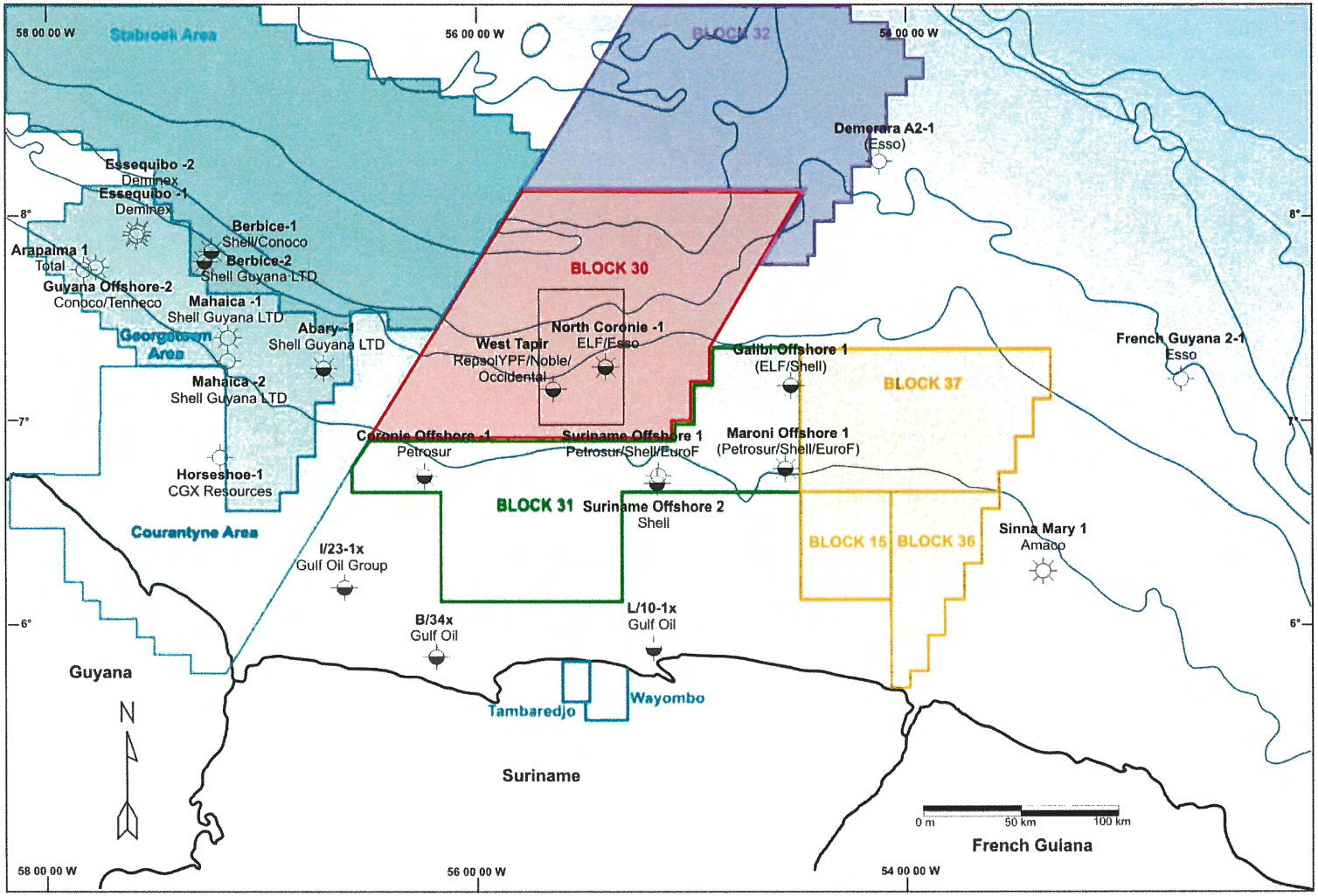

Figure 1.8 Map indicating locations of wells and associated operators on the Suriname/Guyana margins. Highlighted boxes indicate the present day lease block configurations in the offshore/onshore regions.

CHAPTER 2: METHODS

The primary method of investigation for this study of the Suriname margin is interpretation of multi-channel seismic reflection data. The principal dataset is a 40 km x 80 km 3D seismic volume, known as Block30, acquired for RepsolYPF. All seismic interpretations for this study were completed in the time domain for the Block30 3D volume and 2D regional seismic lines. Regional 2D seismic lines extended interpretations from the study area to the outer Demerara Rise. Well data from within Block30 and on the nearby outer Demerara Rise were incorporated into the study using seismic tie lines and synthetic seismograms. Integration of reflection seismic and well data and the application of stratigraphic concepts allows for the establishment of the regional stratigraphic framework of the Suriname margin within the Block30 dataset.

2.1 Seismic Reflection Data

The physics and practical application of marine seismic reflection technology is discussed thoroughly within the literature (for example: Yilmaz 1987, Keary and Brooks 1991, Sheriff and Geldart 1995, Brown 1996, Brown 1999, Hart 1999, and Veeken 2007) and will not be discussed further within this thesis except to address specifics of the datasets used in the investigation.

2.2 Two-Dimensional Seismic Reflection Data

Seismic reflection data for ODP Leg 207 were used in this study to correlate regional 2D lines W99-109, W99-108, W99-150 spanning the western region of the Suriname margin including the 3D Block30 volume to the outer portion of the Demerara Rise (Figure 2.1).

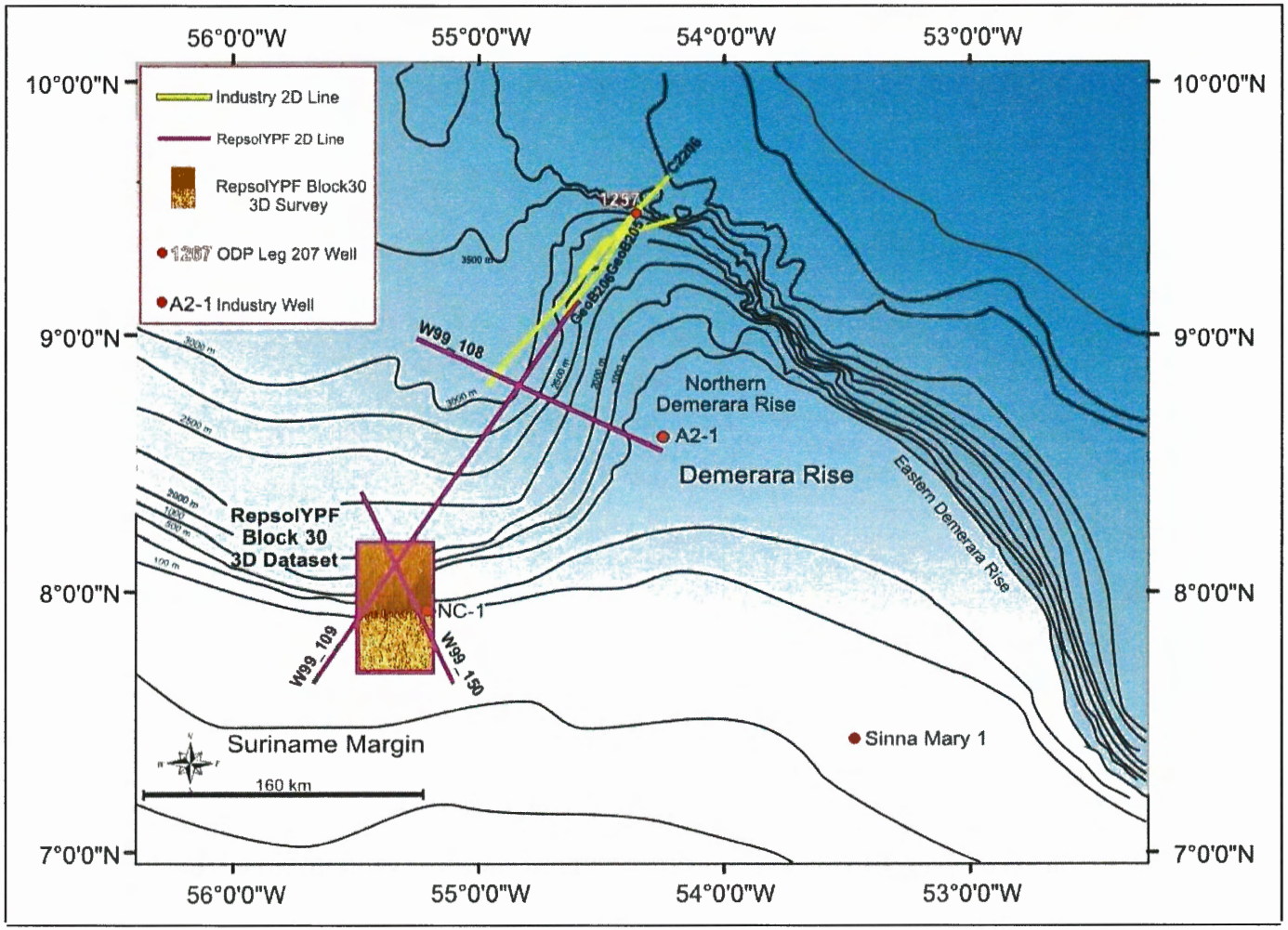

Figure 2.1 Seismic data and well locations used for this study. Seismic lines coloured to segregate vintage. RepsolYPF 2D and 3D data highlighted in magenta, industry profiles highlighted in yellow. ODP Scientific well 1257 indicated in orange, and exploration wells in black. Water depth in metres...

Seismic reflection data for ODP Leg 207 used in this study came from 2 principle sources.

2.2.1 Shell International 1974 Multichannel Seismic Survey

Line C2206 is part of a suite of multichannel seismic reflection lines collected by Shell International in March of 1974, from the survey vessel Petrel. These data were acquired in 1971 with an 12,000 in^3 airgun array using 14 guns towed at a water depth of 7-9 m and a Seismic Engineering Multidyne steamer consisting of 60 channels over 3298 m in length towed at a water depth of 15-20 m. The shotpoint interval was 50 m and the data were sampled at 4 ms over a 10 s window length. Reprocessing of the data by the Federal Institute for Geosciences and Natural Resources, Germany, improved the original data quality using new semblance, stack, deconvolution, FK-migration and time varying bandpass filtering. The data have a frequency bandwidth of 0-50 Hz, centered at 25 Hz.

2.2.2 R/V Meteor 2001 49-4 Site Survey

Line GeoB205, GeoB206, GeoB220 were used to correlate industry data to ODP Leg 207 Site 1257 on the outer portion of the Demerara Rise. This correlation allowed for better age control and to mitigate horizon tie uncertainties from the North Coronie-1 well within the Block30 survey. Lines GeoB205, GeoB206, Geob220 were acquired as part of a 700 line-km high resolution seismic reflection survey on the R/V Meteor in May of 2001 by the University of Bremen. The seismic sound source was a Seismic Systems, Inc. generator injector airgun with reduced chamber volume (2 x 0.411; 100-500 Hz), fired at a time interval between 9-11.5 s with an air pressure of ~1500 PSI. The injector was fired with a 30 ms time delay for the generator shot, which essentially eliminated the bubble

pulse. The gun was towed 1.4 m below the sea surface. The Syntron receiver included six 100 m long active sections, each with 16 hydrophone groups. Streamer tow depth was controlled to 3 m below sea level by 9 digibirds distributed along the 100 m sections. These data span frequencies between 60 and 200 Hz with peak energy around 100 Hz. The high resolution data were processed with a F-K migration, bandpass filtering and gain control adjustment.

2.2.3 Staatsolie 1999 Multichannel Seismic Survey

Seismic lines W99-108, W99-109, and W99-150 were part of a 2D survey spanning the outer Suriname margin, including the western flanks of the Demerara Rise. Burlington Resources were contracted by Staatsolie (State Oil Company of Suriname) in 1999 to acquire these data using the survey vessel M/V Western Inlet. Data collection ranged in water depths of 35 to over 2500 m. The M/V Western Inlet was configured with a single energy source and one streamer. The source comprised a total volume of 3750 in^3, fired at a 25 m intervals. The streamer was a Sentry Solid Stream with a total active length of 6000 m, configured with 480 active channels. Data were reprocessed in 2001 for RepsolYPF, including pre-stack migration.

2.3 RepsolYPF 2005 Block30 Three- Dimensional Seismic Survey

In 2005, a large (~ 2881 km^2) 3D seismic survey was acquired on the Suriname margin for RepsolYPF (Figure 2.1). The Block30 data were acquired by CGG Marine Services Ltd., onboard the vessel M/V CCG Alize. The survey parameters are listed in Table 2.1. The Block30 data used in this study were processed by CCG Americas Inc. The

processing workflow includes: spherical divergence correction, pre-stack zero phasing, velocity analysis, Tau-P deconvolution and Kirchhoff migration.

The data were gathered into 12.5 by 25 m bins and stacked maintaining a 2 ms sample rate. They span frequencies between 0 and 125 Hz with peak energy around 55 Hz. The survey has north-south trending inlines and east-west oriented crosslines.

Table 2.1 List of seismic acquisition parameters for the Block30 3D seismic survey.

Parameter	**Value**
Survey area	2881 km^2
Number of steamers	8
Number of sources	2
Source array	3210 in^2
Streamer depth	8 m
Source depth	6 m
Shot point interval	25.0 m
Receiver group spacing	10 m
Streamer length	7500 m
Inline bin spacing	25.0 m
Crossline bin size	12.5 m
Record length (after T_0)	8.5 s
Sample interval	2 ms
Processed bin size	12.5 m by 25 m

2.4 Seismic Interpretation

SEG-Y formatted files for the Block30 dataset were imported into SMT's Kingdom Suite software for interpretation, where seismic stratigraphic and seismic geomorphologic techniques were applied to the volume. Reflection amplitude, termination patterns, plan-form and 3D geometry were used to distinguish key surfaces, sequence boundaries and seismic facies. Prominent reflections were picked at every 10^{th} inline and crossline and mapped as horizons throughout the 3D Block30 dataset. These horizons were then auto-picked to provide 3D geomorphologic surfaces that provide insight into geologic evolution of the margin.

2.5 Resolution

Understanding the limitations of seismic tools and data for subsurface imaging is critical for interpreting results. Resolution refers to the minimum separation of two objects such that they can be distinguished as two separate entities rather than one (Sheriff and Geldart, 1995). The resolution of seismic data is described in a vertical and lateral sense and both are principally governed by the frequency spectrum and geometry of the source and receiver (hydrophone array).

2.5.1 Vertical Resolution

The temporal or vertical resolution of seismic reflection data is a factor of the frequency bandwidth. In general, the broader the bandwidth, the better the subsurface will be imaged. The maximum resolution (smallest resolvable target) is approximated by the Rayleigh criteria- a ¼ of the highest frequency of the data. A stratigraphic unit, such as a bed that is thinner than a ¼ of the wavelength will still reflect acoustic energy, but may

not be discriminated from surrounding beds. Vertical resolution in depth can be estimated using the following equation:

$$R = v / 4f$$

where v represents velocity and f is the dominant frequency (Yilmaz, 1987). The vertical resolution equation is based on the assumption that there is minimal noise in the recorded seismic data. Increased vertical resolution is achieved by increasing the upper limit on the bandwidth of the input source and decreasing noise (Yilmaz, 1987). A power spectral density plot of the Block30 data shows its frequency bandwidth is ~ 18-55 Hz (Figure 2.2). When using 1500 ms (velocity of water), based on the Rayleigh criteria, the smallest resolvable interval is ~ 7.0 m. Anything less than 7.0 m thick is theoretically not distinguishable.

(1/55 Hz x 1500 ms / 4 = 7 m)

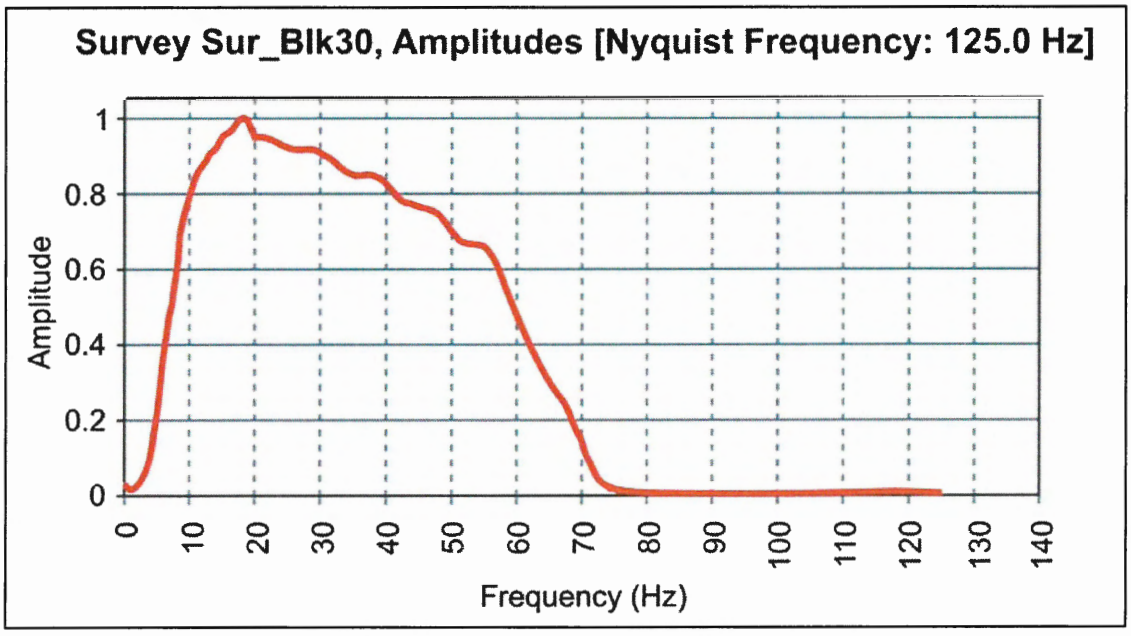

Figure 2.2 Frequency spectrum for the seismic data of the Block30 3D dataset (Kingdom Suite).

2.5.2 Horizontal Resolution

Horizontal, or spatial resolution, refers to the ability to distinguish between features that are displaced horizontally with respect to one another (Sheriff, 2002). The lateral resolution is controlled by the size of the Fresnel zone and the trace spacing from the shot point distances between the subsurface sampling points (Veeken, 2007). The Fresnel zone is a circular area of the spherically spreading wavefront defined according to:

$$r = (z\lambda/2)^{1/2} = (v/2)(t/f)^{1/2}$$

where t is the two-way travel time to the reflector, λ is the wavelength, z is the distance of the source reflector, and v the velocity above the reflector.

Migration of seismic data is an attempt to restore subsurface structure to its in situ geometry by compensating for the spherically spreading wave front. The migration process generally improves the lateral resolution from the Fresnel zone radius to a theoretical limit to one-half wavelength (Veeken, 2007). In general, the migration technique collapses the Fresnel zone and moves dipping reflectors to their approximate correct subsurface position (Yilmaz, 1987). The horizontal resolution of migrated seismic data is then equivalent to ½ wavelength of the source. A 2D migration can only collapse the Fresnel zone in the migration plane direction, whereas 3D migration improves the Fresnel zone completely to the theoretical limit in three dimensions. As the ½ wavelength criteria is less than the bin size of the Block30 3D data, the limiting factor is the bin spacing or data grid size. For the Block30 data, the bin spacing is 25 by 25 m.

2.6 Borehole Data

Data from one industry borehole and multiple scientific wells were available for this study. The hydrocarbon exploration well, known as North Coronie-1 (NCO-1), was drilled in early 1975 under the operator ELF Petroleum Suriname in 129 m water depth on the Suriname continental shelf with a total penetration depth of 5406 m (MD). NCO-1 was logged during various drilling steps. Log data collection for NCO-1 bypassed Pleistocene sediments and initiated at 412 m, determined to represent the top Pliocene interval. Logs for NCO-1 included: gamma ray, sonic, density, caliper, spontaneous potential, neutron, velocity and dip meter analysis. As well, drill core was recovered for the predicted reservoir interval, with associated porosity, bulk and matrix density measurements. Stratigraphic age control for NCO-1 were principally established using a combination of microfauna, nannofossils and pollen.

On the Demerara Rise ODP Leg 207 drilled numerous scientific wells, but for the purposes of this study, only Site 1257 is incorporated. Site 1257 is located in 2951 m water depth on a terrace above the steep northern slope of the Northwest Demerara Rise, ~ 170 km north of the Block30 dataset. The borehole reached a total depth of 287 m, acquiring near continuous down-hole core with multiple holes at the one site. Sediments ranged from Miocene to Albian, with 71% recovery.

2.7 Checkshot Survey and Synthetic Seismograms

Velocities derived from the checkshot surveys were used to convert borehole depths into two-way travel time (TWTT) for NCO-1 and Site 1257. Checkshot surveys are collected by lowering a receiver or a series of receivers into a borehole. The receivers are then

pressed to the side of the borehole at known depths (Yilmaz, 1987). A source is then emitted from a surface vessel and the travel time to the receiver is recorded. The travel time and depth information provides a RMS velocity, which is inverted to construct time-depth pairs for each measurement interval. Interval velocities provide a velocity structure for the stratigraphic column, allowing depth in the borehole to be converted into two-way travel time. Synthetic seismograms are theoretically derived seismic traces generated from physical property information (velocity and density) from wells. Most often, synthetic seismograms are used to correlate well data, which are in the depth domain, to seismic data which are in the time domain. The product of sonic and density data is acoustic impedance. Reflection coefficients (impedance contrasts between lithologic layers) are generated from these data and are mathematically convolved with an appropriate input seismic signal to generate a synthetic seismogram.

Synthetic seismograms for this study were generated as a means to verify the correlation between well information and seismic data. The simulated seismic response computed from velocity and density well data is used to relate geological events and lithologies/ages recognized in wells to seismic traces. The match of the simulated seismic response to the actual seismic profile determines the quality of correlation and confirms velocities used for depth conversion.

2.8 Time Depth Conversion

Time depth conversions were conducted using average interval velocities between picked reflections from checkshot velocities at the NCO-1 well (Table 2.2). These converted depths were used to create isopach maps for interpreted seismic intervals.

Table 2.2 Seismic reflections, depths, velocities and thicknesses

Seismic Reflection	Depth (MD)	Average Velocity (m/s)	Interval Velocity (m/s)	Thickness at NCO-1 (m)
Seafloor	142	1480		
Saramacca	1329	1840	1880	1187
Marowijne	1810	1920	2180	481
(Para)	(N/A)	(2015)	(2340)	(N/A)
Sipaliwini	2907	2110	2510	1097
Nickerie	3203	2140	2530	295
Wanica	3738	2240	3080	535

2.9 Seismic Attribute Analysis

Seismic attributes are characteristics or derivatives of characteristics of seismic signals, including time, amplitude, frequency, and phase. They assist in studies of structure, stratigraphy and rock properties of seismic data (Brown, 2003). Attributes can be extracted along a time surface, a horizon, or from a pre-defined vertical window encompassing any number of reflections. The principle seismic attribute for the Block30 volume was the geometric dip variance attribute. The dip variance represents the difference between the smoothed dip of maximum similarity and the local value of the dip of maximum similarity. The dip of maximum similarity and similarity attributes are computed together but stored differently by scanning adjacent traces within a user-defined range of dips as indicated from the time window. Areas of high similarity are first generated which indicate a high degree of lateral signal similarity. The dip of maximum similarity then detects dip variation and structural discontinuities. The smooth dip of

maximum similarity low-pass filters the dip of maximum similarity values to determine averages over longer windows, detecting any anomalous dip variations and structural discontinuities. Data are viewed in profile to identify local anomalous dips, thicknesses, and offsets. Data may also be viewed as time slices or horizons to asses lateral or vertical attribute changes. A similarity/dip of maximum similarity time window of 0.04 s and a variance time window of .08 s were used to generate two 3D similarity volumes from the Block30 dataset.

2.10 Error and Confidence Analysis

Sources of error in seismic interpretation occur from limitations in acquisition and processing artefacts (physical rock properties, coherent noise, seismic tuning), depth conversion and the ability to pick and correlate horizons.

The main source of error for this study is the ability to pick and correlate seismic reflections (horizons) throughout the data volume. Mapping reflections within a 3D seismic volume consists of picking a series of inlines and crosslines at a defined spacing, and extent. Interpreted reflections in the inline orientation generate seed points at the intersection with crosslines. Interpreted horizons were then autopicked for all inline and crossline data using the manually picked seed points. Complete horizon picks allow generation of a geomorphologic render of a surface. The basic 3D autopicking parameters for autocorrelation begin picking three iterations, with a 3 x 3 smoothing operator. The operator is read inline x crossline using n-1 points (adjacent to the current point) in each of the four directions (total of 2n+2 points).

In order to determine the quality of the autopicks, a series of attribute maps were generated for a 10 x 10 km area of a Early Miocene age horizon in the study dataset (Figure 2.3) using the 3D autoseeker+™ including; pick status, pick order, pick type and confidence (Figures 2.4 to 2.9). The manual picks for the area were interpreted at every 10^{th} inline and crossline for even distribution.

A confidence attribute map (Figure 2.7) is generated based on confidence values ranging from 0.0 - 1.0. Confidence is calculated with the assumption that manual picks have the highest confidence (confidence =1). All other picks have a confidence C_t calculated based on:

$$c(P_t) = X_t^{\,e\,-k(\rho_t\,+\delta_t)}$$

Where:

$c(p_t)$ = confidence for pick pt.

X_t = a measure of affinity between two traces within cross correlation window calculated as:

$$\frac{Q_t \times X_t}{\max\,(Q^T 1 \times Q_\rho X^T{}_1 \times X_t)}$$

Where Q_t is amplitude values at trace 1 and X_t is amplitude values at trace 2.

ρ = maximum vertical shift between all picks in the neighborhood of ρ_t.

δ = the shift to the best cross-correlation sample in the same trace within the correlation widow.

k = smoothing factor of 0.5.

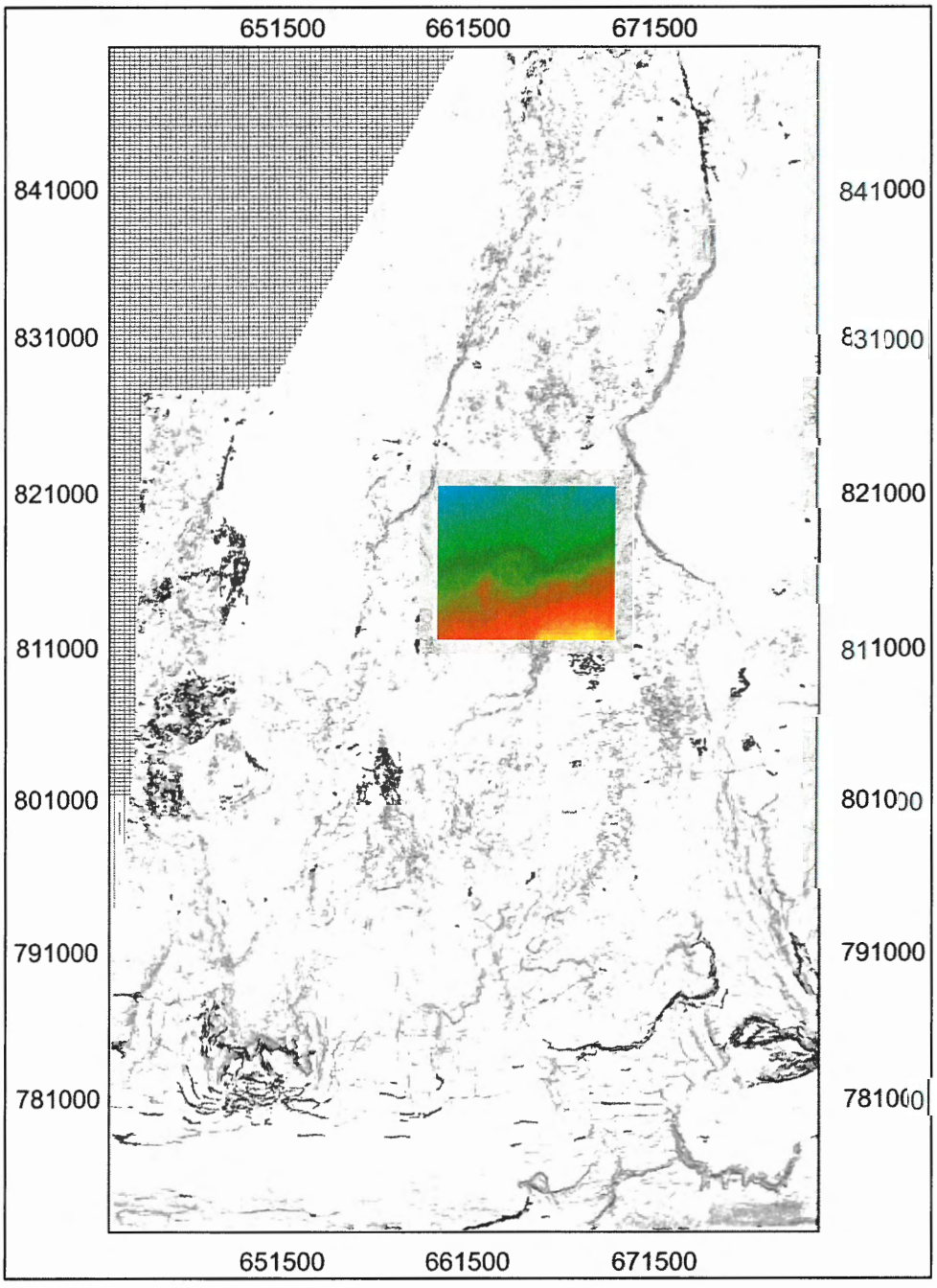

Figure 2.3 Map of the Early Miocene Nickerie reflection surface. The coloured box located in the centre of the surface indicates the location of the 10 km^2 area used to generate a series of attribute maps and the difference map.

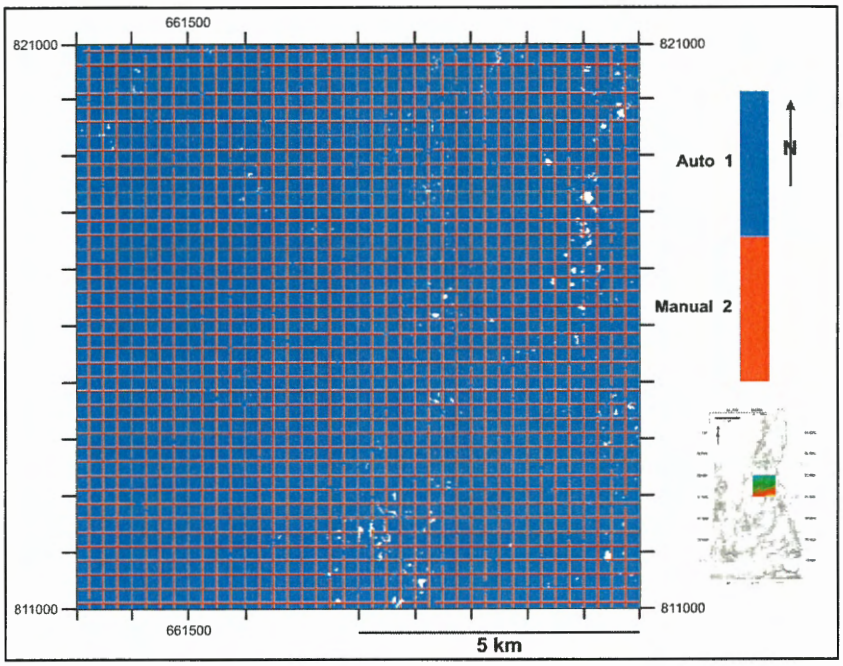

Figure 2.4 Pick type attribute map red showing manual picks and blue are auto picks. In general every 10th line was picked manually.

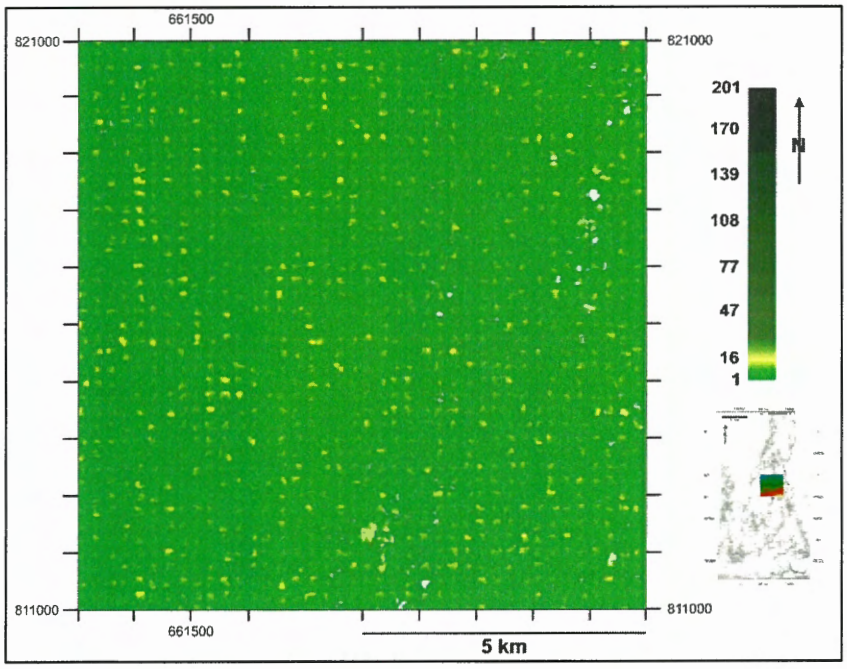

Figure 2.5 Pick order attribute map indicates the generation order of picks determined by the trace selection algorithm. The pick order attribute defines how many steps there are between a particular pick and a possible seed point.

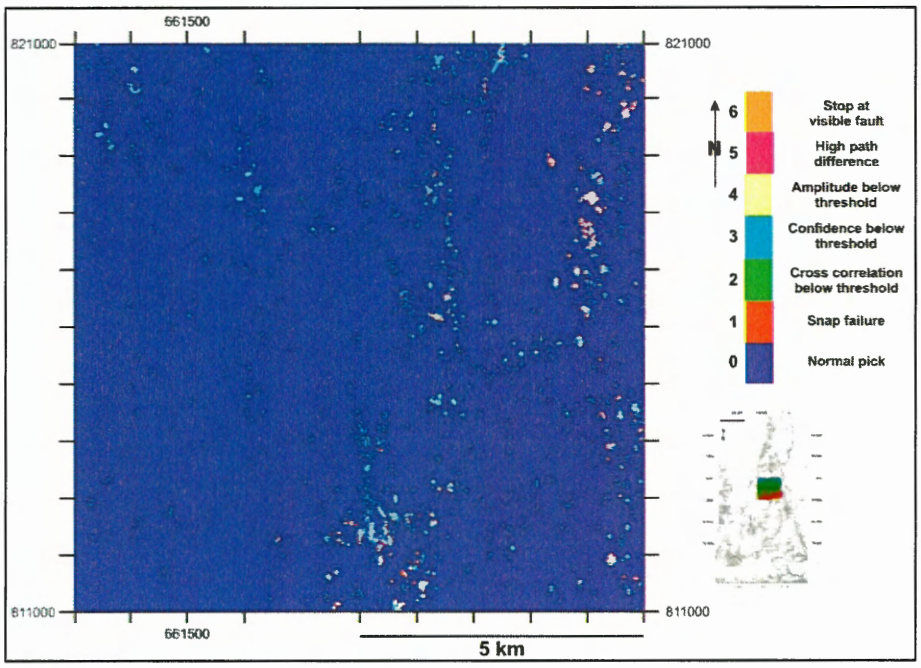

Figure 2.6 Pick statues attribute map indicating directional changes of the autopicker at a particular point. Reasons for changes are noted in the color bar.

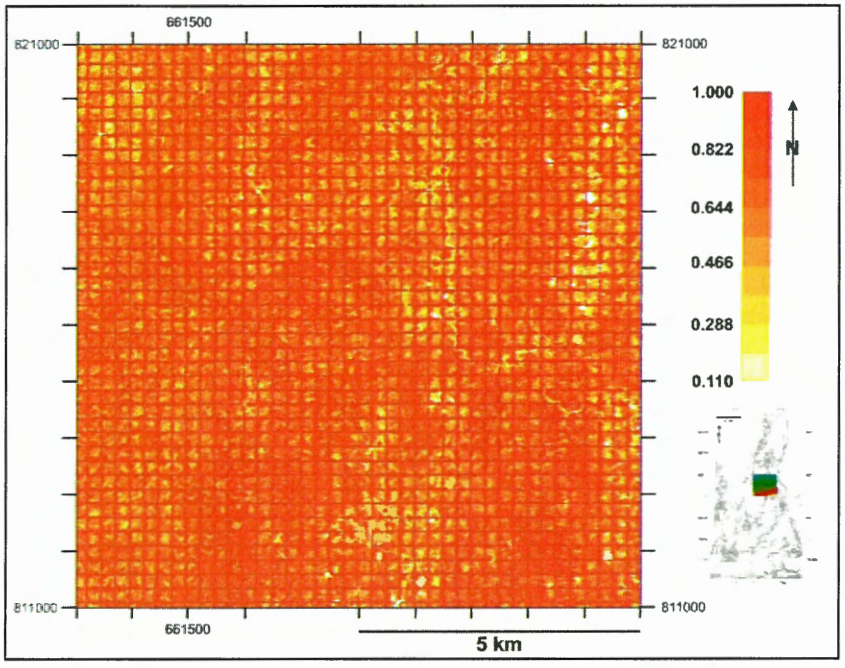

Figure 2.7 Confidence attribute map based on the autopicker values ranging from 0.0 to 1.0. Values of 1.0 are of the highest confidence (manual), lower values indicate a decrease in confidence.

A difference map in time was generated using the basic autopicker over the same 10 x 10 km area of the Early Miocene age horizon (Figure 2.3), using the same manual picks as the autoseeker+™ algorithm. To determine the quality of the autopicks, a difference map was generated between the raw auto picked and the auto smoothed picked surfaces. Results indicate the areas with the greatest potential error (Figure 2.8). The difference map investigated 159881 numerical cells. The differences range from -27.8 ms (~ 31 m) to 26.8 ms (~ 30 m) with an average difference of 0.42 ms, maximum, with a standard deviation range of 1.5 ms (Figure 2.9). The difference values displayed in map form (Figure 2.8) show, as expected, highest confidence in horizon picking is in areas of low morphologic relief and lowest confidence in areas of high variable relief.

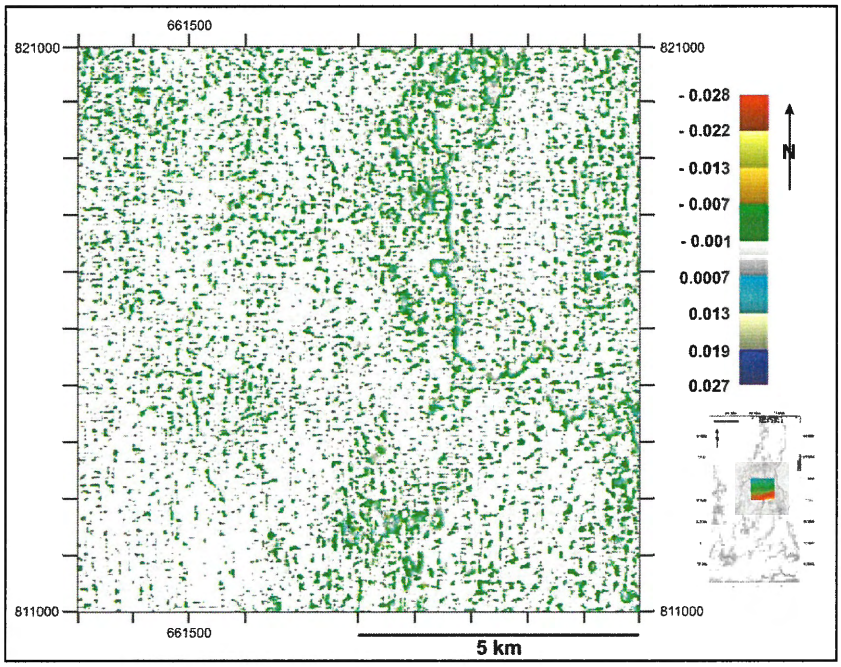

Figure 2.8 Difference map generated for a 10 km^2 area of the Early Miocene Nickerie reflection surface from the Block30 3D dataset. It indicates the greatest potential in error between manual raw picks and the basic autopicks unsmoothed.

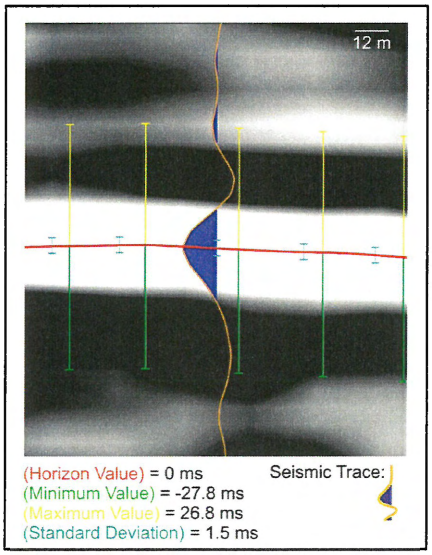

Figure 2.9 Diagram illustrating the range of values from the generated difference map. Orange indicates a single seismic trace and blue represents trough fill through the reflection used to render the 10 km^2 area of the Miocene horizon. Green indicates the minimum ms difference value, yellow indicates the maximum ms difference value, red indicates the reflection used which has a zero difference value, and turquoise represents the standard deviation for the difference values.

2.11 Seismic Stratigraphy

Seismic stratigraphy is a technique used in seismic interpretation that combines seismic reflection geometries and basic stratigraphic concepts to infer depositional architecture (Vail et al. 1977). The unique properties of seismic reflections allowed the direct application of geologic concepts based on physical stratigraphy (Vail et al. 1977). Seismic reflections (often resembling layers) are generated at acoustic impedance contrasts (Z); impedance being the result of changes in the bulk rock properties of velocity and density. With the assumption of normal incidence, seismic reflections are explained through the Zoeppritz equation, which has been reduced to the equation for the normal reflection coefficient.

$$R = \frac{Z_{layer2} - Z_{layer1}}{Z_{layer2} + Z_{layer1}}$$

R = reflection coefficient (ratio between reflected and transmitted energy).

Z = Acoustic impedance (product of the materials bulk density and its seismic velocity).

The equation represents the fact that the reflection amplitude is a function of the magnitude of change of the acoustic impedance. A reflection coefficient is generated at each change in acoustic impedance and collectively the sequence of reflection coefficients are known as the Earth's reflection series. The source wavelet convolves with the Earths reflection coefficient series to produce a series of seismic reflections, the amplitude of the reflection being proportional to the value of the reflection coefficient and of the same sign.

Seismic amplitude and phase (sign) are two "attributes" of seismic reflection data. Other attributes include frequency and coherency and in combination with relationships to neighbouring reflections, reflection configuration and geometry, these elements constitute the basis of seismic interpretation (Figure 2.10). Seismic reflections are grouped into facies or intervals of similar reflection characteristics. Facies are further grouped into seismic sequences based on patterns of occurrence and associations. Seismic facies and sequences are then used to interpret the distribution of sediments and environments of deposition based on internal reflection organization, bounding relationships, external geometry and lateral changes (Mitchum et al. 1977a; Mitchum et al. 1977b; Vail et al. 1977; Vail 1987; Galloway 1989; Christie-Blick 1991, Vail et al. 1991; Catuneanu 2002; Veeken 2007).

2.12 Accommodation Succession Method

Since the introduction of seismic sequence stratigraphy over 30 yrs ago by Mitchum et al. (1977a; 1977b), based on the observations of Vail et al. (1977), the application of seismic sequence stratigraphic methods has generated debate (Posamentier et al. 1992; Plint and Nummedal, 2000). These studies produced a complex jargon that mixes interpretation with observations, often with different genetic names applied to the same surfaces or deposits depending on which conceptual model employed.

A new method of accommodation succession, proposed by Neal and Abreu (2009) for interpreting seismic sequence stratigraphy was applied in this study. Accommodation succession is defined as a regional sedimentary package resulting from changes in rates of shelfal accommodation creation and depositional fill in response to changes in base

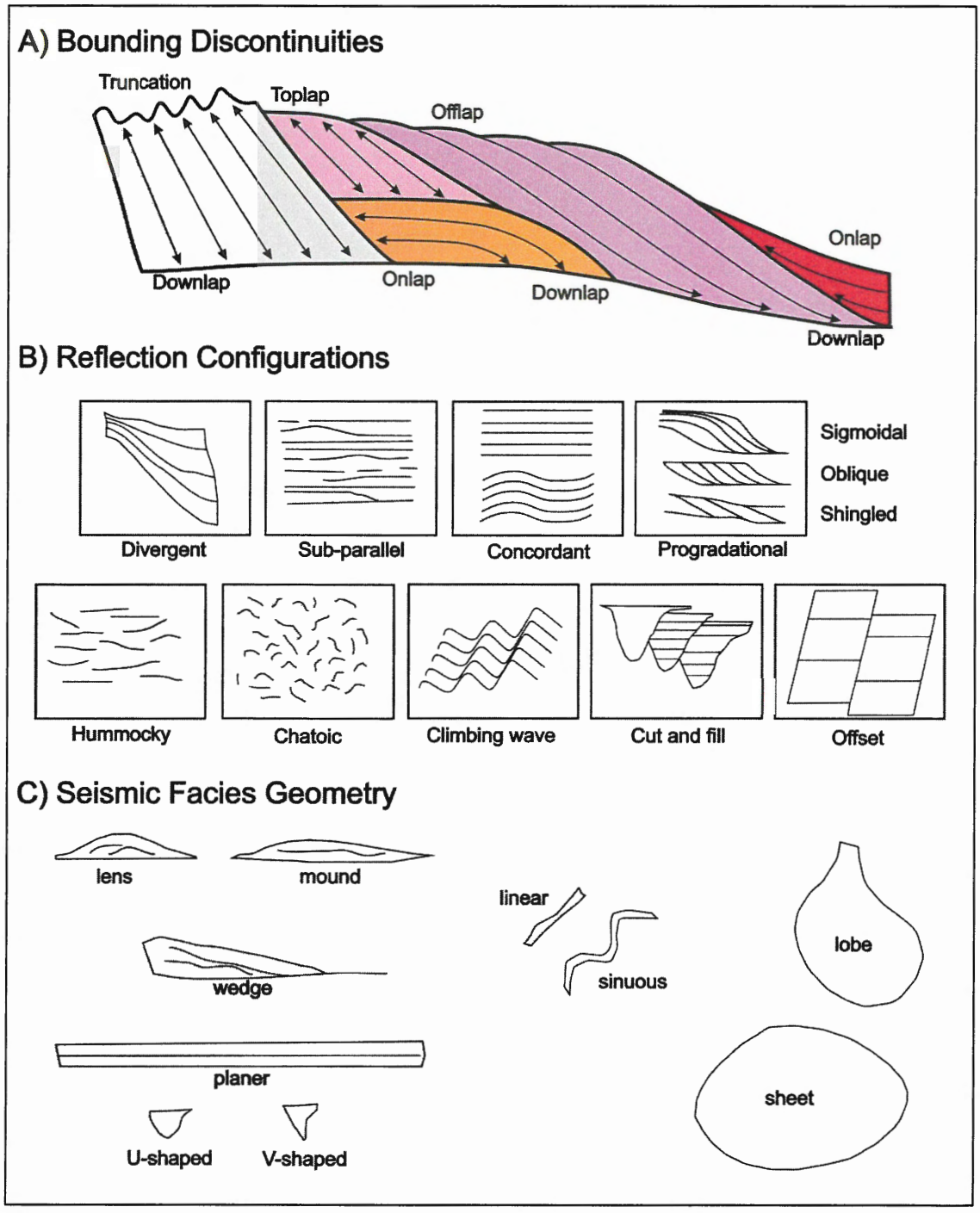

Figure 2.10 Seismic stratigraphic geometries used to describe and interpret stratigraphy, depositional environments and facies distribution (modified after Sloss 1963; Mitchum et al. 1977a; Catuneanu, 2002).

level (Neal and Abreu, 2009). Base level delineates a dynamic surface of balance between erosion and deposition, and is controlled by a combination of eustasy and tectonic subsidence or uplift. The accommodation succession method proposes a framework for the hierarchy of sedimentary sequences observed in seismic data that is based entirely on the geometric relationship of stratal patterns, and facies stacking relative to key bounding surfaces. It is not defined by duration, relative sea level position or inherited depositional profile. Geometries of the strata are assumed to result from repeated successions of accommodation creation and sediment infill. The hierarchal framework of Mitchum and Van Wagoner (1991) was modified to describe depositional sequences resulting from accommodation successions of varying magnitude and duration.

The method proposes the use of classic terms to describe the key bounding surfaces; sequence boundary, transgressive surface (maximum regressive surface), and maximum flooding surface (maximum transgressive surface). The critical stratal pattern of coastal onlap deposition (following the sequence boundary) observed in the rock record is: "lowstand" progradation-to-aggradation (PA), "Transgressive" retrogradation (R), and "highstand" aggradation-to-progradation, degradation and/or basinward shift (APD), then the pattern repeats. The terms "highstand" and "lowstand" are used in the strictest sense of their original definitions from Mitchum et al. (1977), recognizing that highstand (APD) stacking can occur outboard of a shelf edge and lowstand (PA) stacking can occur landward the shelf edge (Neal and Abreu, 2009). The proposed hierarchal framework to describe depositional sequences resulting from accommodation successions of varying magnitude and duration based on the physical stacking is: parasequence, systems tracts, depositional sequence, sequence set, composite sequence set, and mega sequence (Figure

2.11) (Neal and Abreu, 2009). Internally, each hierarchical unit responds to an accommodation succession controlled by the interaction between the rate of accommodation creation and sediment supply rate ($\delta A/\delta S$). The resulting stacking patterns with different rate vectors are: $\delta A/\delta S < 1$ and increasing = PA; $\delta A/\delta S < 1$ and decreasing = APD; $\delta A/\delta S > 1$=R (backstepping) (Figure 2.12) (Neal and Abreu, 2009). Conditions where $\delta A/\delta S = 1$ are found at both the top of PA stacking and base of APD stacking. Subsequent changes in the $\delta A/\delta S$ balance will result in either R or APD stacking (Figure 2.12 and 2.13).

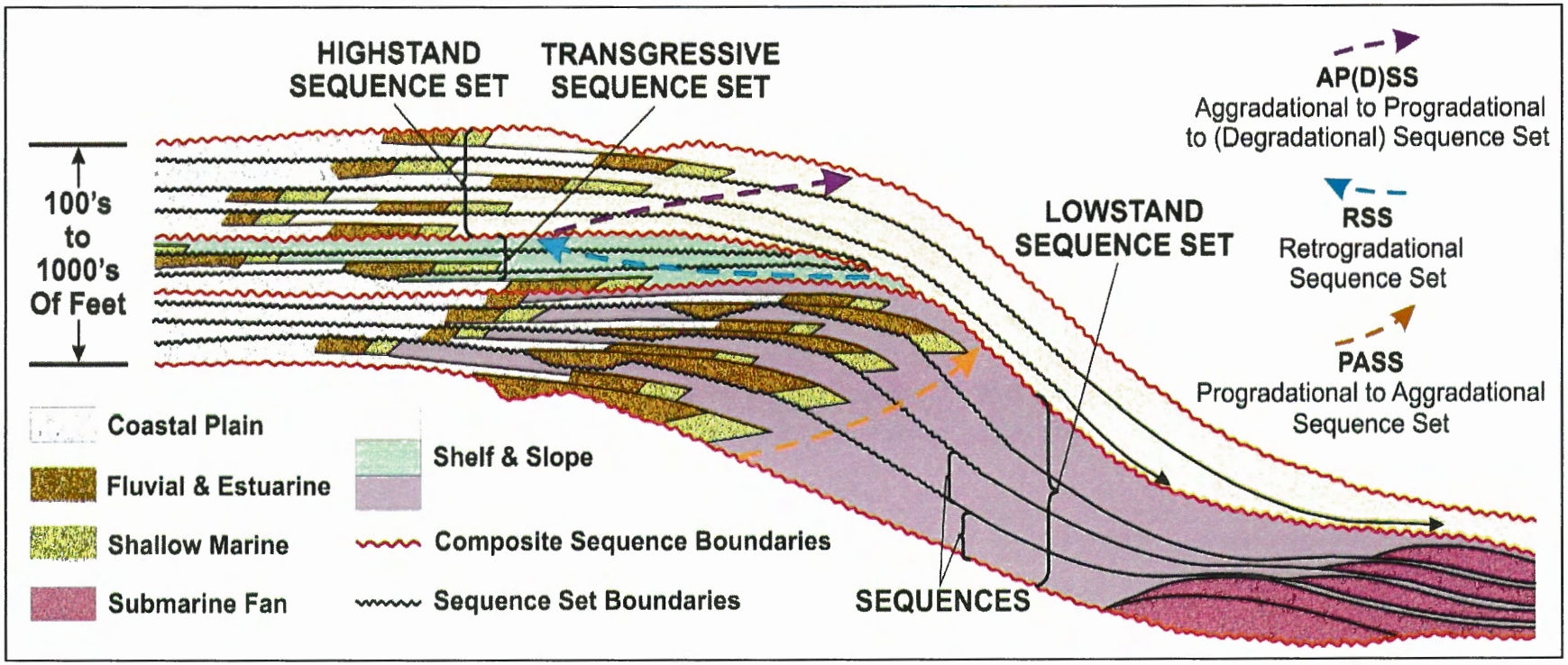

Figure 2.11 Illustration of sequences, sequence sets, and composite sequences. Individual sequences represent parasequences, stacked into lowstand (PA), transgressive (R), and highstand (APD) sequence sets to form composite sequences (modified after Mitchum & Van Wagoner, 1991).

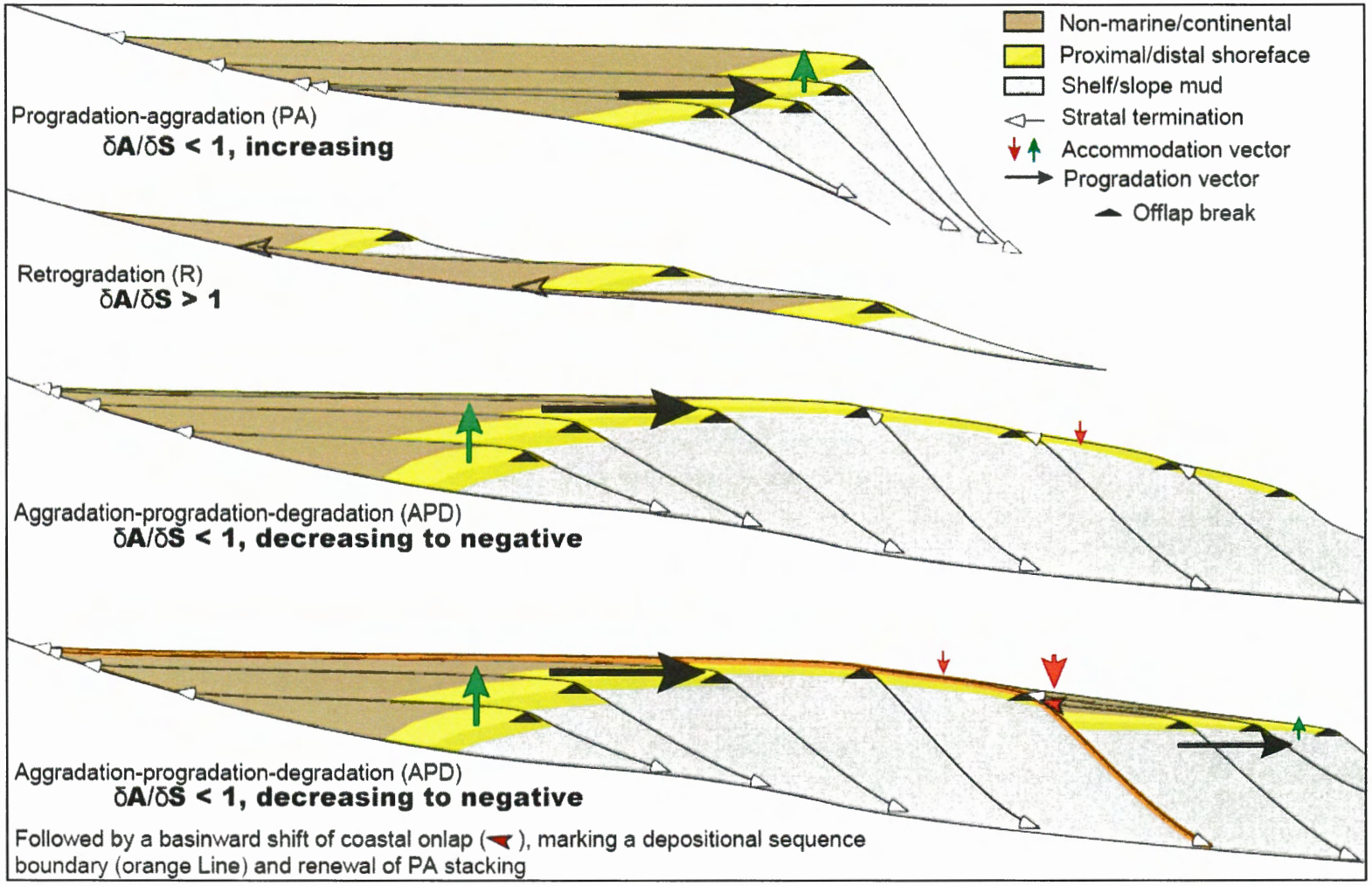

Figure 2.12 Stratal stacking patterns associated with changing rates of coastal accommodation creation and sediment fill, referred to as an accommodation succession (after Neal and Abreu, 2009).

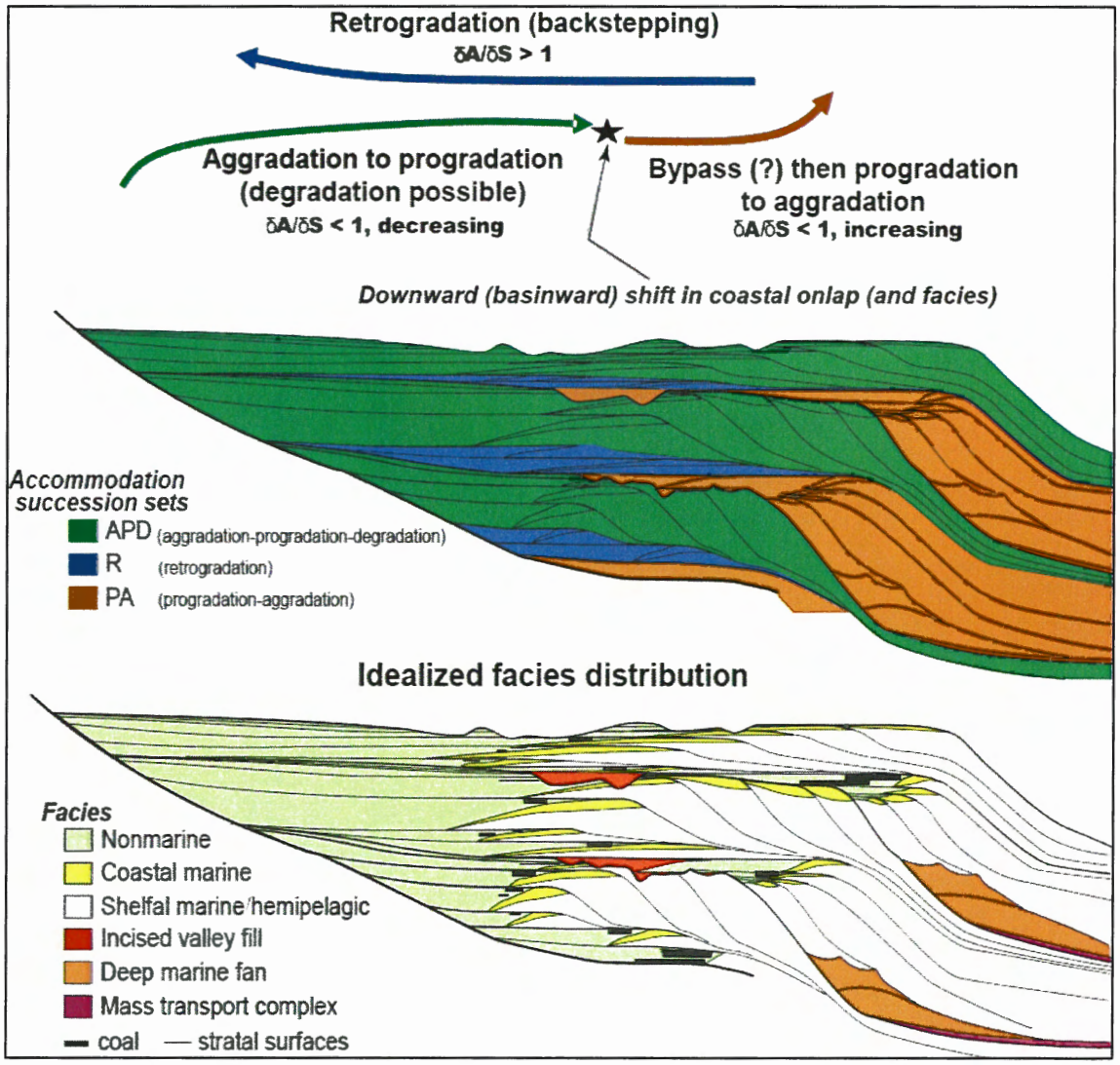

Figure 2.13 Accommodation successions of depositional sequences (A) and idealized facies distribution (B) (after Neal and Abreu, 2009).

CHAPTER 3: RESULTS

3.1 Seismic Facies

The use of seismic facies follows the definitions of Mitchum et al. (1977b) and Sangree and Widmier (1977, 1979). Seismic facies analysis involves "the delineation and interpretation of reflection geometry, continuity, amplitude, frequency and interval velocity, as well as the external form and three-dimensional associations of groups of reflections" (Sangree and Widmier, 1977). Reflection continuity is interpreted to correspond to continuity of strata and the reflection amplitude to the contrast in lithology (Mitchum et al. 1977b). The identification and use of seismic facies is used to determine the age and geometry of depositional sequences, lithology, depositional environments and processes, and sediment transport direction (Figure 2.10 and 3.1).

Geometry of reflections can be sub-divided into packages of reflections composing a unit or "package" of reflections. Commonly within this study, reflection geometries are described as parallel (concordant), sub-parallel (discordant), divergent, progradational, reflection-free, wavy, chaotic, hummocky, or contorted. The external morphology and three-dimensional character of seismic packages is described as sheets, lenses, mounds, wedges, or drapes (Mitchum et al., 1977b). Geologic interpretation made by integrating the facies units to seismic sequences allows for respective inferences to be made on depositional systems, paleo-environments, facies boundaries, paleo-shelf edges and other stratigraphic features (Brown and Fisher, 1980).

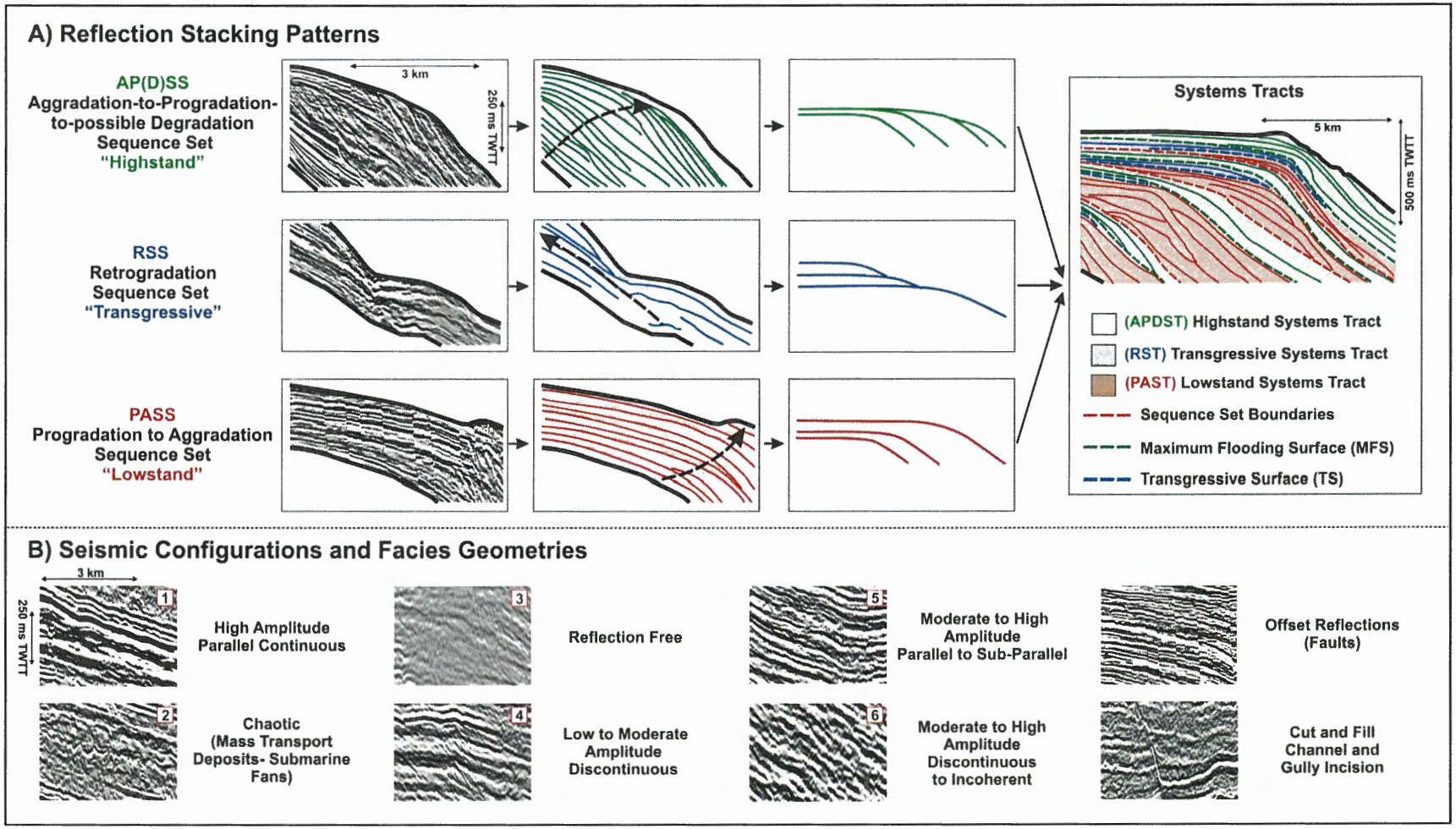

Figure 3.1 Seismic reflection stacking patterns, configurations and facies geometries from the Block30 dataset used to identify depositional environments and establish the seismic stratigraphic framework.

Within the study area, six facies are identified from the 3D Block30 dataset (Figure 3.1). These facies are distinguished by their overall reflection characteristic and geometry of the facies unit in seismic reflection data. Reflection amplitude, strength, continuity and location within the stratigraphic successions helped define these facies. The six facies are defined as 1-6 (Figure 3.1). Facies 1 is composed of mainly high amplitude parallel continuous reflections. The nature of the acoustic facies implies the associated sediment is well stratified. Facies 2 is composed of chaotic reflections. Facies 3 is described as reflection free, representative of homogeneous, nonstratified, or highly contorted strata. Facies 4 is composed of low to moderate amplitude discontinuous reflections. Facies 5 consists of moderate to high amplitude, parallel to sub-parallel reflections. Facies 6 consists of moderate to high amplitude, discontinuous to incoherent reflections.

3.2 Key Reflections and Geomorphologies

In order to establish the seismic stratigraphic framework, seven key reflections were identified and correlated throughout the dataset (Figures 3.2 to 3.4). Reflection names were arbitrarily chosen based on Suriname's 10 districts. From oldest to youngest, these seven key reflections are referred as Wanica, Nickerie, Sipaliwini, Para, Marowijne, Saramacca, and Commewijne.

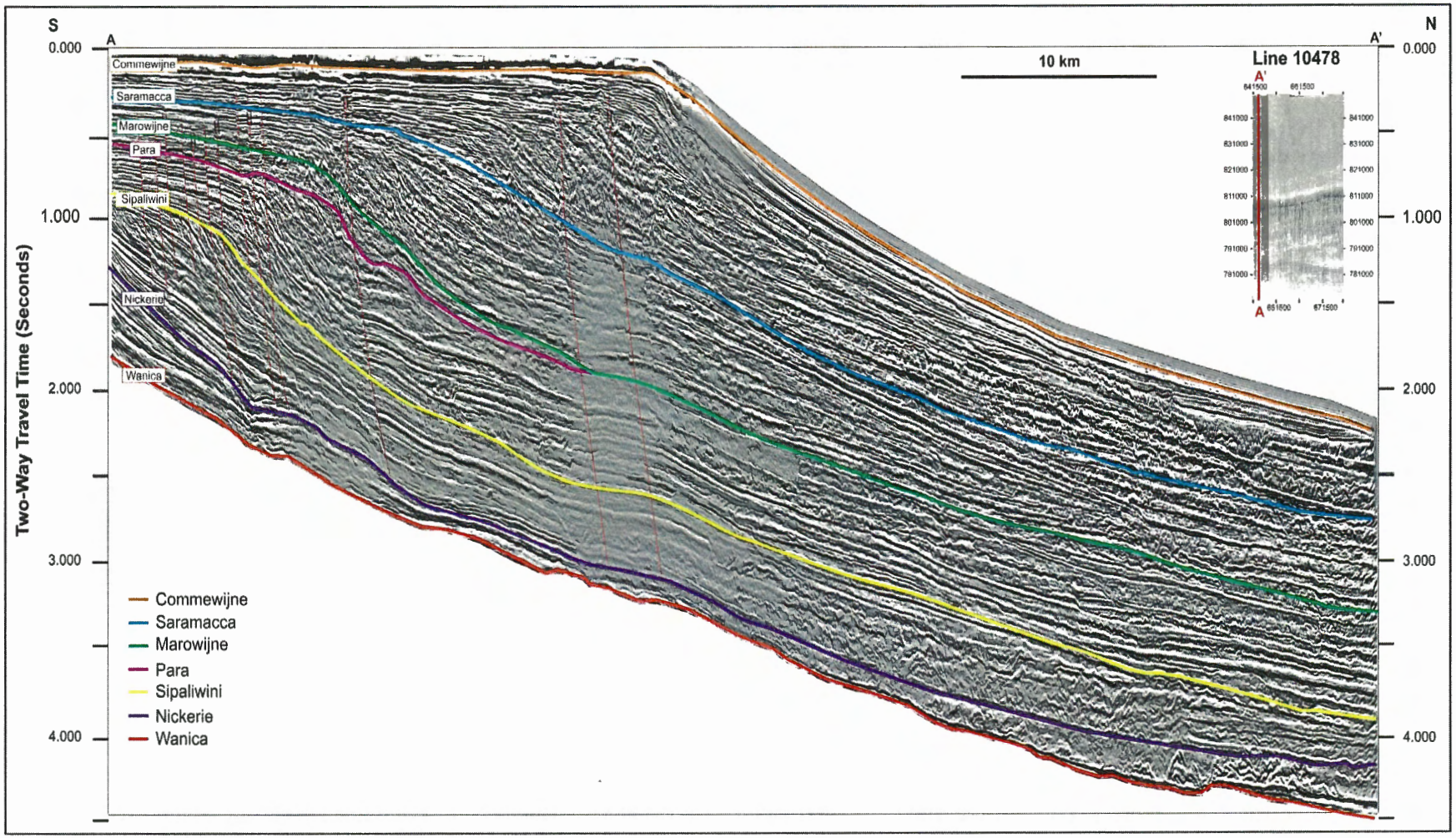

Figure 3.2 Key Cenozoic seismic reflections mapped across the Block30 dataset.

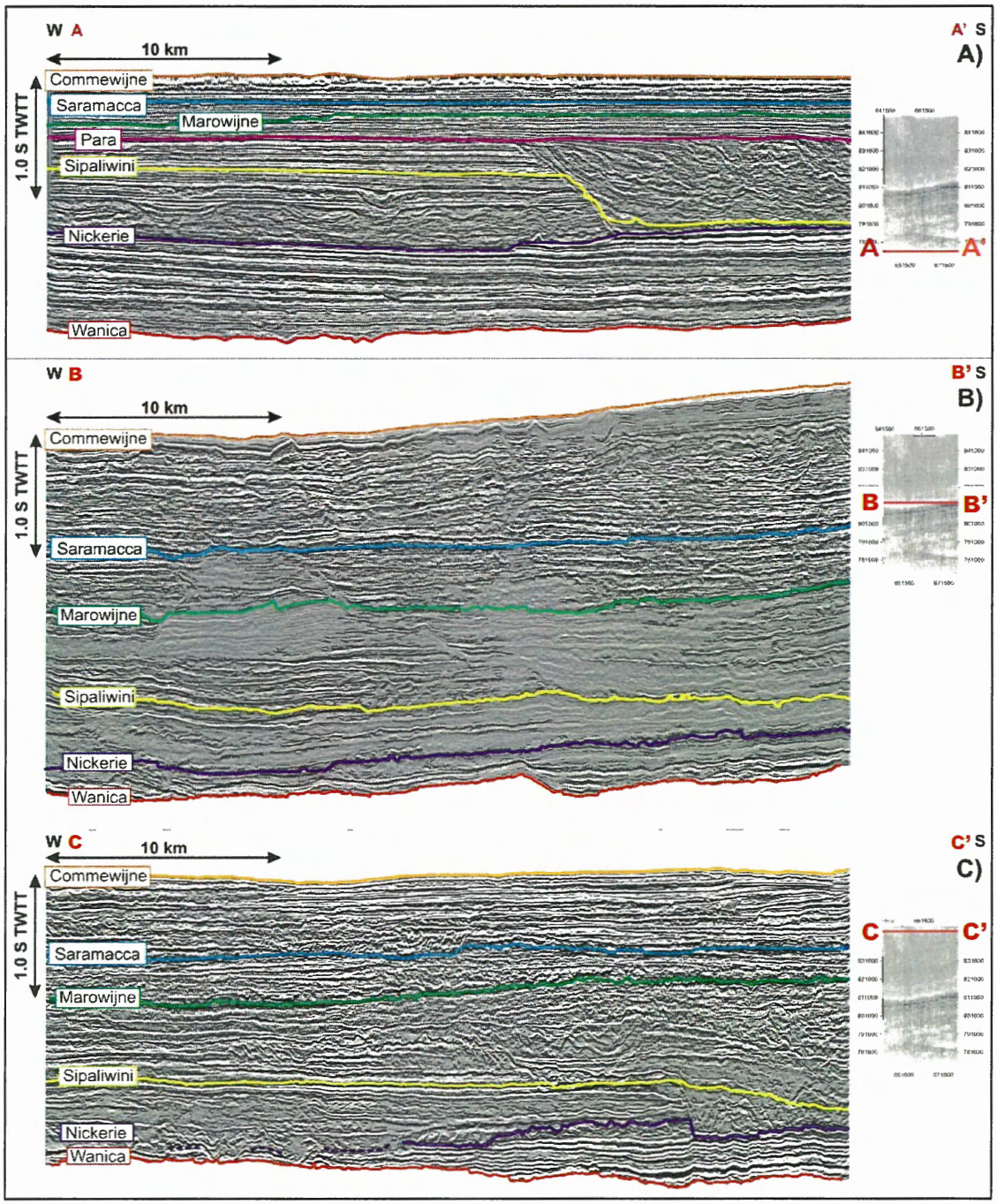

Figure 3.3 Strike profiles with key Cenozoic seismic reflections mapped across the Block30 dataset. A) Strike profile 5266 located across the southern shelf region of the dataset, B) strike profile 8148 located at the present day shelf break location, C) strike profile 11032 located across the northern lower slope region of the Block30 dataset.

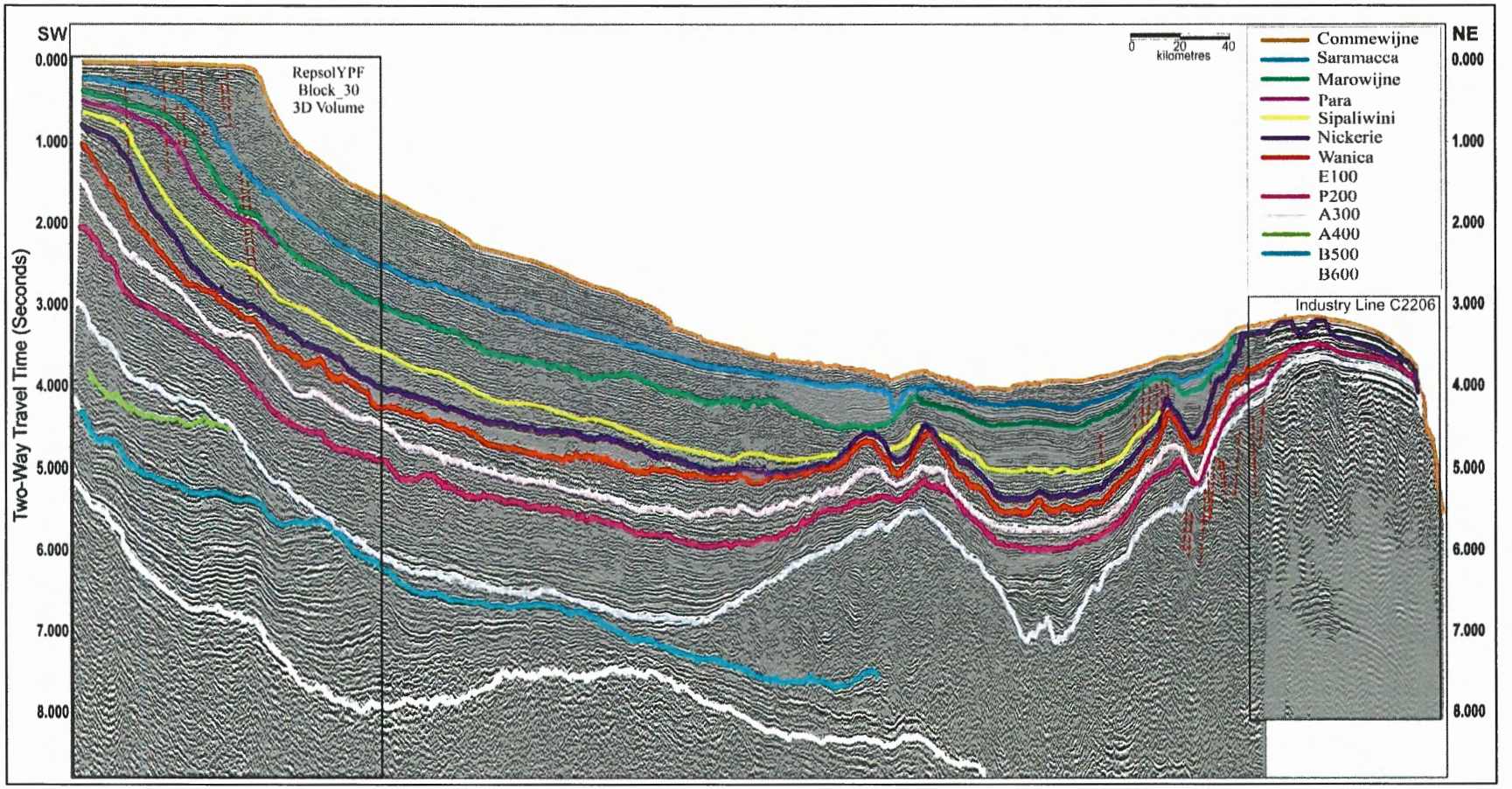

Figure 3.4 Regional RepsolYPF line W99-109 and Shell Line C2206 with the seven key Cenozoic reflections. Reflections deeper then Wanica are used in this study to compare age control between NCO-1 and ODP Site 1257 on the outer Demerara Rise.

The lowest stratigraphic reflection event is referred to as **Wanica**. It is a moderate to high amplitude continuous positive peak, offset by ~ 30 ms TWTT (~ 34 m) normal faulting under the immediate modern shelf region. The reflection is correlated throughout the data and is recognized by its distinctive character; bounded above by a high amplitude trough and below by a moderate to low amplitude trough (Figures 3.2 to 3.4). Interpretation confidence decreases under the inflection point of the modern shelf break as a result of diffraction noise, and to the lower slope region where chaotic reflections bound the reflection above and below. The interval velocity of this horizon averages ~ 2240 m/s (Table 2.2)

The Wanica surface in general hosts a planer geomorphology (Figure 3.5). A series of minor gullies occupy the southern-most region of the dataset (Figure 3.5a). Geomorphologic highs of ~ 90 ms TWTT (~ 100 m) in the middle slope region of the surface are located between the gullies (Figure 3.5b). In the south eastern region of dataset the lower slope exhibits a rugose morphology between two low lying, ~ 20 ms TWTT high (~ 22 m) escarpments.

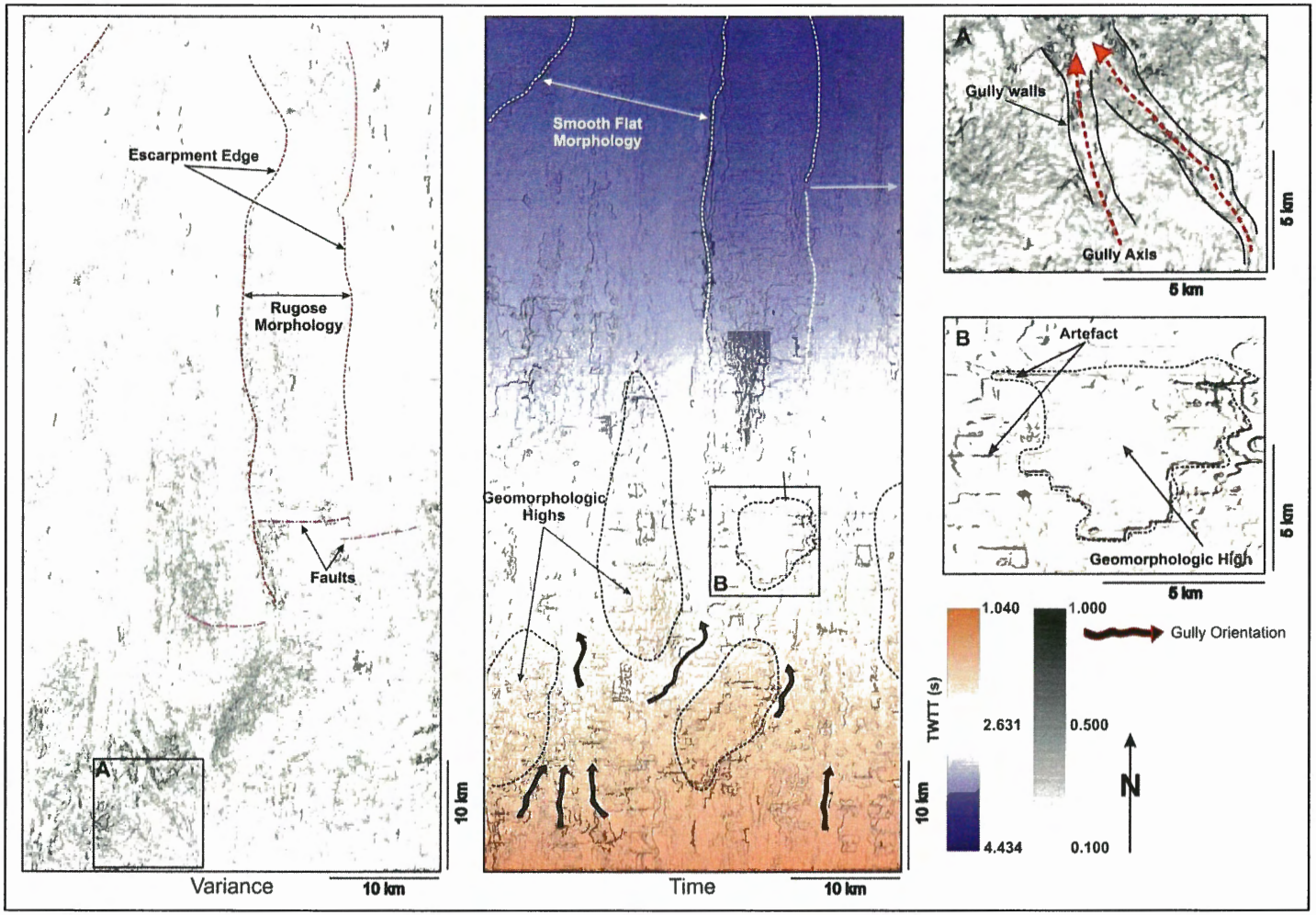

Figure 3.5 Isochron map of reflection Wanica demonstrating the overall morphology of the surface. A) A series of minor gullies and escarpments oriented north-northeast are recognized in the southern region of the surface, B) a structural high separates two minor gullies; artefacts identified are a result of poor reflection continuity. A variance attribute map (far left) of the same surface enhances features of the time domain image.

Reflection **Nickerie** is a distinctive negative trough of moderate to high amplitude that is continuous across the entire span of the dataset (Figures 3.2 to 3.4). The reflection is of high amplitude under the modern shelf break and northernmost lower slope regions. The reflection becomes moderate to high amplitude in the mid-slope region, where it is bounded above and below with moderate to low amplitude positive peak reflections. In the northwest region of the lower slope, reflection continuity is poor and correlation is problematic as the reflection is truncated by a package of low to moderate amplitude chaotic reflections (Figure 3.3c). The interval velocity of this horizon averages ~ 2140 m/s (Table 2.2).

In the upper slope region, the Nickerie surface is cut by a ~ 160 ms TWTT (~ 170 m) deep channel, that extends ~ 9.0 km in length and is oriented north northeast (Figure 3.6). This channel intersects a deeper cut ~ 260 ms TWTT (~ 280 m) channel oriented north northwest, extending ~ 30.0 km in length within the dataset. This deeper channel is confined by steep escarpments to the east and west (Figures 3.3a to 3.6). Two other features on the Nickerie surface incise the paleo-shelf region in a northern direction. To the far west of the surface, a slump scar is identified surrounded by radial fault patterns (Figure 3.6a). To the east of the slump scar, a small ~ 3 km wide and ~ 40 ms TWTT (~ 40 m) deep gully incises the paleo-shelf break and upper shelf. These features coalesce in the mid-slope region where a distinct positive geomorphologic high is identified ranging from ~ 90 to 110 ms TWTT (~ 100 to 120 m) and ~ 20.0 km wide, becoming thicker in lower slope region at ~ 120 to 130 ms TWTT (~ 130 to 140 m) and ~ 10 km wide (Figures 3.3b and 3.6b).

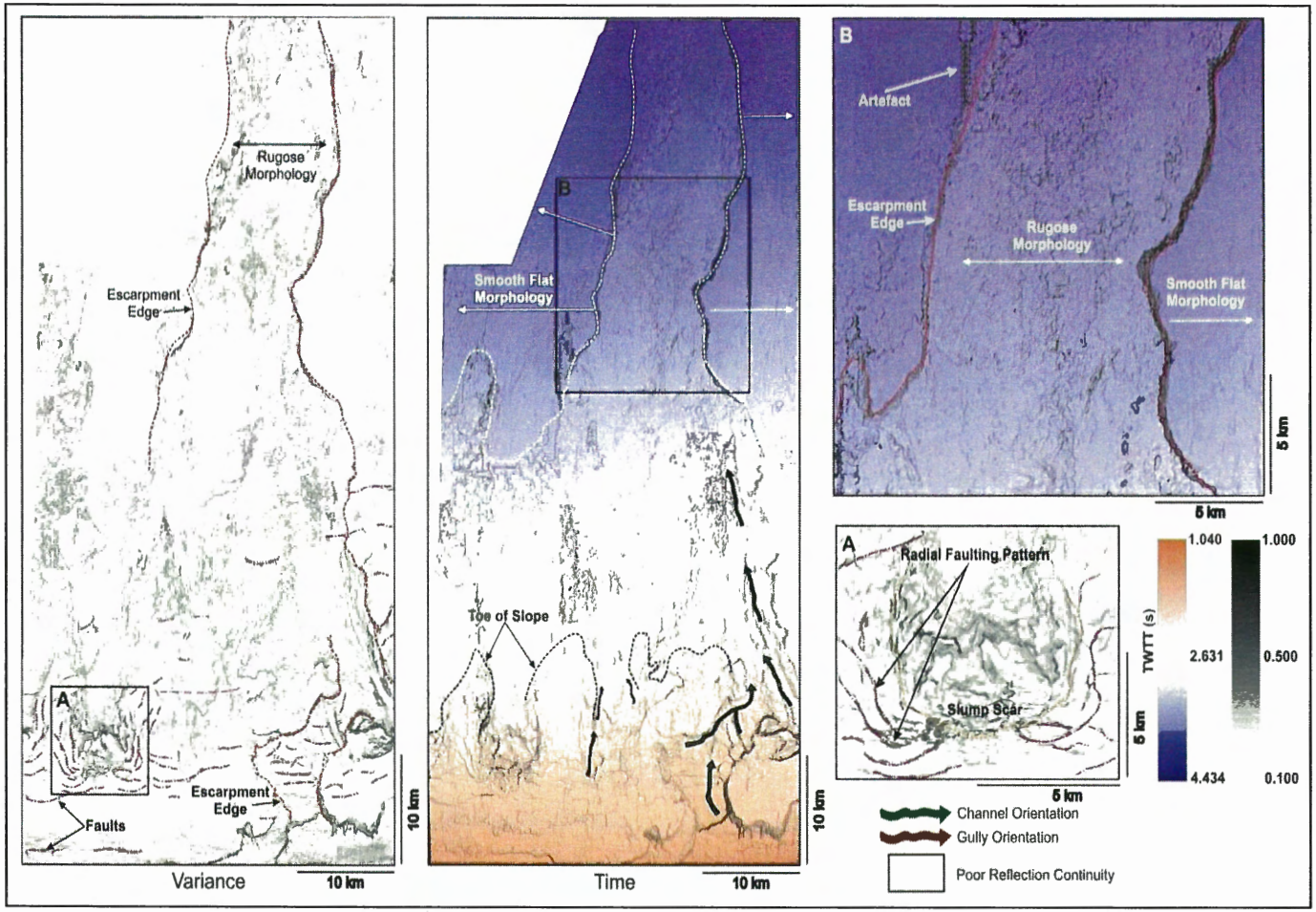

Figure 3.6 Isochron map of reflection Nickerie indicates a large channel system incising the south-eastern shelf, merging with a deeper cut channel downslope oriented north-northwest. A) Indicates a large slump scar surrounded by a series of radial fault patterns, B) displays a large positive bathymetric feature with steep escarpments and a rugose morphology. A variance attribute map (far left) of the same surface enhances features of the time domain image.

The **Sipaliwini** reflection is a moderate to high amplitude negative trough that is easily correlated throughout the extent of the dataset except in the northeast region. In this area reflection continuity is greatly reduced, becoming chaotic. The interval velocity for this horizon averages ~ 2110 m/s (Table 2.2).

The Sipaliwini surface displays the first evidence of a paleo shelf break (Figure 3.7). The north-eastern section of the paleo shelf was incised by a large channel to depths ranging from ~ 370 ms to 460 ms TWTT (~ 400 to 490 m) oriented in a north-northeast orientation with a flat floor (Figures 3.3a and 3.7b). In the mid slope region, the channel diminishes, confined by a ~ 100 ms TWTT (~ 110 m) high escarpment that trends directly north (Figure 3.3b). In the lower slope region, a large ~ 10 km by ~ 25 km geomorphologic low occupies the north-eastern region of the dataset. This low is bounded by escarpment edges ranging from ~ 140 to 240 ms TWTT (~ 150 to 250 m) high to the south and west and by a structural high to the north abutting the escarpment to the west, separated by a small geomorphologic low to a depth of ~ 90 ms TWTT (~ 100 m) (Figure 3.7a). The low spans ~ 20 km in length from the southern extent to the base of the structural high. It is ~ 10 km in width within the extent of the dataset and displays a rugose morphology at its base. A similar geomorphologic low spans the extent of the dataset north of the structural high in the lower slope (Figure 3.3c).

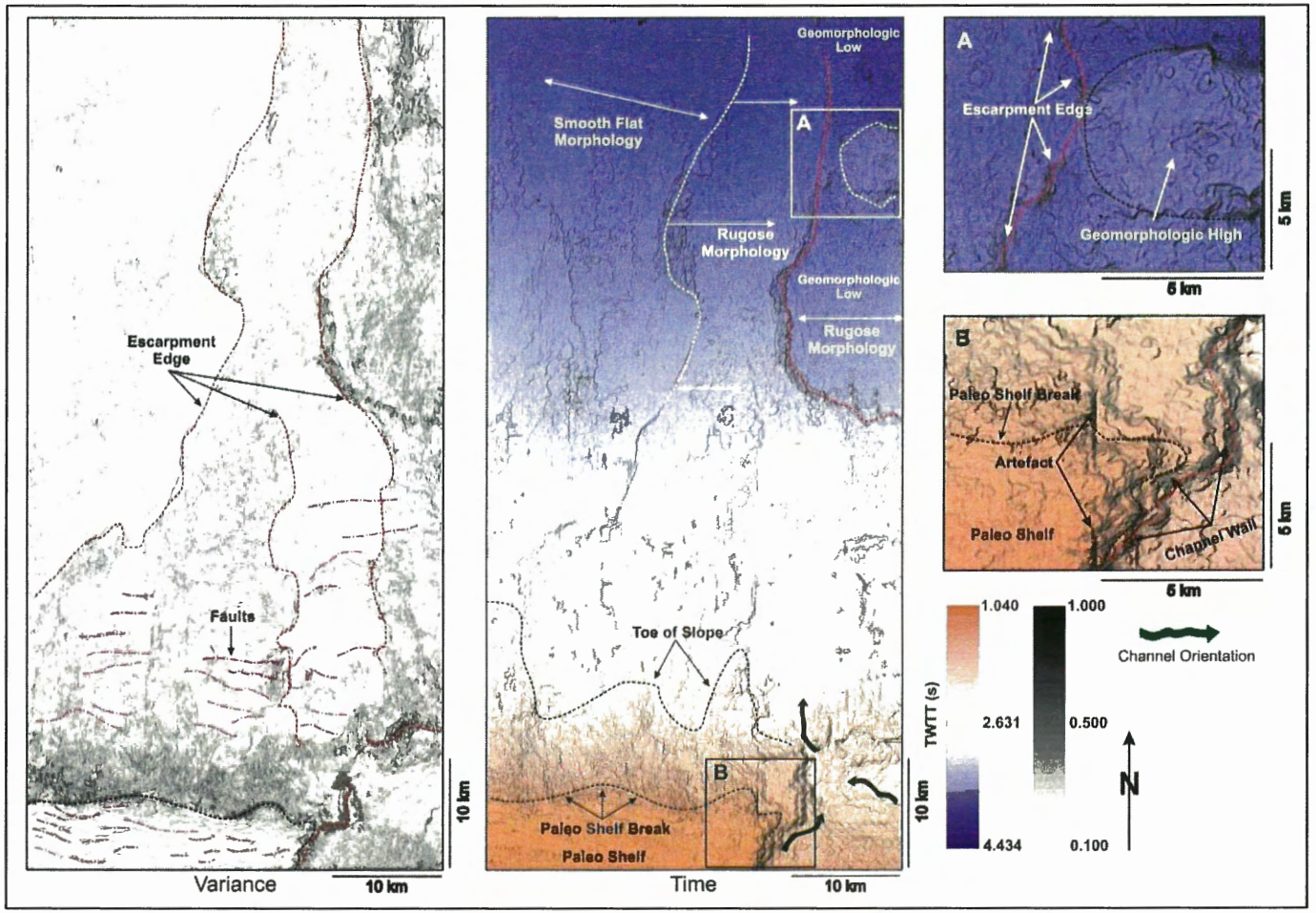

Figure 3.7 Isochron map of reflection Sipaliwini indicates the first evidence of a paleo shelf break incised by a large north northwest oriented channel in the south-eastern region of the dataset. A) Steep escarpments bound a bathymetric low and a large structural high in the northeast region of the lower slope, B) steep channel walls are identified incising the shelf. A variance attribute map (far left) of the same surface enhances features of the time domain image.

The **Para** reflection is a moderate to low amplitude negative trough under the modern shelf and upper slope region of the dataset capped by the overlying Marowijne reflection in the upper paleo slope region (Figures 3.2 to 3.4). Correlation is straight forward except under the shelf-to slope transition zone where reflection geometries become complex; a result of diffraction noise at the modern shelf to slope inflection point. Average interval velocity of the Para reflection is ~ 2015 m/s (Table 2.2).

In the southern extent of the dataset, the paleo shelf break spans the entire region with no channel or gully incisions (Figure 3.8). The paleo shelf is generally expressionless except for shelf margin parallel faults creating minor, ~ 10 ms TWTT (~ 10 m) offsets, varying in length from ~ 2.0 to 32.0 km (Figure 3.8). The upper paleo slope in this region is dipping at ~ 4.5° to the mid-slope where angles diminish < 1°. In the mid-slope, minor gullies oriented north-northeast were identified with 50 ms TWTT (~ 50 m) high walls and flat-bottom floors (Figure 3.8a) along with a large 7 km by 6 km geomorphologic high ~ 50 ms TWTT high (~ 50 m) and minor escarpments. The remaining upper slope region depicts a rugose morphology, becoming more pronounced in the north-eastern region of the surface before it becomes truncated by Marowijne.

.

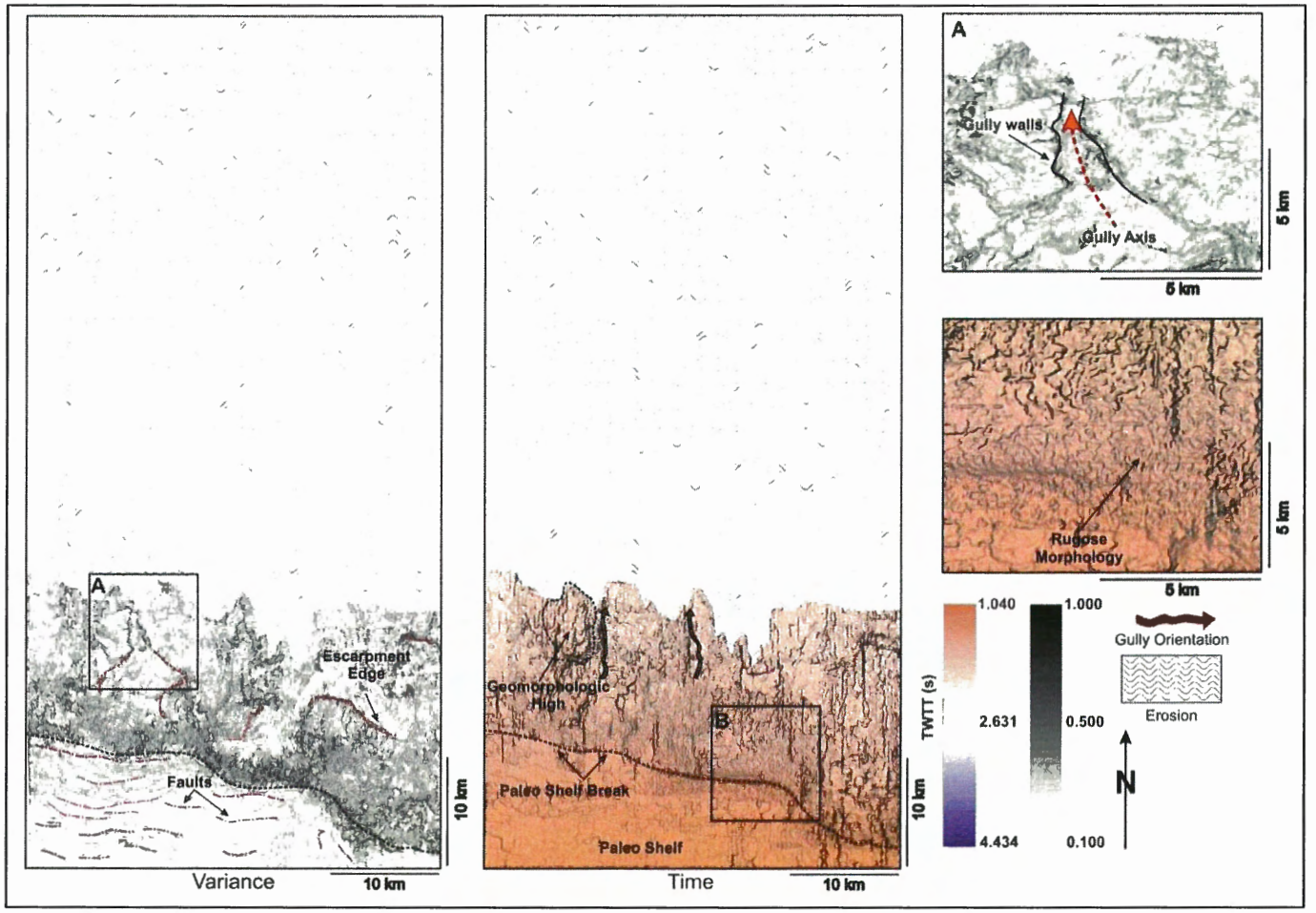

Figure 3.8 Isochron map of reflection Para. Several north-northeast trending gullies are identified below the shelf break. A) Minor gully oriented north northwest, bounded by a geomorphologic high to the west, B) rugose morphology identified below the paleo-shelf break. A variance attribute map (far left) of the same surface enhances features of the time domain image, note the abundance of faults in the paleo-shelf.

The **Marowijne** reflection is a moderate to high amplitude negative trough (Figures 3.2 to 3.4). Under the modern shelf break the reflection is high amplitude. Amplitude strength diminishes downdip under the modern shelf-to-slope inflection point. Reflection amplitude increases in the lower-slope region of the data set. Although the reflection is moderately variable in amplitude, correlation is straight forward. The average interval velocity of the surface is 1920 m/s (Table 2.2).

The paleo shelf and shelf break are easily identifiable on the Marowijne surface in the southern region of the dataset (Figure 3.9). The shelf surface is expressionless, with minor evidence of shallow, margin parallel faulting. The shelf to slope transition is gentle in the western region of the dataset at ~ 3.5° transitioning to ~ 5.0° in the eastern extent of the dataset. In its mid-slope region, slope angles reduce to < 2.0°, exhibiting a rugose morphology with a series of gullies oriented north northwest. A large ~ 6 km by ~ 5 km structural dome in the eastern region of the dataset is apparent (Figure 3.9a). Transitioning to the lower slope region, a gully is identified oriented north-northwest. The gully is shallow, bounded by ~ 20 to 30 ms TWTT (~ 19 to 29 m) high walls to the east and west (Figure 3.9b). This gully extends over ~ 45 km past the extent of the lower slope region in the dataset.

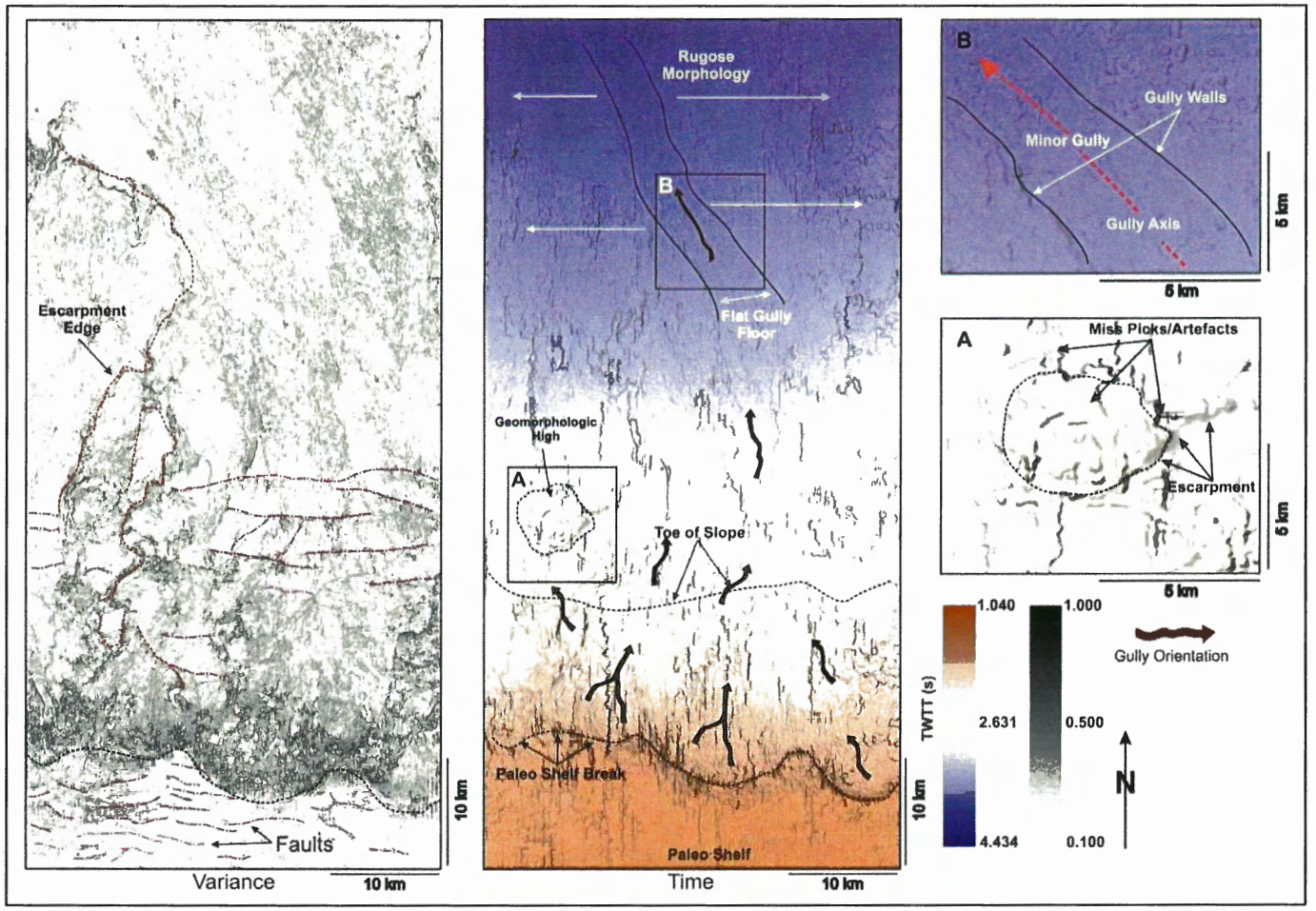

Figure 3.9 Isochron map of reflection Marowijne. A broad shelf spans the entire southern region of the dataset. Several north-northeast oriented gullies were identified in the mid-slope region that coalesce downslope. A) Large dome structure identified in the mid-slope region, B) minor gully with a flat floor, surrounded by a rugose morphology and smooth gully walls. A variance attribute map (far left) of the same surface, enhances features of the time domain image.

The **Saramacca** reflection is a distinctive high amplitude negative trough that is moderately continuous across the dataset, except where it is disrupted by chaotic reflections in its shelf-to-slope transition zone (Figures 3.2 to 3.4). The reflection is of high amplitude in nature under the modern shelf and seaward regions, and variable within the poorly imaged zone under the present shelf break. The reflection event is strongly coherent throughout much of the data, thus correlation was completed with minimal difficulty. The interval velocity of this horizon averages ~ 1840 m/s (Table 2.2).

The Saramacca surface relatively featureless (Figure 3.10). The shelf region is broad with minor fault offsets ~ 10 ms TWTT (~ 9 m) in the southern-most portion of the dataset. Faults span ~ 20 km from the southern extent in the western region of the data; to nearly ~ 12 km in the easterly direction (Figure 3.10). The paleo shelf break indicates a smooth transition to the lower slope region at ~ 4° to the mid-lower slope regions where slope angles diminish to < 2° (Figure 3.10). The mid-slope region indicates several circular pockmarks in a cluster surrounded by a series of radial fault vs, and a highly rugose morphology in the distal extent of the dataset (Figure 3.10a).

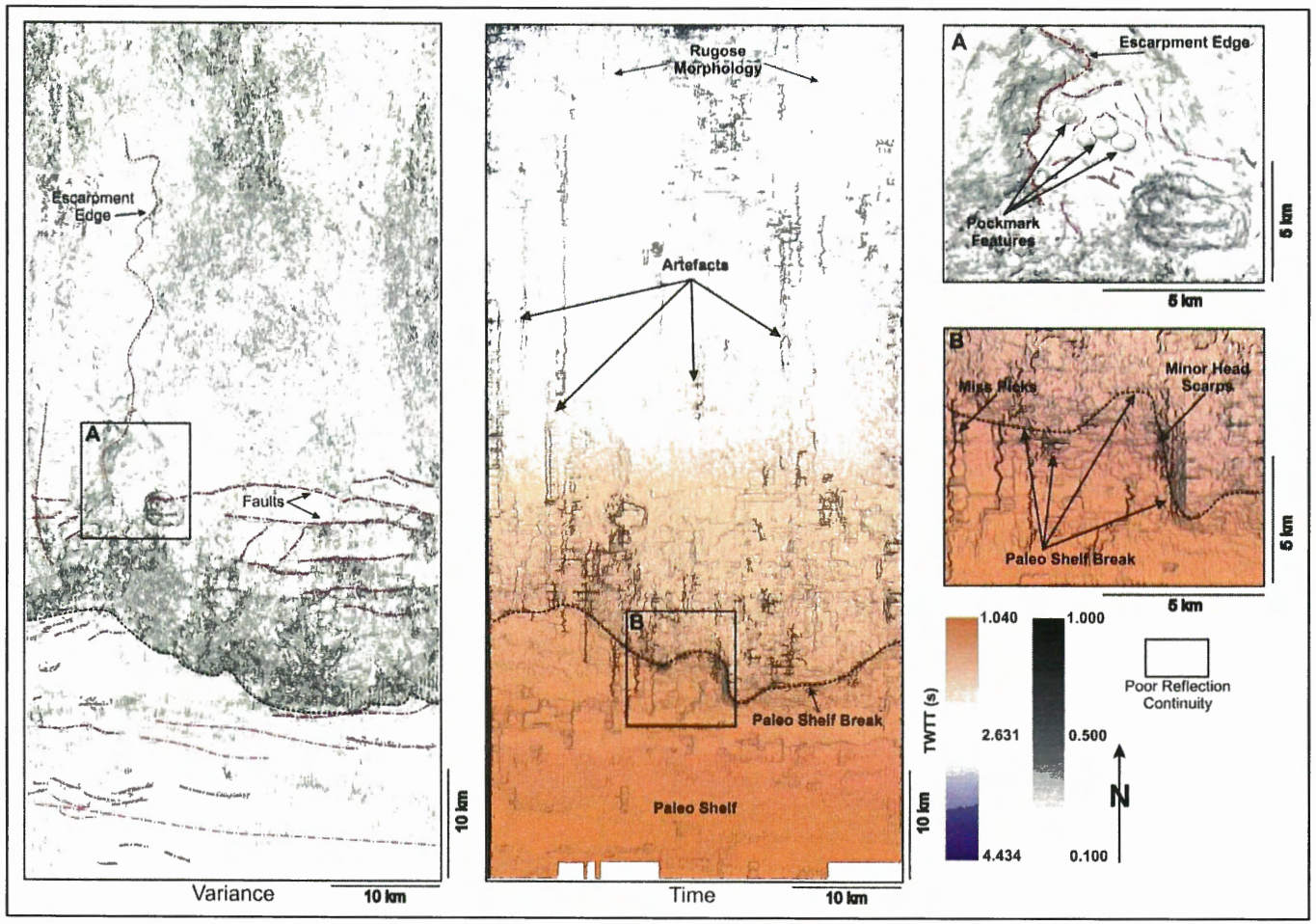

Figure 3.10 Isochron map of reflection Saramacca demonstrating a broad expressionless shelf with minor fault offsets. A) Smooth shelf-to-slope transition with smooth scalloped morphology, B) small cluster of pockmarks interpreted as gas escape features. A variance attribute map (far left) of the same surface enhances features of the time domain image.

The first arrival, seismic reflection **Commewijne**, represents the seafloor (Figure 3.11). Correlation of this surface was completed with great certainty. In the southern-most region, the reflection is discontinuous and of poor data quality, but transitioning the shelf-to-slope inflection point the reflection becomes high amplitude and continuous (Figures 3.3a and 3.11). Water velocity is assumed to be ~ 1480 m/s, permitting travel time to depth conversion (Table 2.2).

The modern seafloor displays a relatively featureless geomorphology. The shelf is rugose due to poor data quality in this region. Although noise is apparent in the shelf region, shelf margin parallel faults are easily recognized (Figure 3.11a). These faults range in lengths from ~ 5 km to ~ 40 km with offsets reaching ~ 20 ms TWTT (~ 15 m). At the shelf-to-slope transition zone, minor gullies are recognized, oriented in a northerly direction. These gullies extend for ~ 3.5 km to ~ 5 km downslope (Figure 3.11b). In general seafloor slope angles are < 2° and diminish in the lower slope region. A moderately rugose morphology extends from the mid-lower slope region, with evidence of minor buried scarps in the immediate subsurface.

3.3 Seismic Sequence Distribution within the RepsolYPF Block30

The distribution and thickness of seismic sequences is highly variable, and changes along strike and dip within the Block30 seismic survey (Figures 3.12 - 3.15). The five main sequences are described sequentially from oldest (deepest) to youngest (shallowest) below.

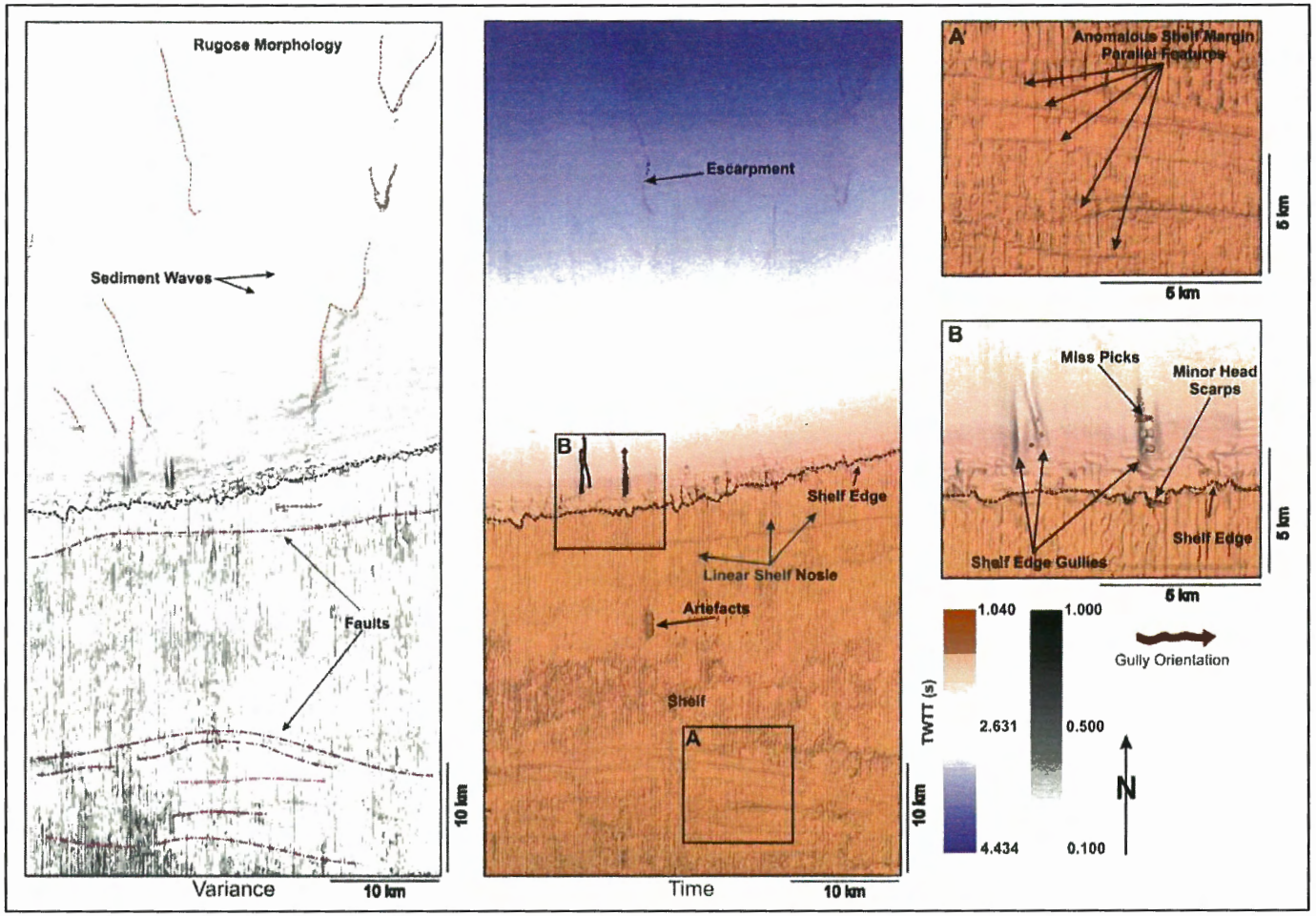

Figure 3.11 Isochron map of reflection Commewijne representing the modern seafloor. A rugose morphology dominates the shelf region transitioning to an expressionless slope with minor escarpments. A) Shelf margin parallel faults display anomalous features on the seabed, B) small shelf edge gullies with smooth walls incise a scalloped shelf edge. A variance attribute map (far left) of the same surface, enhances features of the time domain image.

The deepest of the seismic sequences, the **Wanica Sequence**, comprises the interval between sequence boundaries Wanica to Nickerie. Thickness of the sequence ranges from 124 to 1299 m, based on interval velocities shown in (Table 2.2) with the greatest thickness in the southernmost region of the dataset (Figure 3.16). The eastern region of the lower slope indicates a typical thickness range between ~ 400 to 700 m, with the thickest section located in the most northern portion of the dataset (Figure 3.15a). The western half exhibits a much shallower interval where thicknesses range from ~ 124 to 400 m (Figure 3.15c).

The southernmost (landward) section of the Wanica Sequence consists of moderate to high amplitude, continuous, parallel and sub-parallel, gently dipping reflections (Facies 1 and 5, Figure 3.1) up to the base of the Nickerie Sequence Boundary (Figures 3.12 to 3.14). Reflections are noted onlapping the Wanica Sequence Boundary, stacking to form a condensed package prior to being truncated by the overlying Nickerie Sequence Boundary. Reflections become moderate to low amplitude, chaotic and fairly incoherent down dip in the mid-slope with little internal structure (Facies 2 and 6, Figure 3.1). These reflections continue to the northernmost (seaward) extent of the dataset before becoming high amplitude continuous reflections in the eastern and central regions of the dataset.

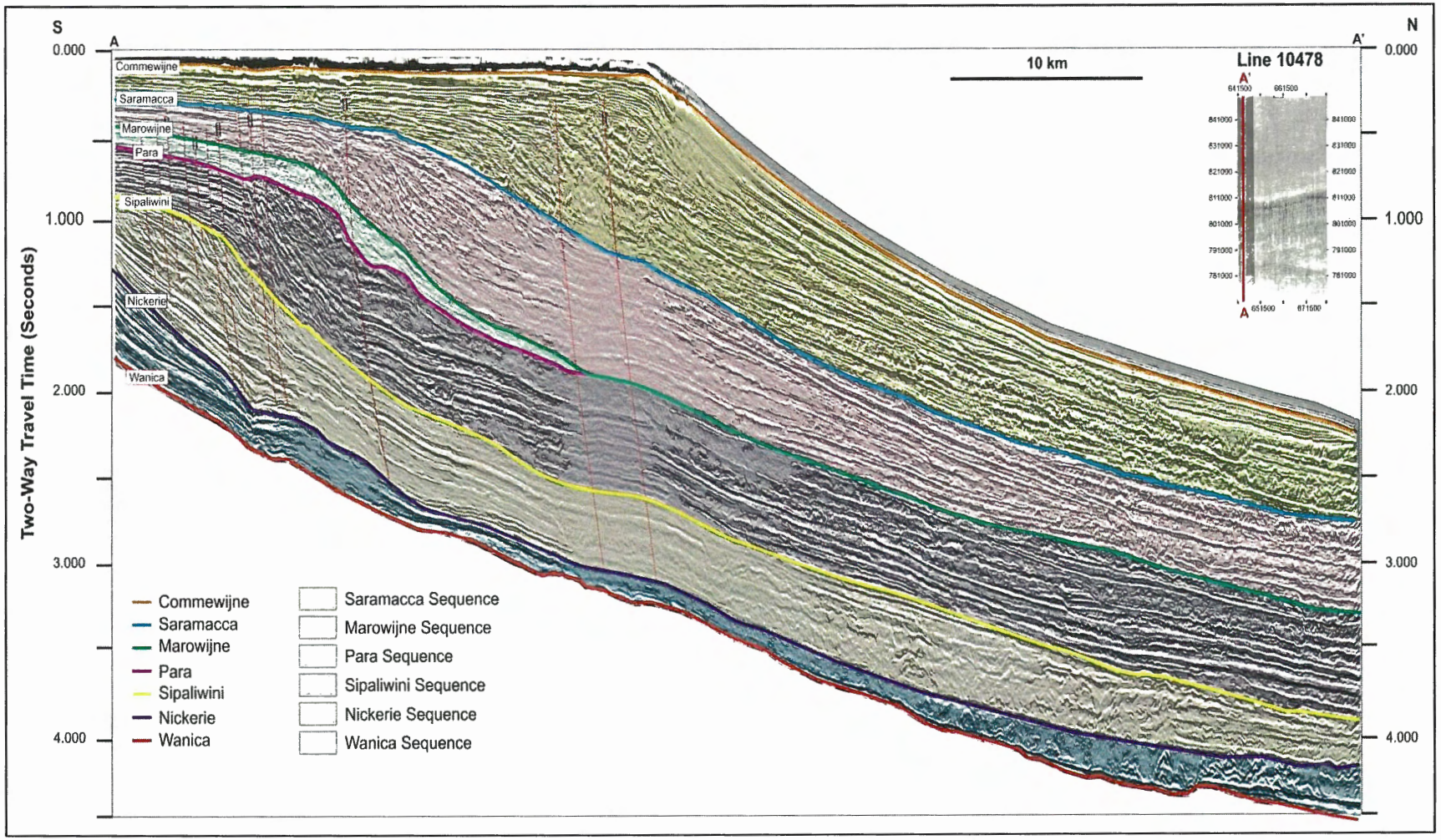

Figure 3.12 Interpretation of seismic reflections and associated sequences displayed on dip-profile 10478 from the western extent of the Block30 dataset. Note thicknesses are not distributed evenly across the profile.

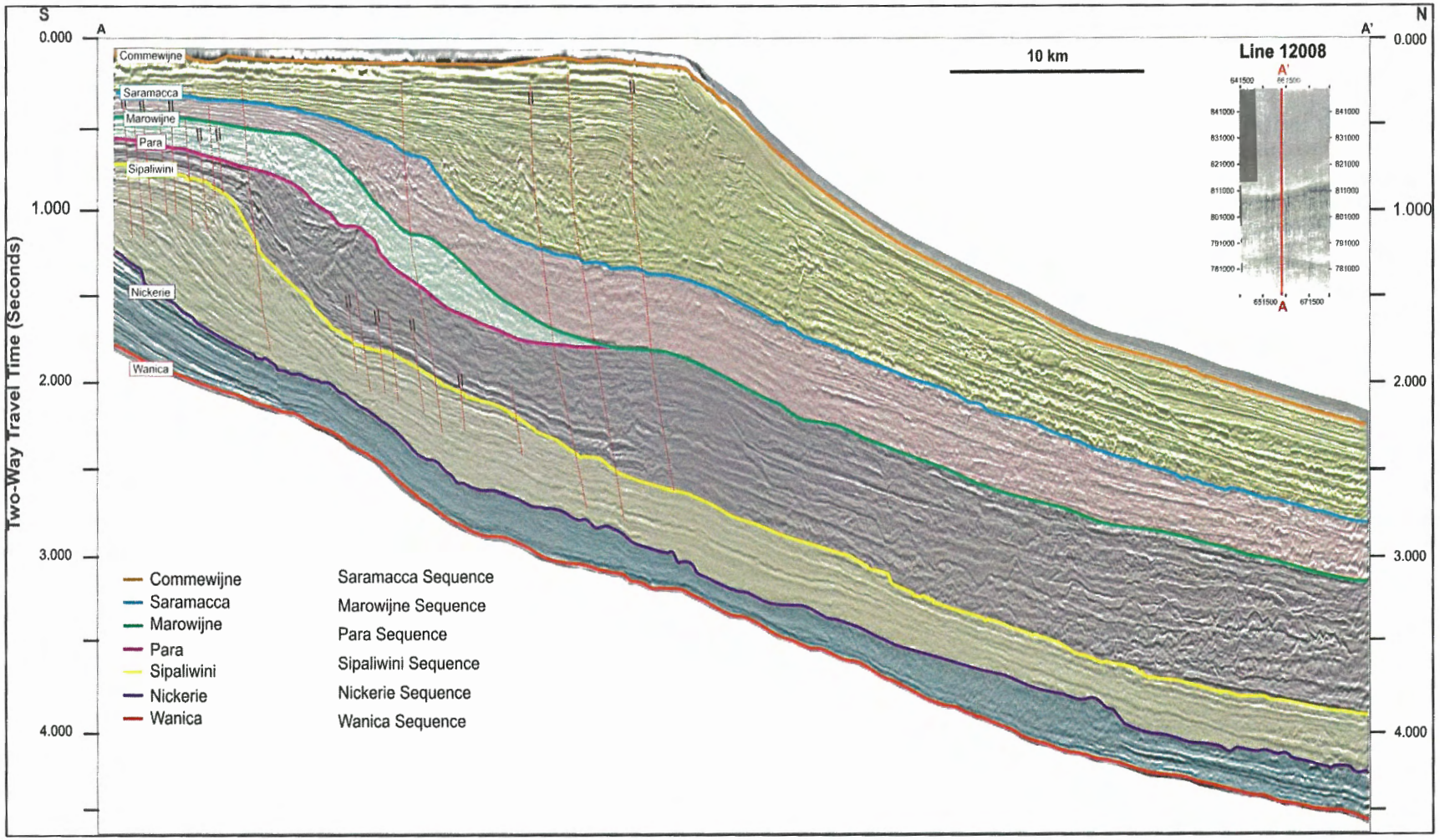

Figure 3.13 Interpretation of seismic reflections and associated sequences displayed on dip-profile 12008 from the centre of the Block30 dataset. Note thicknesses are not distributed evenly across the profile.

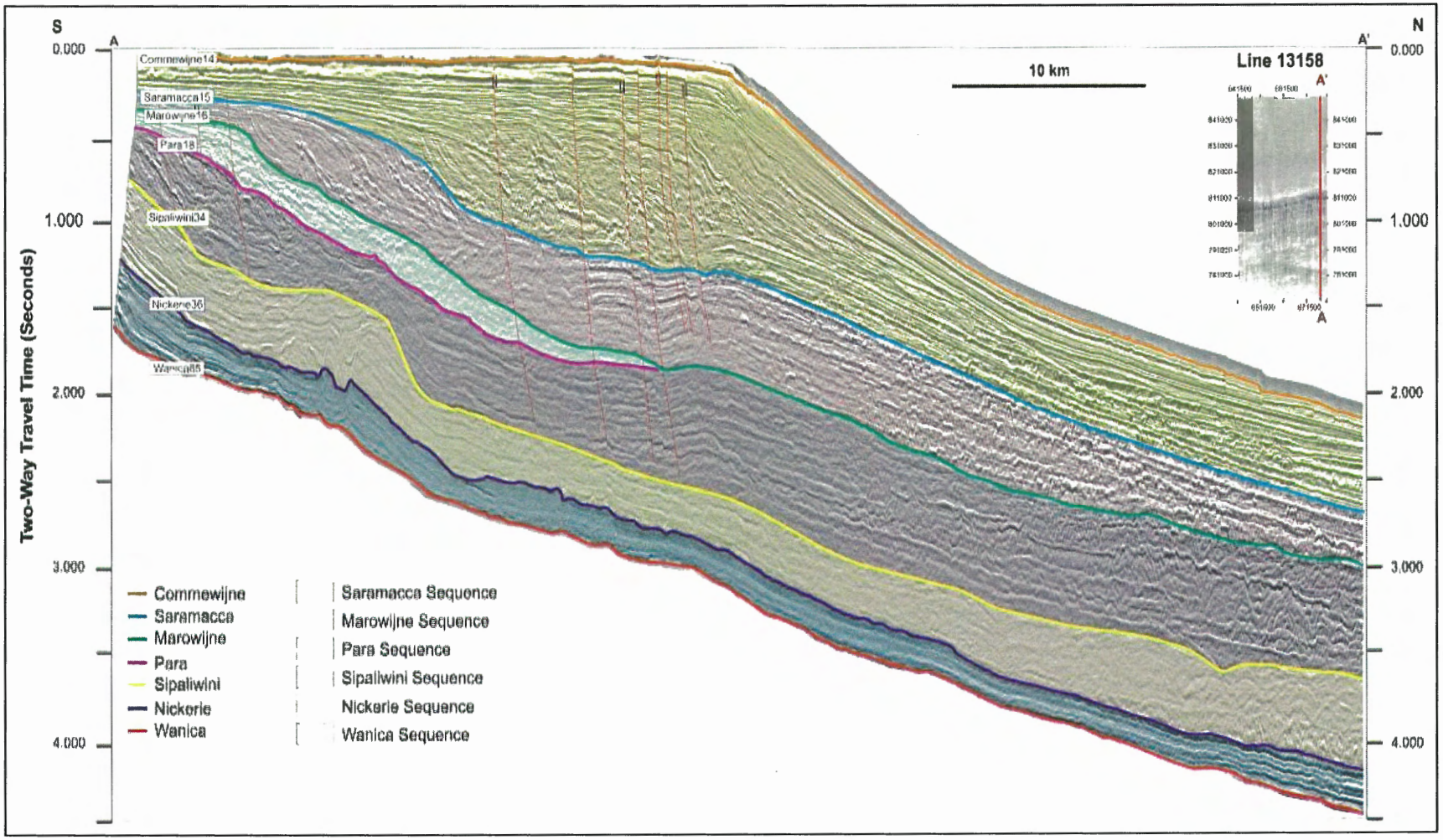

Figure 3.14 Interpretation of seismic reflections and associated sequences displayed on dip-profile 13158 from the eastern extent of the Block30 dataset. Note thicknesses are not distributed evenly across the profile.

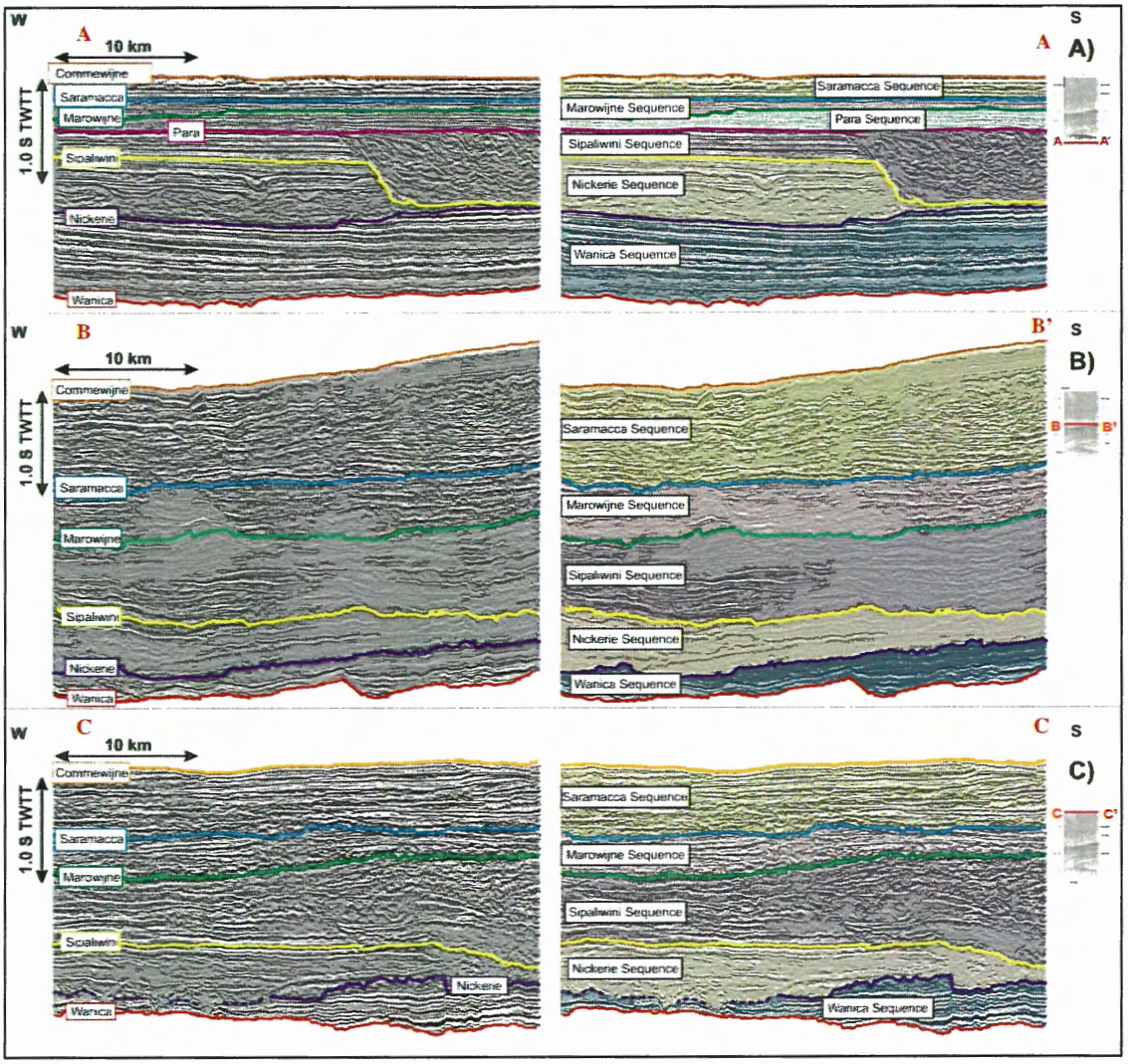

Figure 3.15 Interpretation of seismic reflections and associated sequences. A) Strike profile 5266 located across the southern shelf region of the dataset, B) strike profile 8148 located at the present day shelf break location, and C) strike profile 11032 located across the northern lower slope region of the Block30 dataset.

Reflections in the western extent of the dataset are high amplitude and chaotic to the limit of which correlation from the overlying Nickerie Sequence Boundary was possible (Figure 3.15c).

The deepest of the seismic sequences, the **Wanica Sequence**, comprises the interval between sequence boundaries Wanica to Nickerie. Thickness of the sequence ranges from 124 - 1299 m (assuming an average interval velocity of 3076 m/s), with the greatest thickness in the southernmost region of the dataset (Figure 3.16). The eastern region of the lower slope indicates a typical thickness range between ~ 400 - 700 m, with the thickest section located in the most northern portion of the dataset (Figure 3.15a). The western half exhibits a much shallower interval where thicknesses range from ~ 124 - 400 m (Figure 3.15c).

The southernmost (landward) section of the Wanica Sequence consists of moderate to high amplitude, continuous, parallel and sub-parallel, gently dipping reflections up to the base of the Nickerie sequence boundary (Figures 3.12 - 3.14). Reflections are noted onlapping the Wanica sequence boundary, stacking to form a condensed package prior to being truncated by the overlying Nickerie sequence boundary. Reflections become moderate to low amplitude, chaotic and fairly incoherent down dip in the mid-slope with little internal structure. These reflections continue to the northernmost (seaward) extent of the dataset before becoming high amplitude continuous reflections in the eastern and central regions of the dataset. Reflections in the western extent of the dataset are high amplitude and chaotic to the limit of which correlation from the overlying Nickerie sequence boundary was possible (Figure 3.15c).

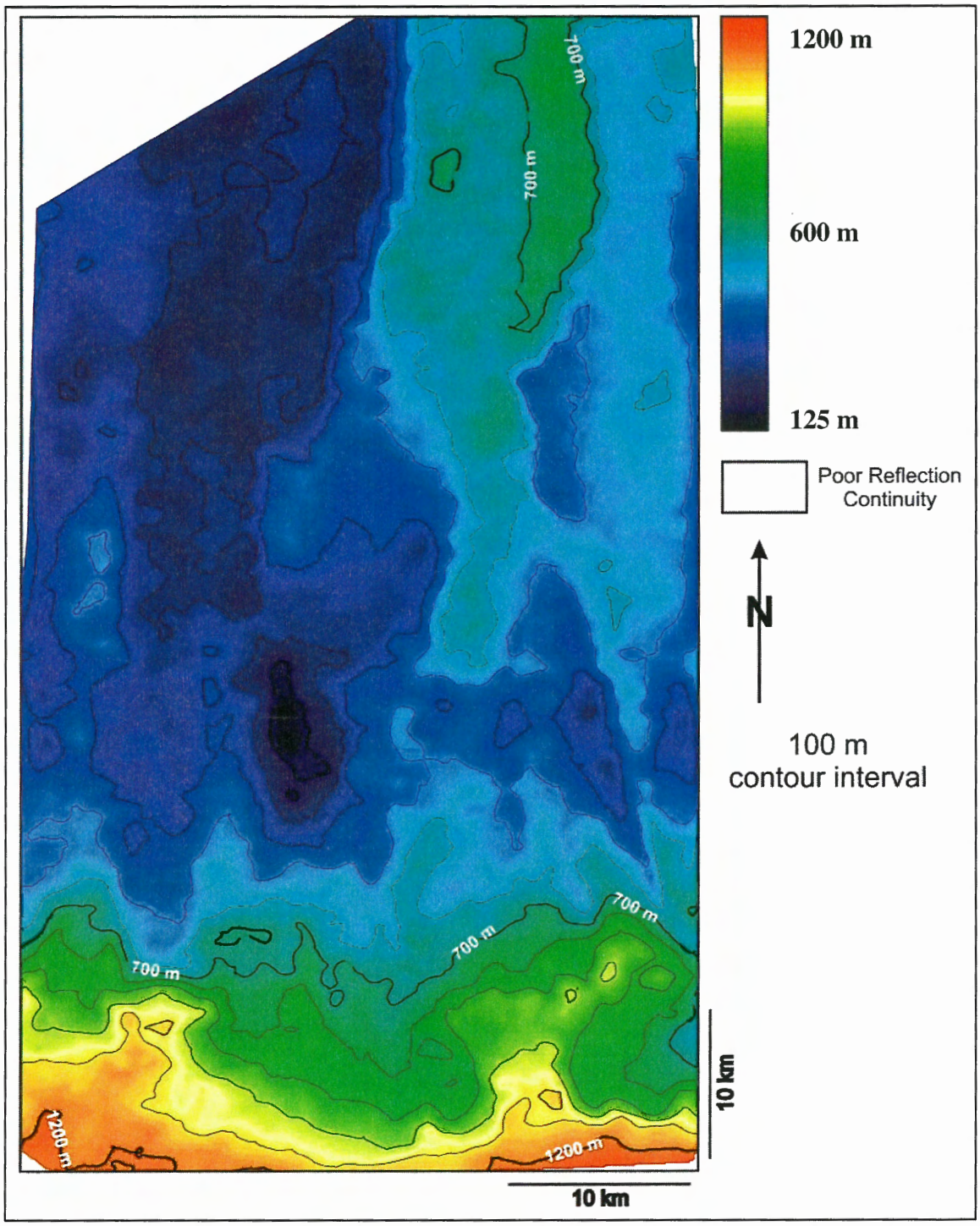

Figure 3.16 Isopach map indicating the true stratigraphic thickness and distribution of the Wanica Sequence. Sequence thickness is unavailable in the north western region of the dataset where the reflections could not be reliably correlated.

The **Nickerie Sequence** thickness cannot be quantified in the north western region of the dataset due to lack of reflection continuity of the Nickerie reflection horizon. Elsewhere, thickness of this interval varies from ~ 22 to 916 m thick (Table 2.2) (Figure 3.17). The greatest thickness (> 600 m) is located under the modern shelf. This thickness is greatly reduced to < 300 m where the shelf was incised by a channel (Figure 3.15a). The interval thickness ranges from ~ 22 and 400 m down-dip of the shelf break in the central to eastern extent of the dataset. From the central to western extent of the dataset down-dip of the shelf break, the interval ranges from ~ 400 to 700 m, with the exception of a narrow corridor of ~ 200 to 300 m thick section in the mid-slope region.

Reflections at the base of the Nickerie Sequence are high amplitude, continuous to moderately continuous, and parallel to sub-parallel (Facies 1 and 5, Figure 3.1) under the modern shelf break, except in the south eastern region of the dataset (Figures 3.12 to 3.14). In this area, channel incision removed much of the interval. Reflections under the shelf appear faulted with offsets of ~ 13 m (Table 2.2) where reflections are high amplitude and continuous down-dip to the paleo shelf break. Reflections then begin to split and expand into a clinoform wedge on the outer shelf, capped by a package of onlapping-downlapping reflections that are truncated down-dip by the overlying Sipaliwini Sequence Boundary. Down-dip, these reflections become moderate to low amplitude sub-parallel to chaotic (Facies 2 and 5, Figure 3.1) from the top of the Nickerie Sequence Boundary (Figures 3.12 to 3.14).

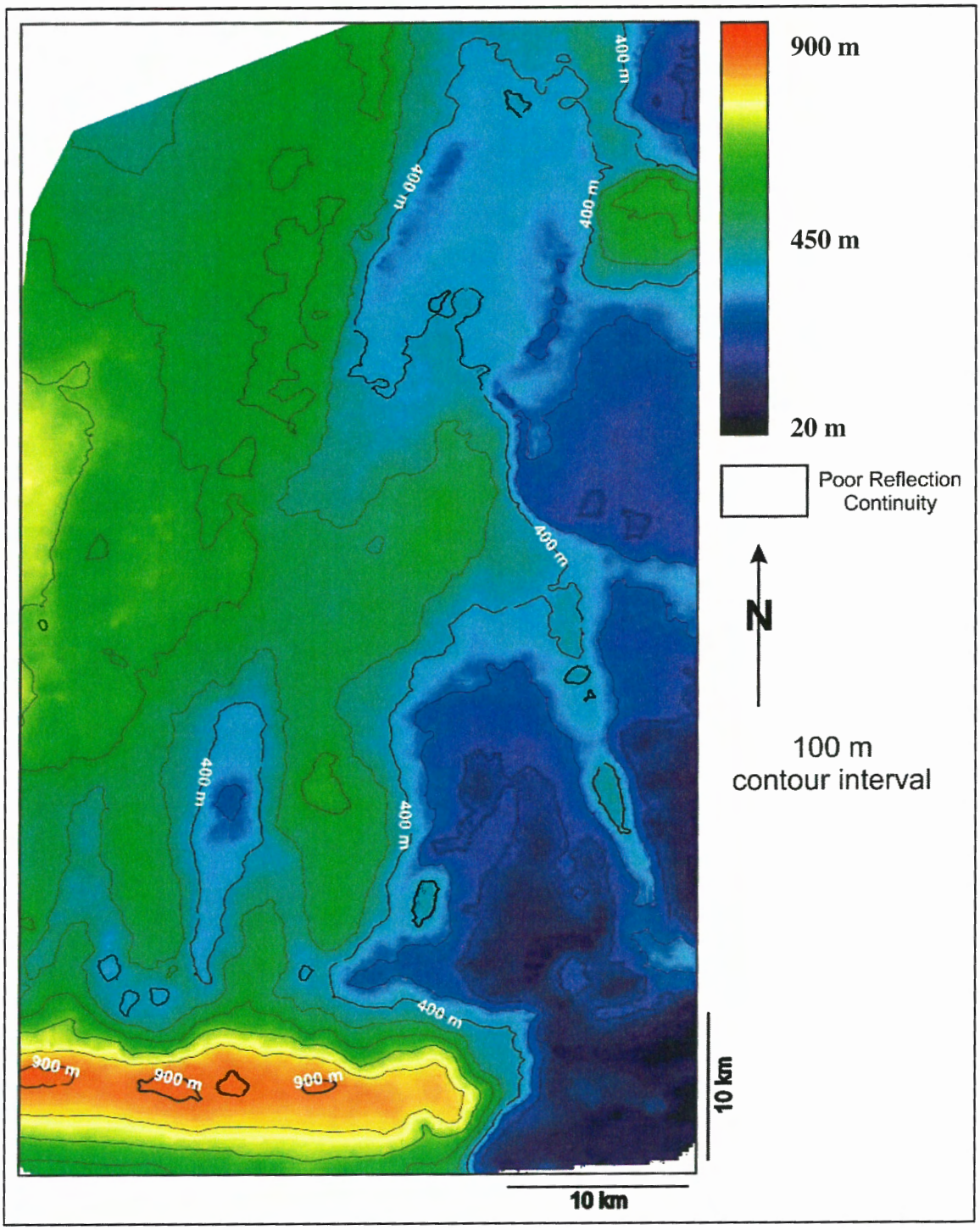

Figure 3.17 Isopach map indicating the true stratigraphic thickness and distribution of the Nickerie Sequence. Sequence thickness is unavailable in the north western region of the dataset where the reflections could not be reliably correlated.

The **Sipaliwini Sequence** comprises the interval from the Sipaliwini to Para Sequence Boundaries, ranging in thickness from 247 to 1368 m (Table 2.2) (Figure 3.18). This interval exhibits a ~ 247 to 600 m thick paleo shelf from the western extent of the data to the position of the incised channel, where thickness increases from ~ 600 to 900 m (Figures 3.15a and 3.18). This thicker section expands to the majority of the mid-slope section down-dip of the paleo-shelf. In the mid-lower slope region, thicknesses range from ~ 600 to 1300 m, with the exception of the north-easternmost section where sediment thickness exceeds 1300 m.

Reflections in the Sipaliwini Sequence are of moderate to high amplitude with variable reflection geometries. Under the modern shelf, reflections are gently dipping and high amplitude, parallel, and continuous in nature (Facies 1, Figure 3.1). They extend out to the paleo shelf-break and up to the Para Sequence Boundary (Figures 3.12 to 3.14). Normal faults are responsible for offsetting reflections in this region from 13 to 226 m (Table 2.2) (Figures 3.6 to 3.7 and 3.12 to 3.14). Reflections at the shelf-to-slope transition zone split and expand into a clinoform package that builds down-dip, becoming aggradational up to the Marowijne Sequence Boundary. In the south-eastern region, the paleo shelf has been incised and high amplitude discontinuous to chaotic reflections (Facies 2 and 6, Figure 3.1) on-lap the western channel wall. These reflections become low to moderate in amplitude down-dip and are sub-parallel to discontinuous (Facies 5 and 6, Figure 3.1). They span the entire mid-lower slope region of the dataset. In this area faults are identified, offsetting reflections from ~ 25 to 33 m (Table 2.2).

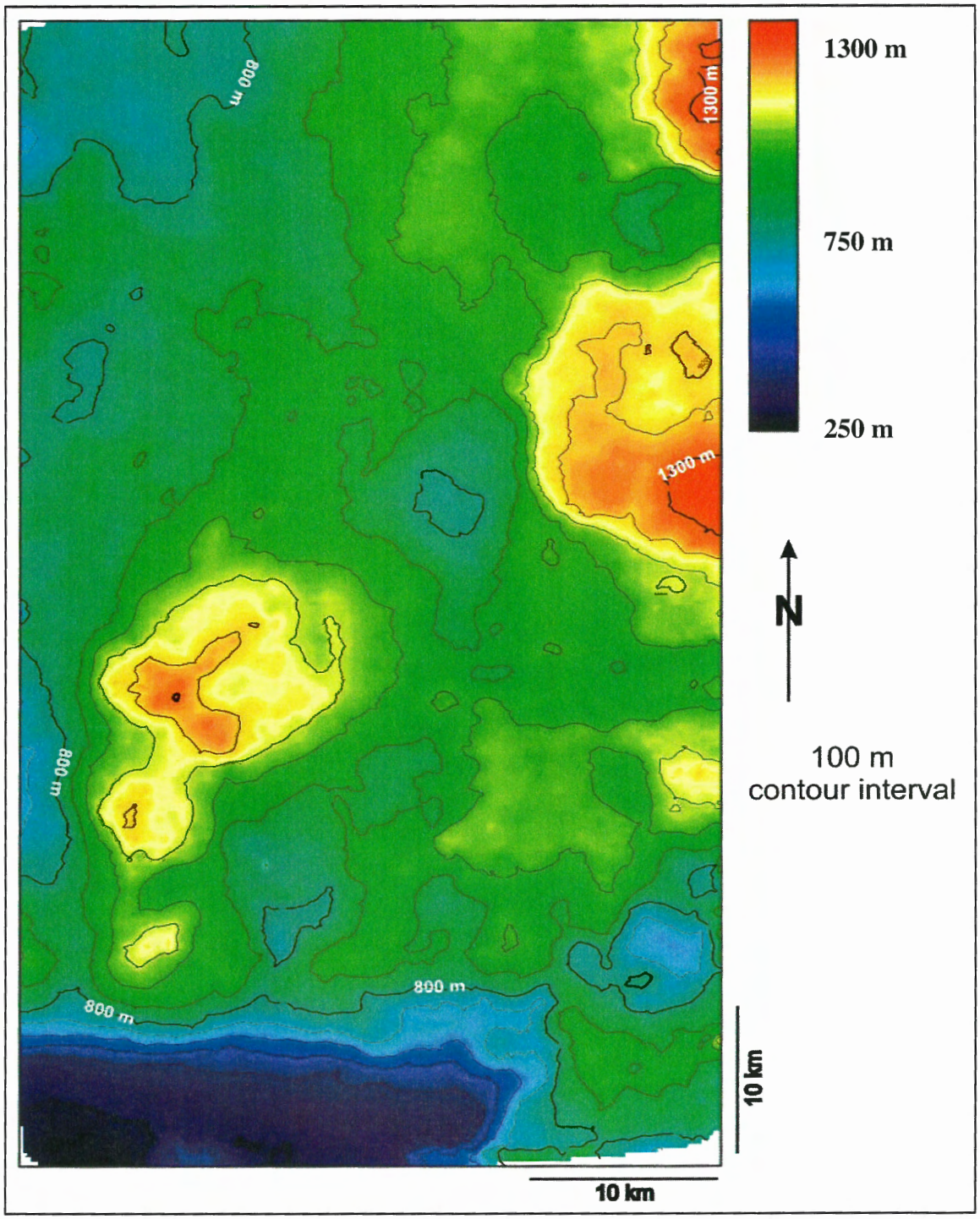

Figure 3.18 Isopach map indicating the true stratigraphic thickness and distribution of the Sipaliwini Sequence.

The **Para Sequence** is much thinner in comparison to underlying sequences. Typical thicknesses range from 0 to 693 m (Table 2.2) (Figure 3.19). The paleo-shelf in this sequence ranges from ~ 0 to 300 m in thickness from east to west. The thickest region in this interval exceeds 600 m in the south-eastern region directly down-dip of the paleo-shelf break, becoming gradually thinner to the west. Down-dip, the interval is absent where it is truncated by the overlying Marowijne Sequence Boundary.

Reflections in the Para Sequence exhibit a moderate to high amplitude package of sub-parallel continuous reflections (Facies 5, Figure 3.1). These reflections span the entire dataset to the east and west, onlapping the Para Sequence Boundary in the middle to upper slope region, up to the Marowijne Sequence Boundary (Figures 3.12 to 3.14). Similar to the underlying sequences normal faults in the upper and middle slope regions offset reflections up to 12 m (Table 2.2) (Figure 3.9).

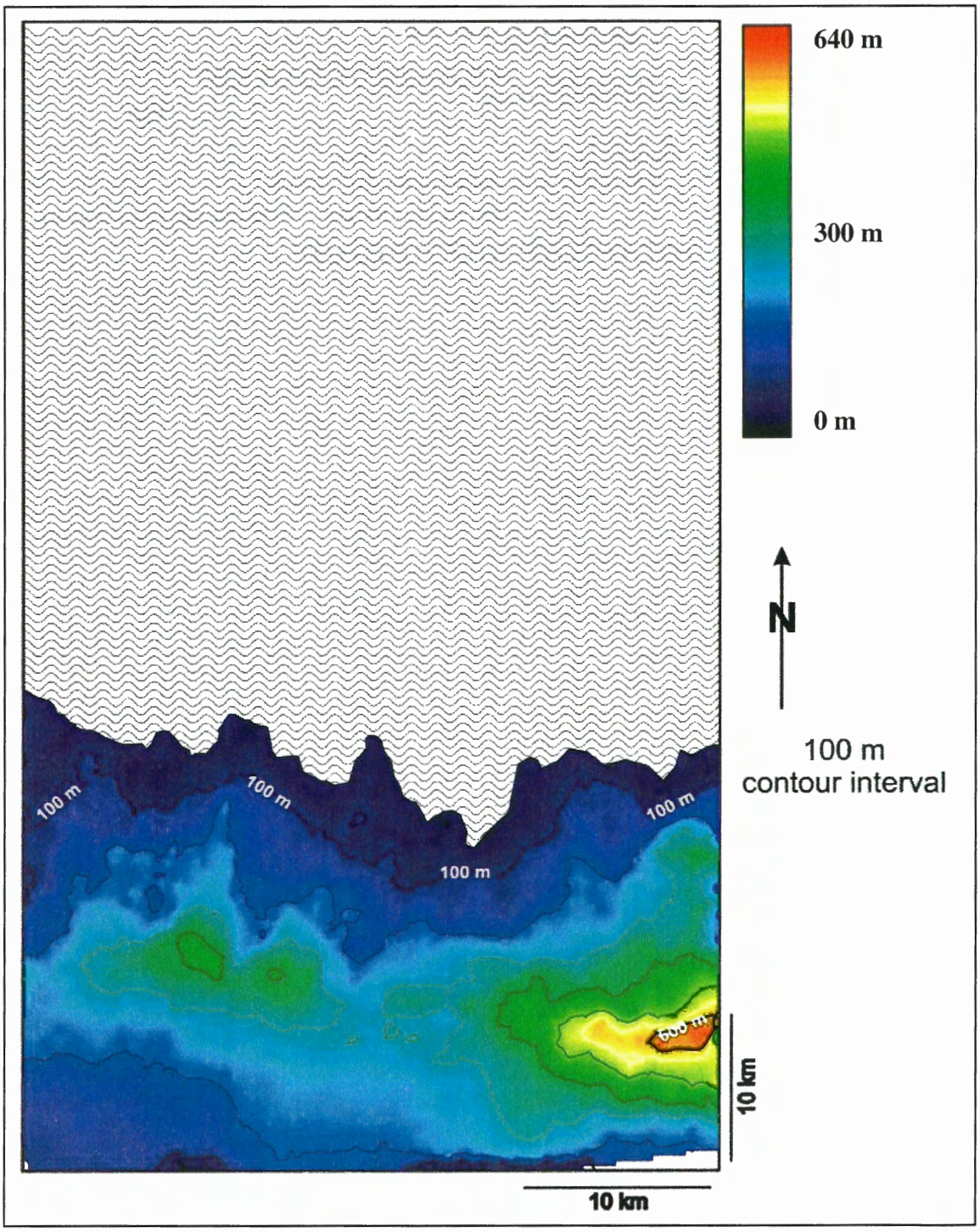

Figure 3.19 Isopach map indicating the true stratigraphic thickness and distribution of the Para Sequence.

The **Marowijne sequence** has thicknesses ranging from ~ 86 to 917 m (Table 2.2) (Figure 3.20). The paleo shelf region has sediment thicknesses on the order of < 350 m, spanning the entire southern region of the dataset. Down-dip of the of the paleo-shelf break, thickness in the mid-slope region generally ranges between ~ 350 m to 650 m, with the exception of a > 850 m region extending ~12 km in dip profile by 5 km in strike extending beyond the extent of the dataset. In the lower slope to the most northern extent of the dataset, thicknesses ranges from ~ 200 to 400 m. The central region increases in thickness, ranging from 350 to 550 m.

Reflections in the Marowijne Sequence are variable; from high amplitude parallel continuous, to low-moderate amplitude discontinuous, sub-parallel to chaotic in nature (Facies 1, 2, and 4, Figure 3.1, 3.12 to 3.14). Under the modern shelf break, reflections are largely parallel and continuous, dipping slightly down-slope. They span the entire dataset east and west. In the position of the paleo-shelf break reflections split into a clinoform wedge, up to the Saramacca Sequence Boundary where these reflections are truncated. Reflections in the upper-mid slope region are offset by normal faults with up to ~ 11 m (Table 2.2) (Figures 3.9 and 3.10). Down-dip, in the mid-lower slope region, the clinoform package of reflections are largely low-moderate amplitude and discontinuous. They mimic the Marowijne reflection. Periodic packages of chaotic reflections ranging from low-high amplitudes (Figures 3.12 to 3.14).

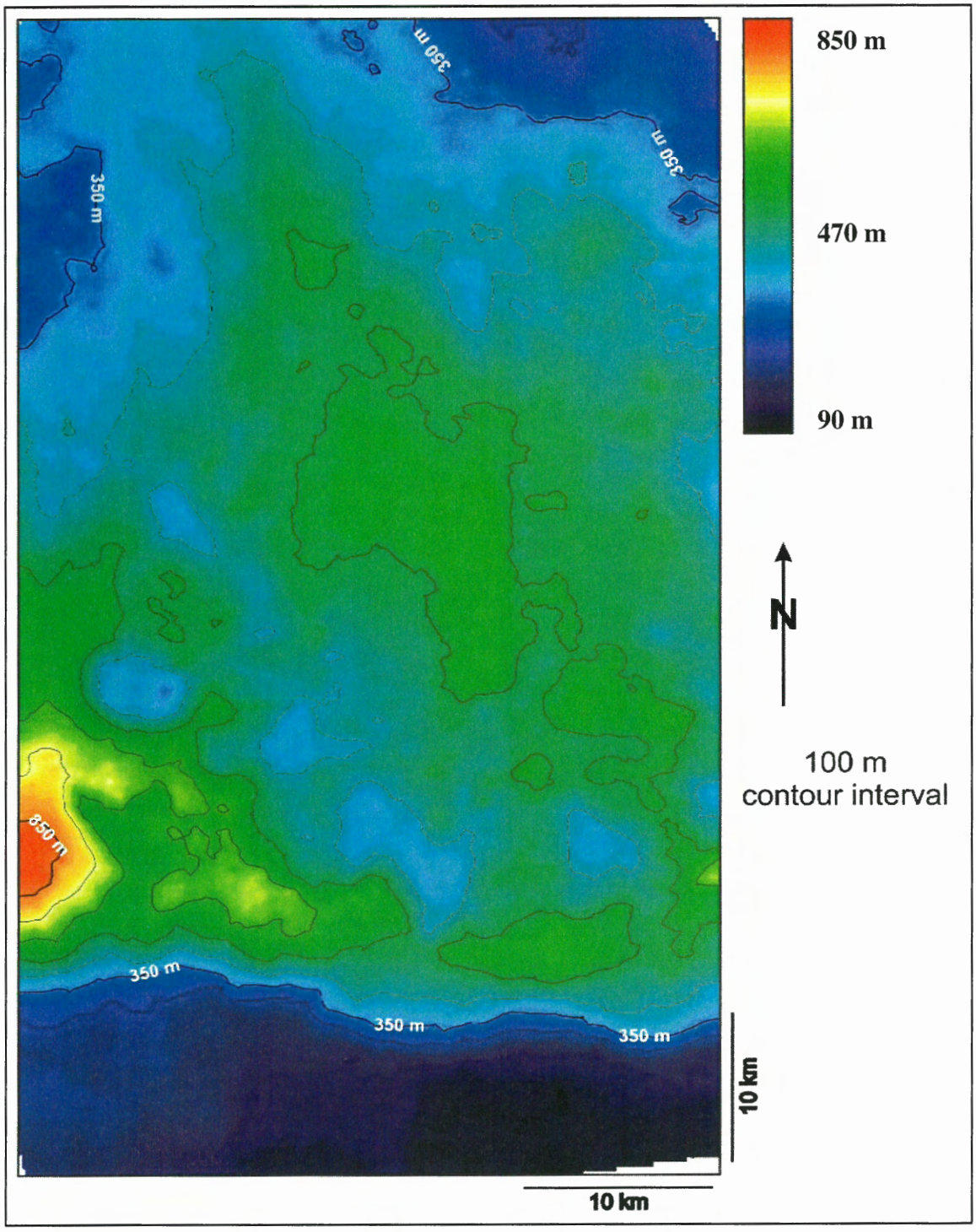

Figure 3.20 Isopach map indicating the true stratigraphic thickness and distribution of the Marowijne Sequence.

The **Saramacca Sequence** ranges in thickness from ~ 158 to 1224 m (Table 2.2). The shelf in this sequence is broad, extending nearly 20 km from the southern limit of the dataset (Figure 3.21). Thickness in the shelf region gradually increases from ~ 158 to 650 m where the modern shelf break is located. Down-dip of the shelf break, a narrow ~ 10 km east-west trending band ranges in thickness from ~ 650 to 1050 m, before increasing from ~ 800 m to 1150 m. The thickest region extends from the eastern limit of the dataset nearly 25 km by 15 km down-dip (Figure 3.15b). The remainder of the mid-lower slope is characterized by a gradual thinning of the sequence from ~ 400 to 1050 m towards the northern limit of the dataset.

Reflections in the Saramacca Sequence exhibit similar characteristics as the underlying Marowijne Sequence. In general, above the Saramacca Sequence Boundary, reflections are of high amplitude and continuous (Facies 1, Figure 3.1, 3.12 to 3.14). These reflections split in the position of the paleo shelf break into prograding clinoform packages that become high amplitude sub-parallel to parallel continuous reflections (Facies 5, Figure 3.1) in the mid-lower slope region. The paleo shelf-break in this sequence shifted basinward nearly 20 km, as identified by inflection points though the sequence. Reflections are continuously offset by ~ 10 m (Table 2.2) normal faults spanning from the southern extent of the dataset to the modern shelf break (Figures 3.10 and 3.11). Reflection geometries under the modern shelf in the middle of this sequence generally shift from a largely progradational stacking pattern to an aggradational stacking pattern.

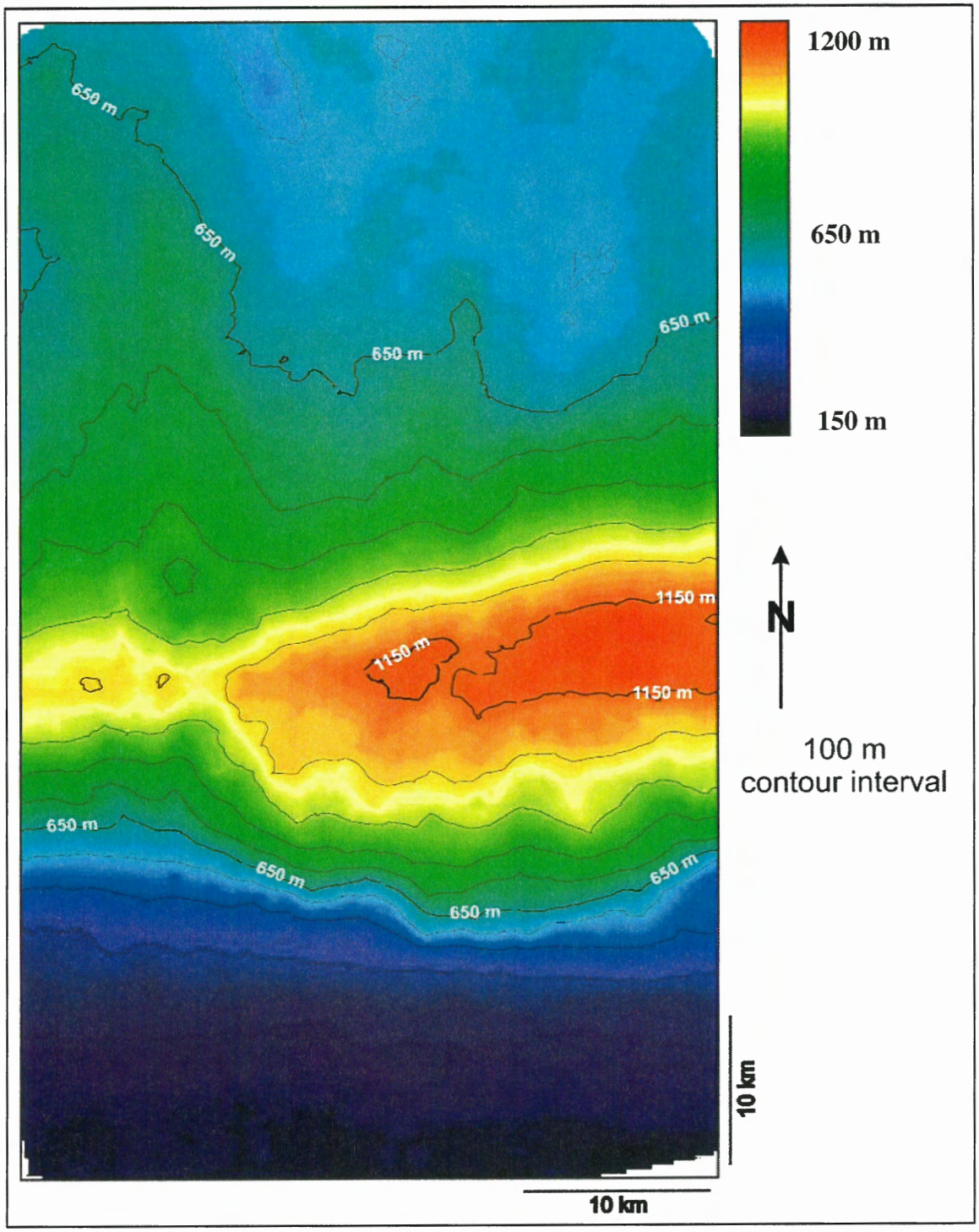

Figure 3.21 Isopach map indicating the true stratigraphic thickness and distribution of the Saramacca Sequence.

3.4 Seismic to Well Correlation

Well data, including available age control, were correlated to seismic profiles with synthetic seismograms (Figure 3.22). Modeling allows extension of well data to a regional scale with seismic profiles. Well to seismic correlations are available in the RepsolYPF Block30 using the North Coronie-1 (NCO-1) well and are extended to the outer Demerara Rise to ODP Leg 207 scientific well 1257 using RepsolYPF regional line W99-109 and Shell line C2206. Correlating reflections from the Suriname continental shelf, through the slope and across the Demerara Rise is difficult because of incoherent reflection geometries at the shelf to slope transition zones.

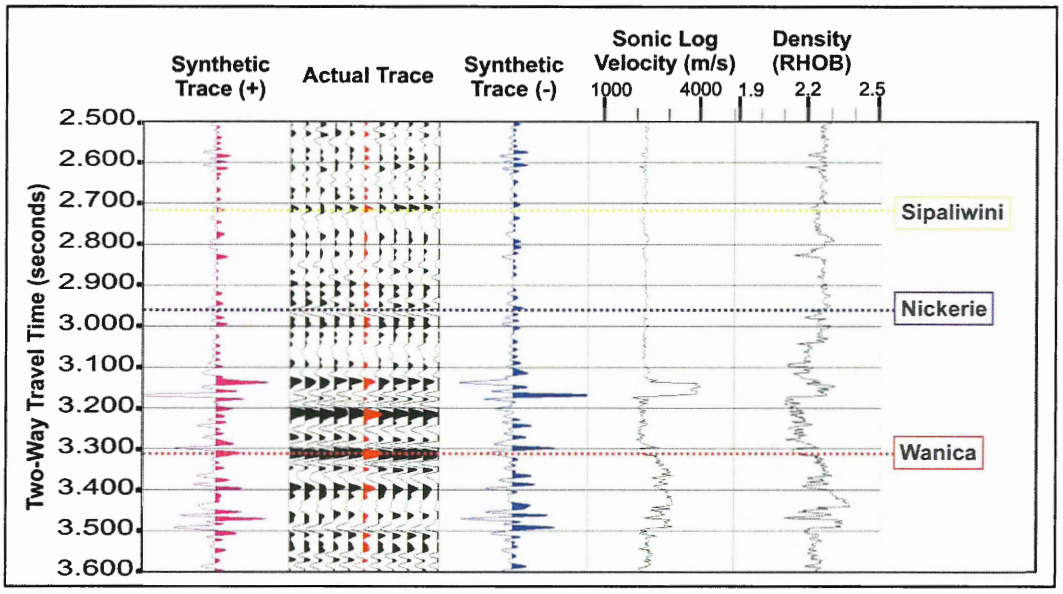

Figure 3.22 Synthetic seismograms for NCO-1 well calculated from sonic and density logs. The pink and blue single traces indicate the resultant synthetic + and – traces, with the actual seismic response at the well highlighted red.

3.4.1 North Coronie-1

The NCO-1 well is located on the Suriname continental shelf, ~ 1 km south of the modern shelf break. It is within the Block30 volume, 3.8 km west of its eastern edge (Figure 1.8).

In general, two main formations define the Cenozoic interval in the NCO-1 well; (1) 3185 to 3995 m (MD) consists of indurated calcareous claystones alternating with chalky limestones. (2) 412 to 3185 m (MD) essentially consists of silty plastic clays with rare components of lignite, pyrite and organic remains. Based on biostratigraphic data, several unconformities are apparent in the NCO-1 well (Staatsolie, 1976). Oligocene strata are noticeably absent and represent an unconformity at ~ 3400 m (measured depth below Kelly Bushing (MD)). At ~ 3185 m (MD) a sudden sedimentological and lithological break, correlative to a strong reflection is representative of an Early Miocene eroded section. Existence of stratal deformation and Eocene fauna immediately above the 3185 m break reinforces the interpretation of this sedimentary discontinuity. In the Late Miocene to Late Pliocene 450 to 1700 m (MD) lithologic data suggest several unconformities.

Six of the seven correlated reflections discussed earlier (excluding Para) correlate with confidence to the NCO-1 well. The Wanica Sequence Boundary falls within the early Oligocene age sediments which range in depth from 3728 m to 3400 m (MD). The overlying interval from 3400 m to 3185 m (MD) is defined by a regional unconformity at 3185 m (MD) with absent strata, correlating to the Nickerie Sequence Boundary. The age range for this interval therefore incorporates upper Oligocene to Early Miocene strata.

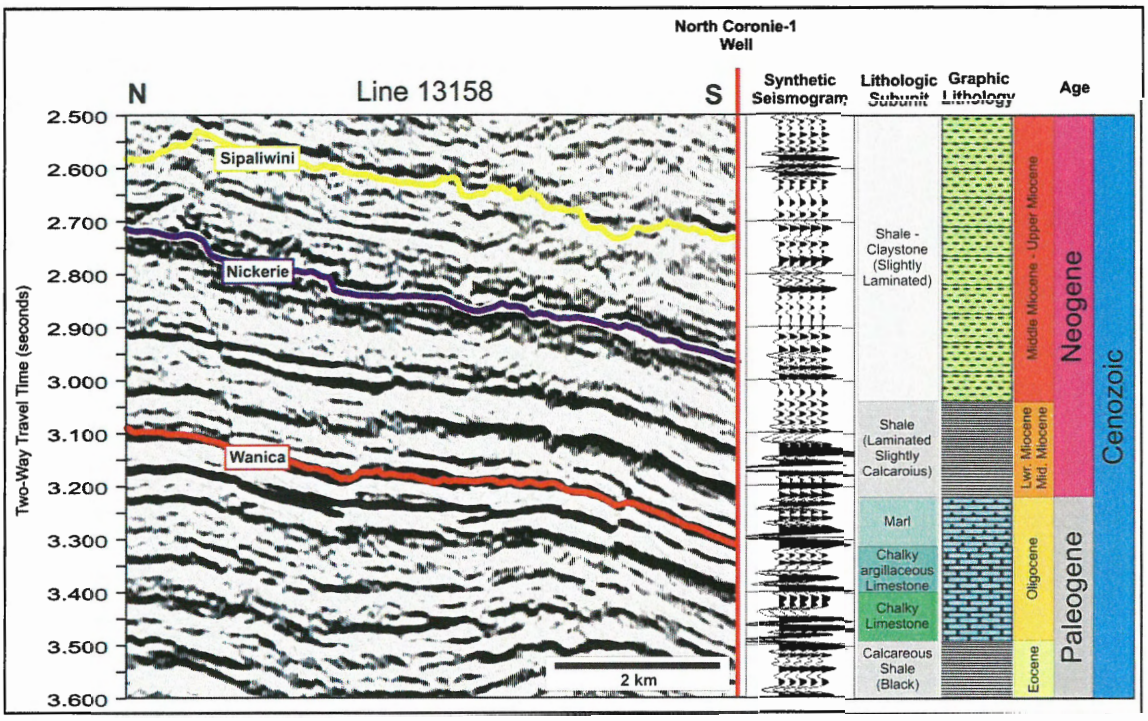

Figure 3.23 Age control diagram for NCO-1 well. Seismic reflections are displayed as wiggle traces and compared to the synthetic seismogram, lithology and biostratigraphic results to assign an age range to the reflections. The projected well location is represented as a vertical red line.

The overlying interval ranges in depth between 3185 m to 1700 m (MD), consisting of sequence boundaries Sipaliwini, Para, and Marowijne representing Early Miocene to Late Pliocene. This interval is separated by an unconformity with reworked strata and Eocene fauna lying just above the 3185 m reflection. As a result of this reworking, age determinations are more uncertain above 3185 m (MD). The Nickerie Sequence Boundary correlates to 3085 m (MD) which may be problematic in constraining its age at the NCO-1 location. The remaining sequence boundaries Sipaliwini, Para, and Marowijne therefore range in age between Early Miocene to Late Pliocene. The youngest interval between 1700 m and 412 m (MD) can then be assigned an age range of Late Pliocene to Early Pleistocene. Saramacca Sequence Boundary is located at 1391 m (MD)

at NCO-1 and has been assigned a tentative age of Early Pleistocene based on its erosive nature with the underlying strata and the published stratigraphic charts.

3.4.2 ODP Leg 207 Site 1257

ODP Leg 207 Site 1257 is located on the north eastern Demerara Rise (Figure 2.1). Correlation of reflections from the Block30 dataset were possible using RepsolYPF line W99-109, Shell line C2206 and GeoBline 220. Age control for Site 1257 is based on biostratigraphic analyses of calcareous nannofossils, planktonic foraminifers, and radiolarians (Erbacher et al. 2004a).

One reflection within the Cenozoic interval in the Block30 dataset was correlated across the margin along with two older reflections below the extent of this study: Cenozoic reflection Nickerie and two underlying older reflections P200 and A300 (Figures 3.4 and 3.24). A300 is the deepest reflection that was correlated from the Block30 dataset to Site 1257. At Site 1257, this reflection is recognized as the "C" reflection (Erbacher et al. 2004a; Erbacher et al. 2004b), and has an age range of Late Albian to Upper Cenomanian. When correlated to the NCO-1 well, A300 age control has a high confidence with Site 1257. A300 is located at ~ 4900 m (MD), which constrains its age between Albian 5050 m (MD) to Upper Cenomanian 4698 (MD). Therefore the reflection was given a tentative age of Albian. P200 at Site 1257 was defined as the "B" reflection and given an age of Early Paleocene (Erbacher et al. 2004a; Erbacher et al. 2004b). When correlated to the NCO-1 well this reflection is located at 3958 m (MD) placing within the Upper Maastrichtian 3995 m (MD) to Thanetian 3900 m (MD) in age. This reflection is defined as Paleocene in age. Nickerie is a much younger reflection defined as Upper

Oligocene to Early Miocene in the NCO-1 well. Results from ODP Site 1257 indicate a similar age of this reflection dated as Early Miocene (Erbacher et al. 2004a, Erbacher et al. 2004b). Nickerie is then tentatively given an Early Miocene age.

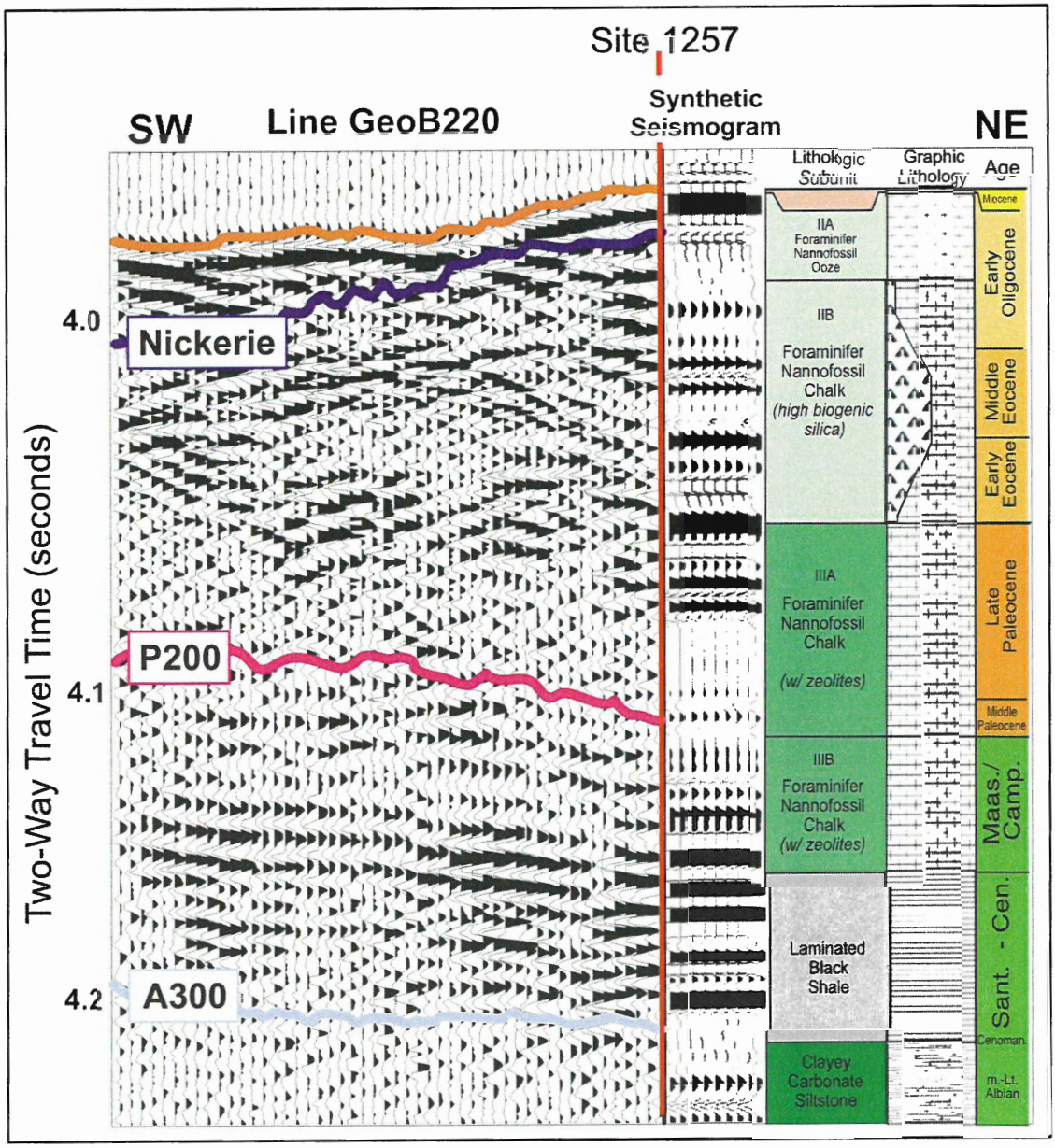

Figure 3.24 Age control for scientific well ODP Site 1257. Comparison wiggle plot, synthetic seismogram, lithology and biostratigraphic results to assign an age range to the reflections. The projected well location is represented as a vertical red line (modified from Erbacher et al. 2004a).

CHAPTER 4: DISCUSSION

4.1 Cenozoic Stratigraphy

Investigation of seismic sequences of the Suriname margin within the Block30 dataset and regional 2D seismic profiles provides evidence of erosion and deposition caused by sea level and sediment input variation. The six seismic sequences defined in chapter three (Figures 3.12 to 3.15) are addressed in section 4.1 of this chapter in relation to the Cenozoic composite sequence of the Suriname margin (Figures 4.1 to 4.3). Section 4.2 describes the detailed sequence stratigraphic interpretation that defines depositional sequences, in which each depositional sequence is composed of highstand "AP(D)" (aggradation to progradation to possible degradation), transgressive "R" (retrogradation), and lowstand "PA" (progradation to aggradation) systems tracts (ST).

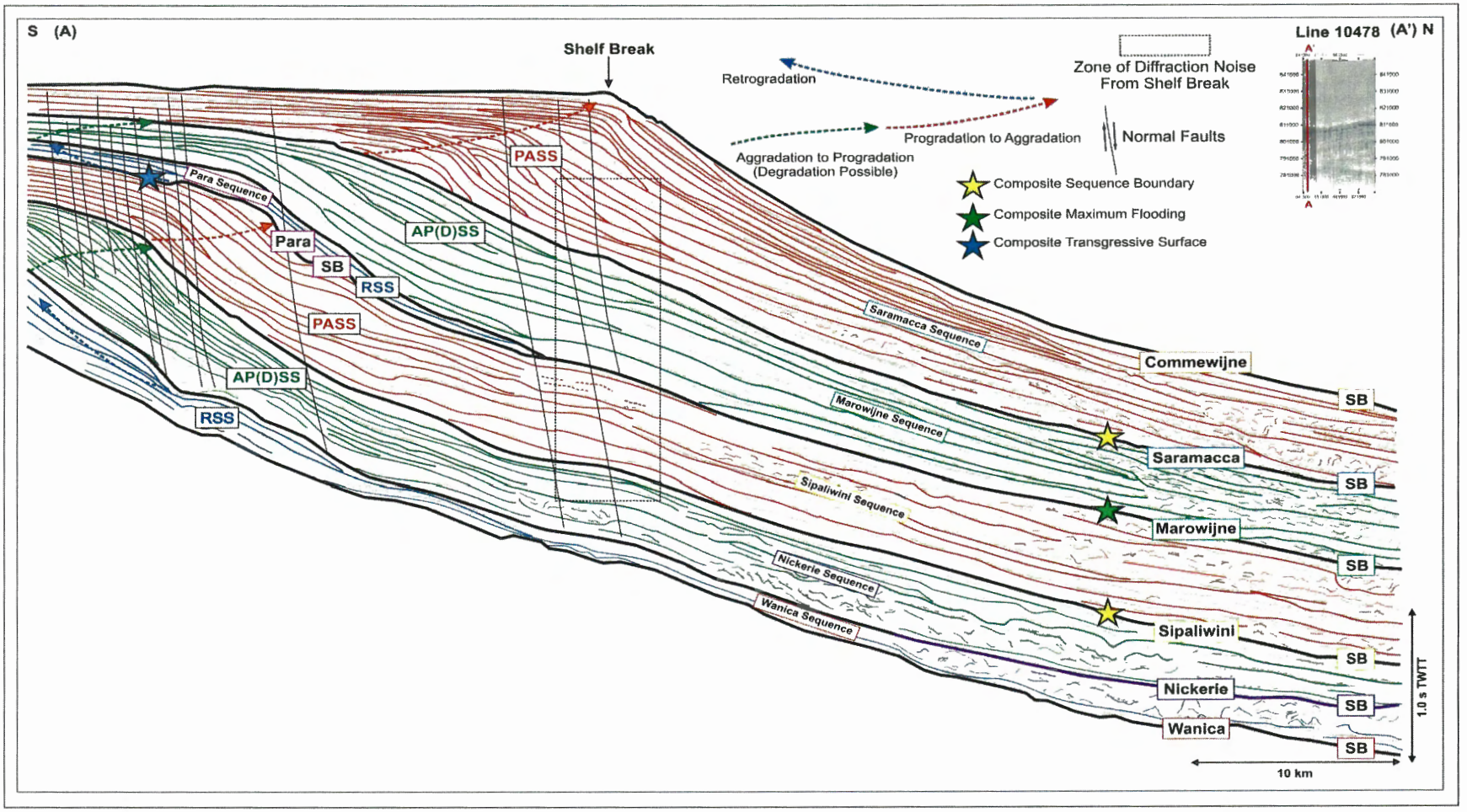

Figure 4.1 Seismic reflection dip profile used in Figure 3.12 for the outer shelf-to-slope in the western portion of the Block30 study area. This profile illustrates the interpretation of PA (progradation to aggradation), R (retrogradation), and APD (aggradation to progradation to degradation) sequence sets (PASS, RSS, and APSS, respectively). Sequence boundaries between sequence sets are in black.

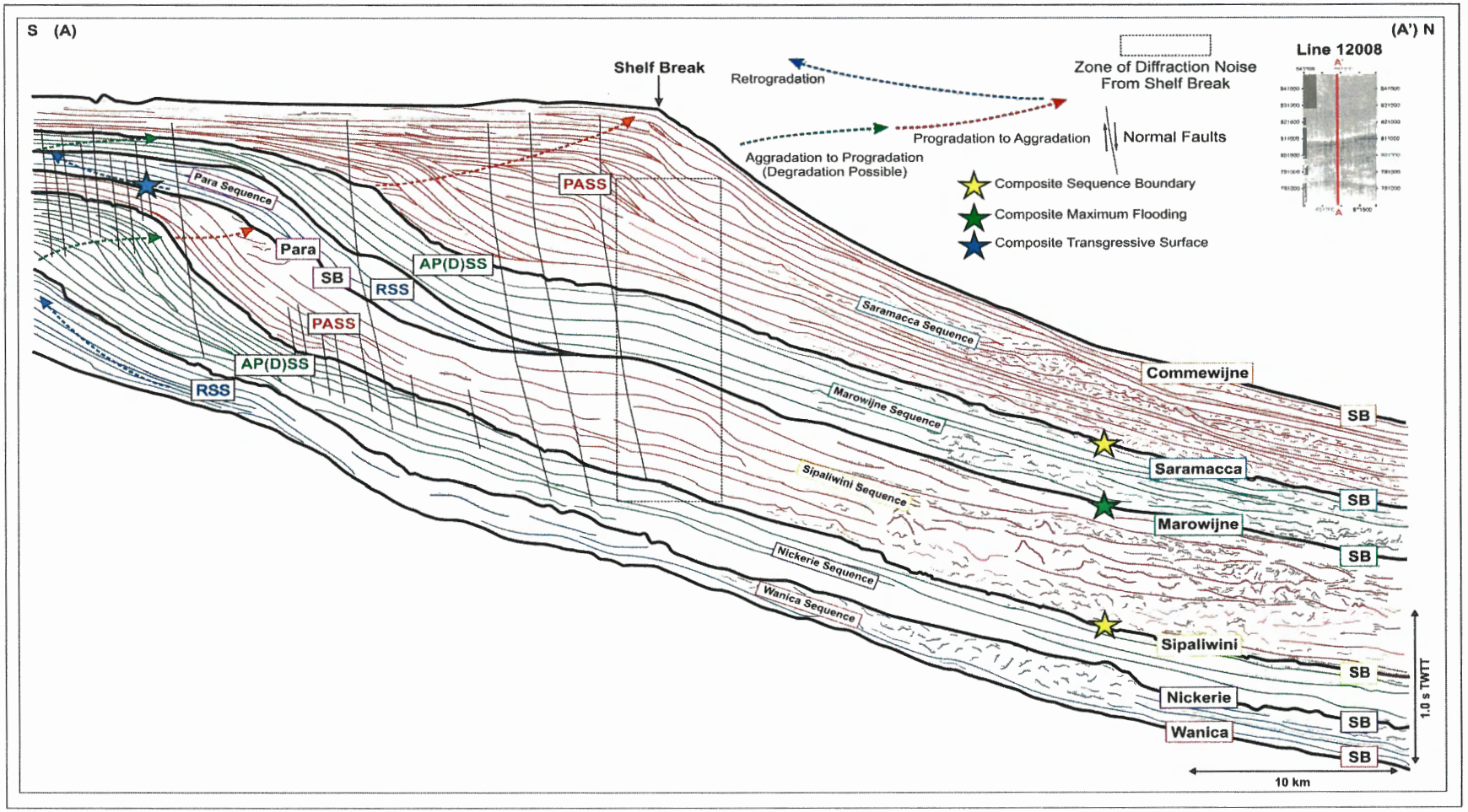

Figure 4.2 Seismic reflection dip profile used in Figure 3.13 for the outer shelf-to-slope in the central portion of the Block30 study area. This profile illustrates the interpretation of PA (progradation to aggradation), R (retrogradation), and APD (aggradation to progradation to degradation) sequence sets (PASS, RSS, and APSS, respectively). Sequence boundaries between sequence sets are in black.

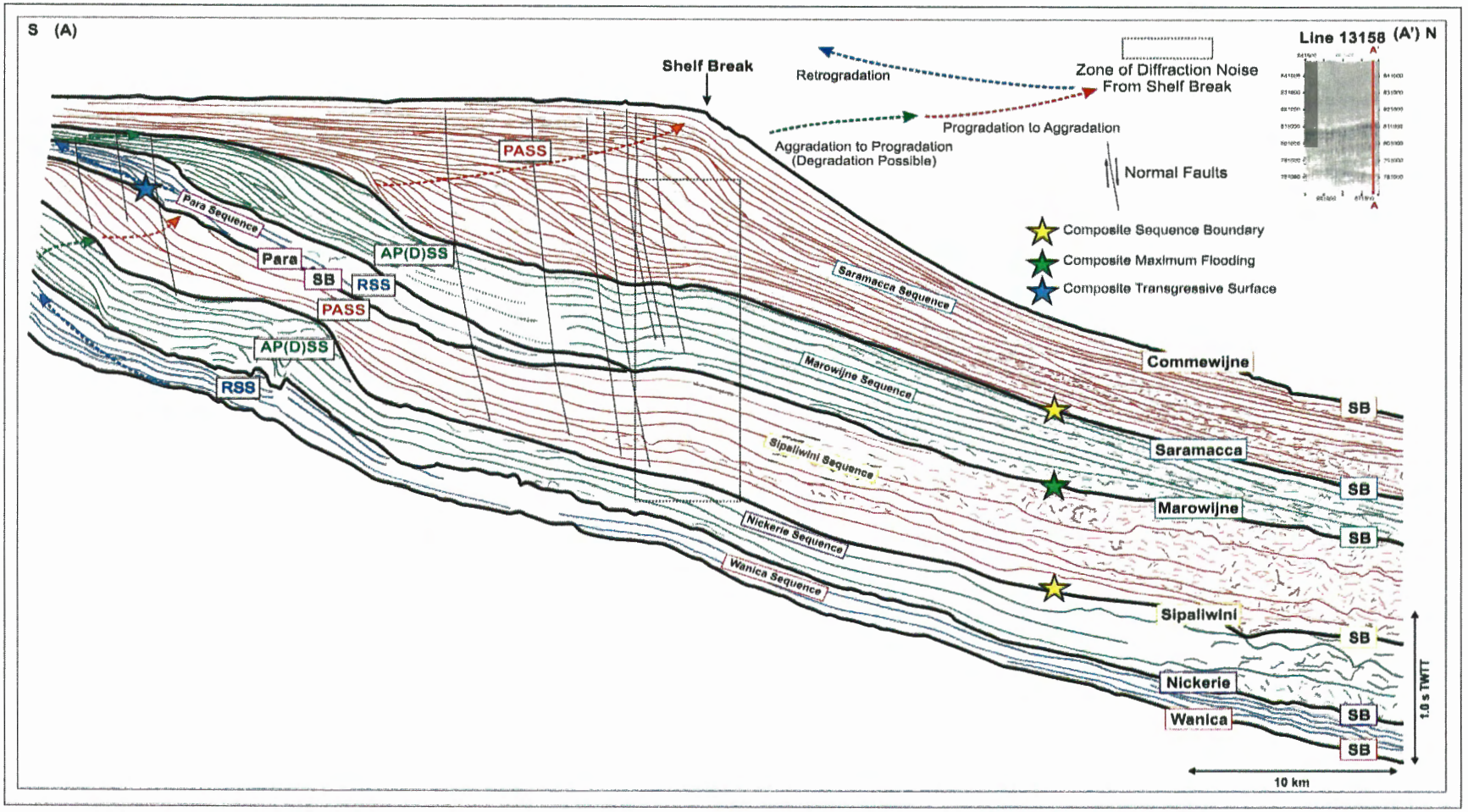

Figure 4.3 Seismic reflection dip profile used in Figure 3.14 for the outer shelf-to-slope in the eastern portion of the Block30 study area. This profile illustrates the interpretation of PA (progradation to aggradation), R (retrogradation), and APD (aggradation to progradation to degradation) sequence sets (PASS, RSS, and APSS, respectively). Sequence boundaries between sequence sets are in black.

4.1.1 Wanica Sequence Set (RSS)

The lowermost interval of the Cenozoic composite sequence, the Wanica Sequence, represents an overall transgressive sequence (Figures 4.1 to 4.3). It's lower surface, the Wanica Sequence Boundary, is interpreted to represent an erosional unconformity which presumably formed during a period of major sea-level lowstand. Following the formation of the Wanica Sequence Boundary a transgressive phase ensued as reflections backstepped and onlapped the inherited depositional profile. The sequences top surface, is the Nickerie Sequence Boundary.

4.1.2 Nickerie Sequence Set (AP(D)SS)

The Nickerie Sequence represents an overall highstand sequence (Figures 4.1 to 4.3). The Nickerie Sequence Boundary represents a major sea-level lowstand and is recognized as a wide spread erosional unconformity throughout the Block30 study area. The Nickerie Sequence Boundary is correlated to the outer Demerara Rise where it is defined as the "C" unconformity by Erbracher et al. (2004) (Figure 3.4). Reflections within the Nickerie Sequence are identified onlapping the inherited depositional profile of the Nickerie Sequence Boundary as clinoforms aggraded, with slow then rapid progradation into the basin. This pattern is followed by degradational reflection geometries as the rate of sea-level rise began to decrease. Subsequent, rapid progradation produced offlap breaks that step down into the basin without topsets onlapping the depositional profile of the Nickerie Sequence Boundary. This sequence is bounded at the top by the Sipaliwini Sequence Boundary, interpreted to represent the first composite sequence boundary within the Cenozoic composite sequence deposited during the last phase of the highstand.

4.1.3 Sipaliwini Sequence Set (PASS)

The Sipaliwini Sequence is bound at the top by the Para Sequence Boundary and Marowijne Sequence Boundary. It represents a lowstand to early transgressive sequence (Figures 4.1 to 4.3). Since all shelf accommodation was presumably filled with sediment, clinoforms rapidly prograded then aggraded, shown by topset reflections that onlapped the depositional profile of the Sipaliwini Sequence Boundary. The top of the sequence set is bound by the Para Sequence Boundary under the modern shelf, and this sequence boundary represents the composite transgressive surface of the composite sequence as sea-level continued to rise. The Marowijne Sequence Boundary represents the composite maximum flooding surface conformable to the Para Sequence Boundary, in the middle to lower slope region of the Sipaliwini Sequence Set.

4.1.4 Para Sequence Set (RSS)

The Para Sequence is bound at its base by the Para Sequence Boundary and the Marowijne Sequence Boundary and represents an overall transgressive phase (Figures 4.1 to 4.3). Reflections from the base of this interval onlap the Para Sequence Boundary and reflections display retrogressive stacking geometries. Rapid sea level rise created shelf accommodation faster then sediment could infill, and reflection packages backstepped as the shoreline transgressed. The Marowijne Sequence Boundary therefore represents the composite maximum flooding surface as sea-level reached its most landward position.

4.1.5 Marowijne Sequence Set (AP(D)SS)

The Marowijne Sequence represents the second highstand sequence set within the composite sequence (Figures 4.1 to 4.3). Following formation of the composite maximum

flooding surface, shelfal accommodation was presumably filled with sediment generated by a presumed decrease in the rate of sea level rise. As a result, clinoforms aggraded with slow then rapid progradational basinward wedges. These progradational clinoforms are overlain by degradational reflection geometries. Degradational reflection geometries indicate rapid progradation with offlap breaks that step down into the basin without topsets onlapping the inherited depositional profile. This sequence is bound by the Saramacca Sequence Boundary, which represents the second composite sequence boundary of the Cenozoic composite sequence.

4.1.6 Saramacca Sequence Set (PASS)

The Saramacca Sequence is bound below by the Saramacca Sequence Boundary and above by the modern seafloor. This Commewijne reflection represents the last lowstand sequence within the Cenozoic composite sequence (Figures 4.1 to 4.3). The Saramacca Sequence Set is dominated by PA stacking geometries, formed as sea level began to rise and shelfal accommodation filled. Clinoforms indicate rapid progradation of ~20 km, followed by aggradation as topsets onlap the inherited depositional profile.

4.2 Detailed Sequence Stratigraphic Interpretation

Six sequences are recognized in this study and are compiled into three distinct packages with characteristic stacking patterns defined as PA, R, and AP(D) Sequence Sets within the Cenozoic composite sequence. The composite sequence therefore contains a composite sequence boundary, composite maximum flooding surface, composite transgressive surface and internal sequence boundaries that are interpreted to represent separate cycles of deposition in response to changes in sea-level (Figures 4.1 to 4.3).

Although the stratigraphic framework was developed independently of any assumptions regarding base level fluctuation, interpretation into the timing and nature of slope deposition requires consideration of changes in base level and oceanographic processes.

Although six sequences are documented, it is recognized that within each sequence set, smaller order sequences are present (Figure 4.4). The six sequence sets discussed are considered representations of deposition related to base level change during the Cenozoic. Each sequence set of a composite sequence has likely gone though a lowstand "PA" sequence, followed by a transgressive "R" sequence resulting from a rise in base level, followed by the development of maximum flooding surface (MFS) into the highstand "AP(D)" sequence. Erosion and hiatuses in stratigraphic succession have removed complete or near complete sequence sets truncating unconformities and correlative conformities. Interpretations are made on the development of highstand "AP(D)", transgressive "R" and lowstand "PA" system tracts (ST) in relation to reflection geometry, facies and the magnitude of base level change.

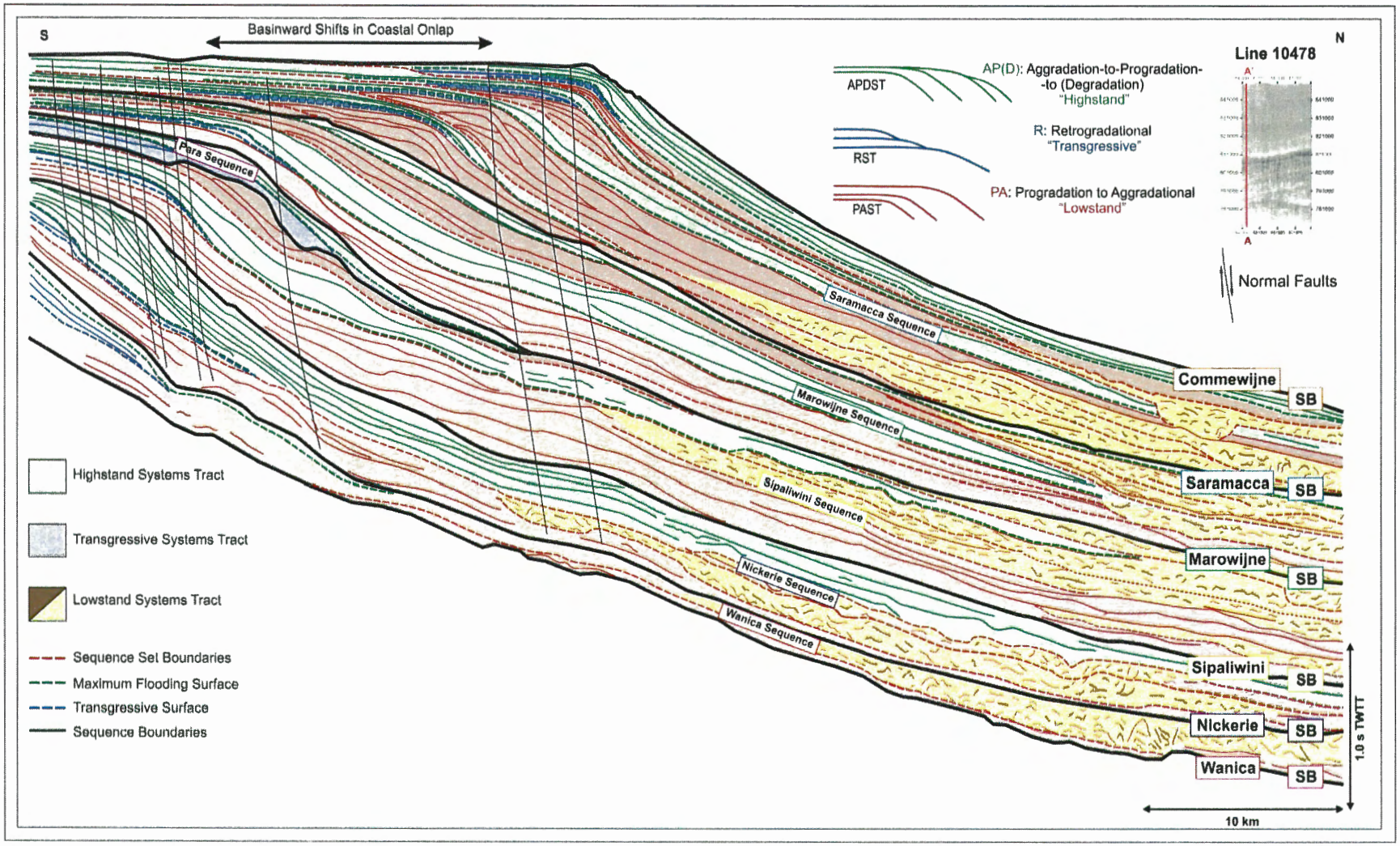

Figure 4.4 Proposed sequence stratigraphic model for the outer shelf and slope of the Block30 study area. Each depositional sequence set is composed of PA (progradation to aggradation), R (retrogradation), and APD (aggradation to progradation to degradation) systems tracts (ST).

4.2.1 Wanica Sequence Set (RSS)

The Wanica Sequence Set of the composite sequence (Figures 4.1 and 4.4) for the Suriname margin is subdivided to show the depositional sequences within the Wanica R (retrogradational) sequence set (Figure 4.5). The base of this sequence is bound by the Wanica Sequence Boundary which represents a wide-spread Early Oligocene erosional unconformity that correlates to a major eustatic sea-level lowstand (Haq et al. 1988) (Figure 4.5). Since the position of the paleo-shelf break is further up-dip than the extent of the dataset, down-dip predictions of the Wanica Sequence Set relate to the generalized cycle of sequences. "PA" stacking predicts "R" stacking; "R" stacking predicts "AP(D)" stacking; and "AP(D)" stacking predicts the sequence boundary before the cycle repeats (Neal and Abreu, 2009). Since reflection geometries in the Nickerie Sequence Set indicate AP(D) stacking, the Wanica Sequence Set is therefore (R) stacking (Figures 4.1 to 4.3). Following the formation of the Wanica Sequence Boundary, a lowstand systems tract (PAST) is interpreted to comprise the lower half of this interval in the mid to lower slope region. The lowstand is defined by the aggradational character of the reflection geometries. The presence of minor gullies occupying the middle slope region at the base of the interval are interpreted to be the result of lowered base level, as incision and bypass delivered sediments to the lower slope (Campbell, 2005) (Figures 3.5 and 4.5). Bypass and incision is represented in the lower slope, down dip of these gullies by extensive packages of chaotic/incoherent internal reflections indicative of mass transport deposits. These features typically lie above interpreted sequence set boundaries that normally form within the lowstand systems tract (PAST) (Posamentier et al, 2003). Transgressive (R) stacking patterns identified by reflection terminations and geometries

form the transgressive surface, resulting from an interpreted rapid sea level rise. Reflection geometries indicate backstepping, as the shoreline began to transgress forming the transgressive systems tract (RST) as base level rise accelerated. Transgressive deposits healed over incised gullies within the underlying lowstand systems tract (PAST) (Figure 4.5). The maximum flooding surface was formed resulting from an interpreted sea level rise which continued to increase to a maximum landward position. Largely progradational to aggradational geometries built as the rate of base level rise decelerated over the previously deposited transgressive and lowstand systems tracts, forming the highstand system tract (AP(D)ST). The Wanica Sequence Set is then bound at the top by the Nickerie Sequence Boundary, which is representative of a major Early Miocene erosional unconformity (Erbacher et al. 2004a, Erbacher et al. 2004b) that signifies a significant drop in sea level. This lowstand presumably eroded a significant portion of the Wanica Sequence Set. This conclusion is further supported by the eustatic curve where the Nickerie Sequence Boundary correlates to a drop in sea level (Haq et al, 1988) (Figure 4.5).

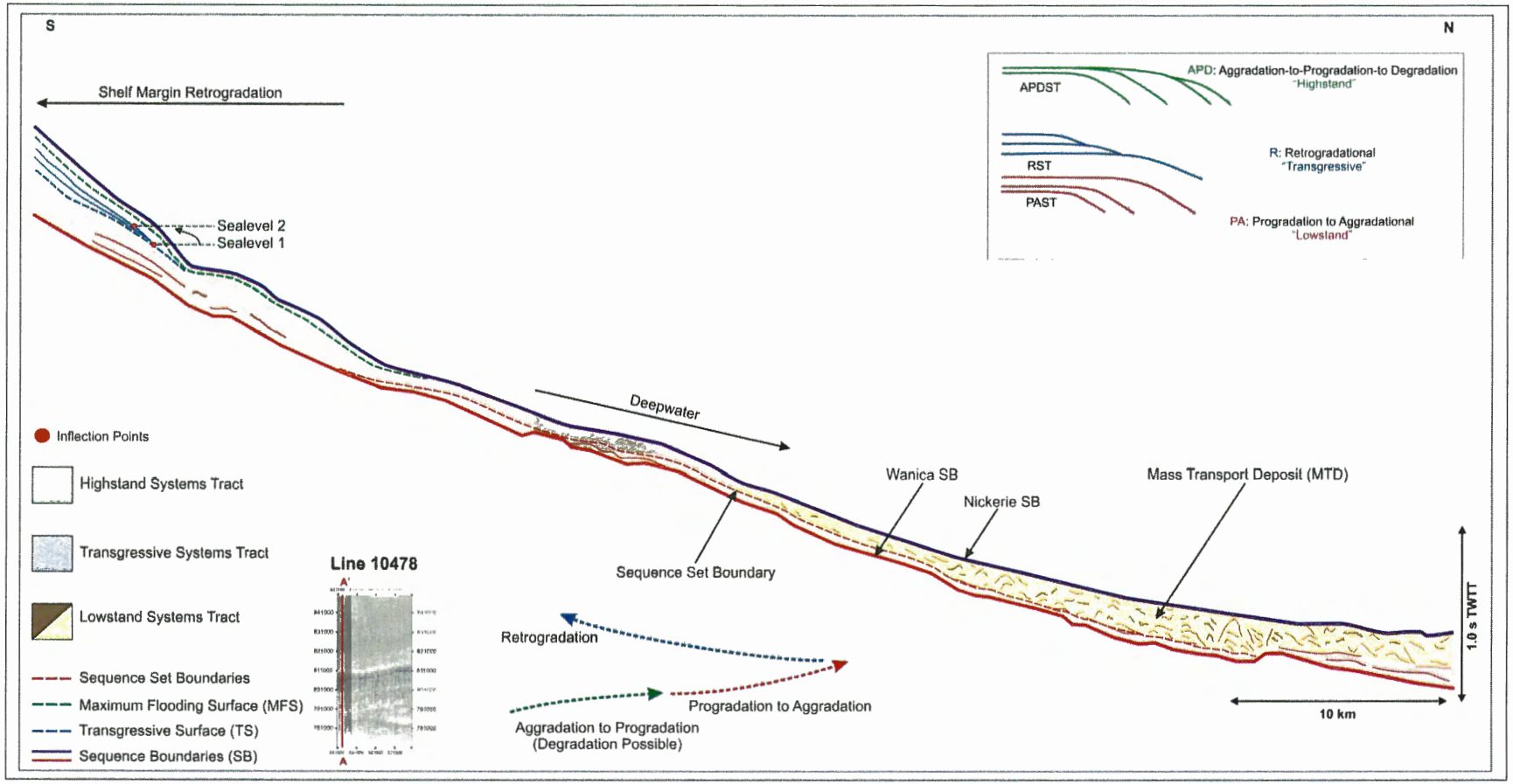

Figure 4.5 Detailed sequence stratigraphic interpretation of the seismic line shown in Figures 3.12 and 4.1, showing depositional sequences within the Wanica RSS (Retrogradation Sequence Set) of the Suriname margin's Cenozoic composite sequence. PA, R, and APD systems tracts are identified within the sequence set.

4.2.2 Nickerie Sequence Set (AP(D)SS)

The Nickerie Sequence Boundary represents a major Early Miocene erosional unconformity. As the lowstand system tract (PAST) developed, a significant amount of material was eroded. This process was occupied by down-cutting and channel incision of the paleo shelf and upper paleo slope in the south-eastern region of the Nickerie Sequence Boundary surface (Figures 3.6 and 4.6). Down-dip of the channel incision, reflections within the lowstand systems tract (PAST) formed similar patterns as the Wanica Sequence Set: two packages in the lower slope exhibit chaotic/incoherent internal reflections, presumably representing mass transport deposits (Figure 4.6). The first of these packages is thicker than the overlying package, lying above an interpreted sequence set boundary. A 20 ms (~ 25 m) thick layer of lowstand deposit separates this unit from the overlying unit, which has similar internal reflection characteristics. The characteristics of these two units represent the result of multiple phases of incision and bypass which delivered sediments to the lower slope regions. Overlying the lowstand system tract (PAST) in the middle to upper slope region, reflection geometries backstep and migrate landward, partially filling the previously eroded channel system. This package forms the transgressive system tract (RST) as sea level began to rapidly rise (Figure 4.6). The transgressive system tract (RST) is capped by the maximum flooding surface as rising sea level reached its maximum landward position and base level rise ceased. Following the development of the maximum flooding surface, the highstand system tract (AP(D)ST) formed and reflection geometries stacked into progradational to aggradational clinoforms (Figure 4.6). Clinoform inflection points indicate progradation which produced offlap breaks that step down into the basin. The interval capped by the

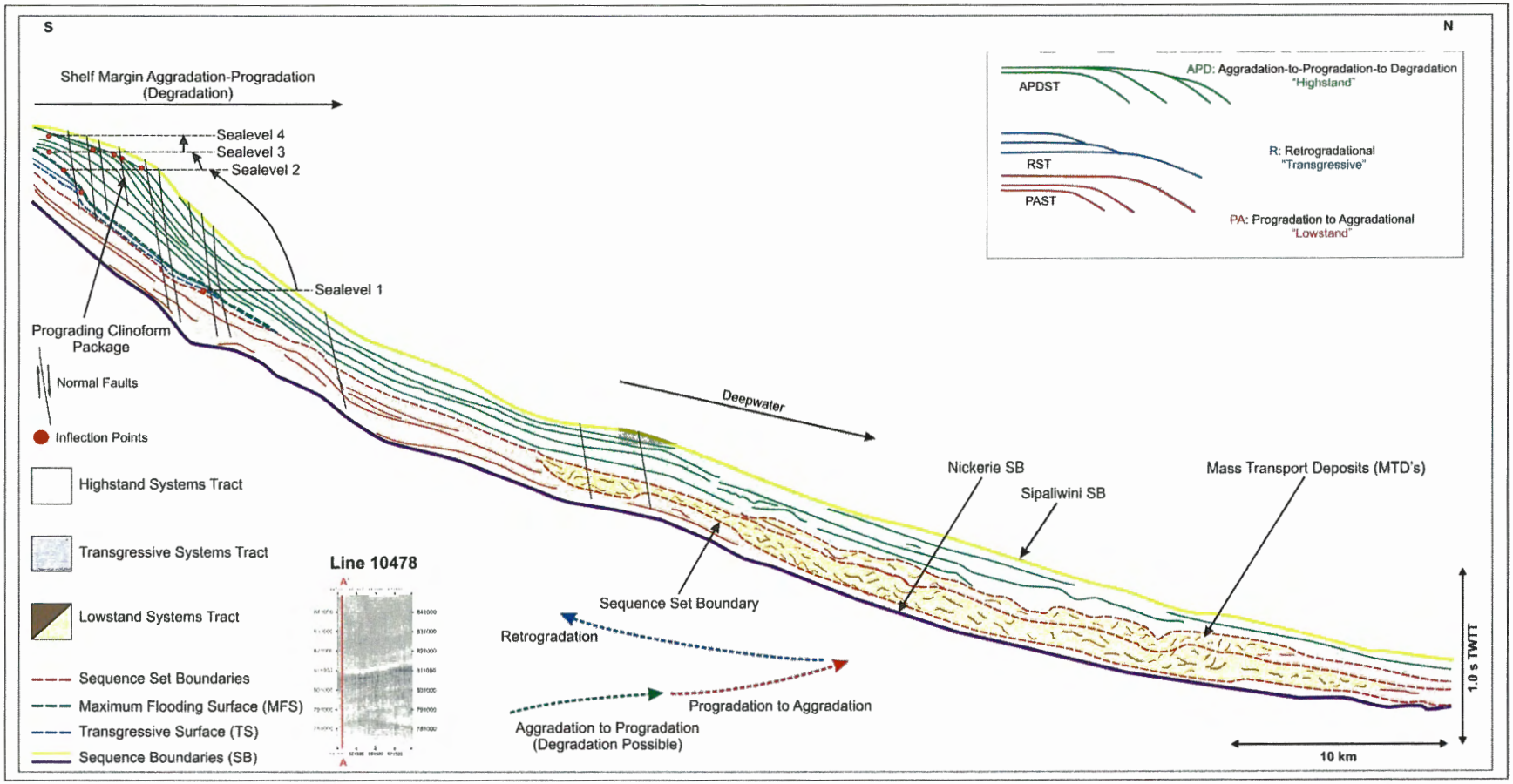

Figure 4.6 Detailed sequence stratigraphic interpretation of seismic line shown in Figures 3.12 and 4.1, showing depositional sequences within the Nickerie APDSS (Aggradation to Progradation to Degradation Sequence Set) of the Suriname margin's Cenozoic composite sequence. PA, R, and APD systems tracts are identified within the sequence set.

lower Middle to Late Miocene Sipaliwini Sequence Boundary which represents the first composite sequence boundary of the Suriname Cenozoic composite sequence.

4.2.3 Sipaliwini Sequence Set (PASS)

At the base of the Sipaliwini Sequence Set is the lower Middle to Late Miocene Sipaliwini composite sequence boundary. Following the formation of this composite sequence boundary, a lowstand system tract (PAST) developed. The composite sequence boundary is identified by progradational to aggradational stacking geometries that formed a thick sedimentary wedge during this period of sea level lowstand (Figure 4.7). Erosion re-occupied the south-eastern region where the channel system had previously developed in the underlying sequence set, during this period of sea level lowstand (Figures 3.7 and 3.15a). Down-dip of the channel system in the middle to lower slope, a series of stacked mass transport deposits formed above interpreted sequence set boundaries. These features presumably formed as a result of material bypassing through the channel system (Figure 4.7). Up-dip reflection geometries indicate a transgressive phase as inflection points backstepped and migrated landward, under the paleo-shelf of the Early Pliocene Para Sequence Boundary. As a result, the transgressive systems tract healed channel and gully incisions as sea level rise increased. The transgressive system tract (RST) is capped by the formation of the maximum flooding surface as sea level presumably reached is maximum landward position. The flooding surface is followed by the development of the highstand system tract (AP(D)ST). Clinoforms of the highstand systems tract (AP(D)ST) indicate rapid aggradation followed by a slow progradation, indicating a decrease in the rate of base level rise. Outer shelf deltas migrated basinward at this stage. (Figure 4.7). In the lower slope, the highstand system tract (AP(D)ST) formed a condensed wedge of

sediment which terminates in the lower slope mass transport deposits. Under the paleo shelf of the Para Sequence Boundary, a lowstand systems tract (PAST) lies above the highstand system tract (AP(D)ST) separated by the interpreted sequence set boundary. The lowstand systems tract (PAST) interval is thin ~70 ms (~ 87 m) on the outer shelf as reflection geometries indicate rapid progradation. This thinning is associated with the development of a mass transport deposit that eroded the underlying highstand (AP(D)ST) deposits in the lower slope region. The entire sequence is bound in the upper slope by the interpreted Early Pliocene composite transgressive surface (Para Sequence Boundary) and the overlying Late Pliocene composite maximum flooding surface (Marowijne sequence boundary) (Figures 4.1 to 4.3).

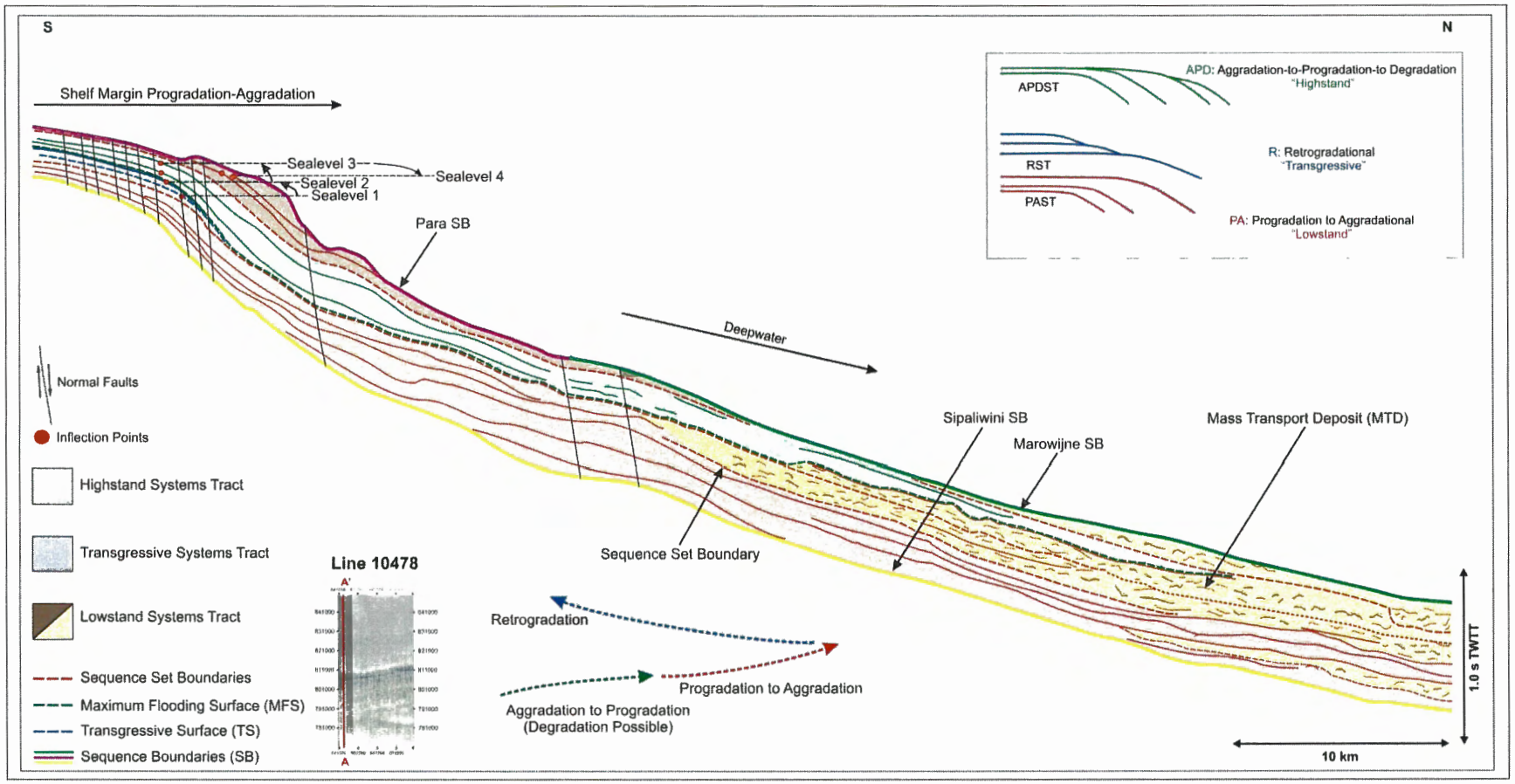

Figure 4.7 Detailed sequence stratigraphic interpretation of seismic line shown in Figures 3.12 and 4.1, showing depositional sequences within the Sipaliwini PASS (Progradation to Aggradation Sequence Set) of the Suriname margin's Cenozoic composite sequence. PA, R, and APD systems tracts are identified within the sequence set.

4.2.4 Para Sequence Set (RSS)

The Para Sequence Set of the composite sequence (Figures 4.1 and 4.4) for the Suriname margin was interpreted to show the depositional sequences within the Para R (retrogradational) Sequence Set (Figure 4.8). The early Pliocene Para Sequence Boundary represents the composite transgressive surface of the Suriname composite sequence. The middle slope region of this interval exhibits evidence of a lowstand system tract development (PAST), in which minor gullies formed on the Para Sequence Boundary surface (Figure 3.8). Following the lowstand system tract development, sea level presumably began to rapidly rise. As transgressive sediments healed over these minor gullies, reflections backstepped and migrated landward. Following the transgressive system tract, the maximum flooding surface developed which marked the onset of the highstand system tract (AP(D)ST). Reflections of the highstand systems tract indicate strong aggradation, before the formation of the Late Pliocene composite maximum flooding surface (Marowijne Sequence Boundary) as the rate of base level rise decreased.

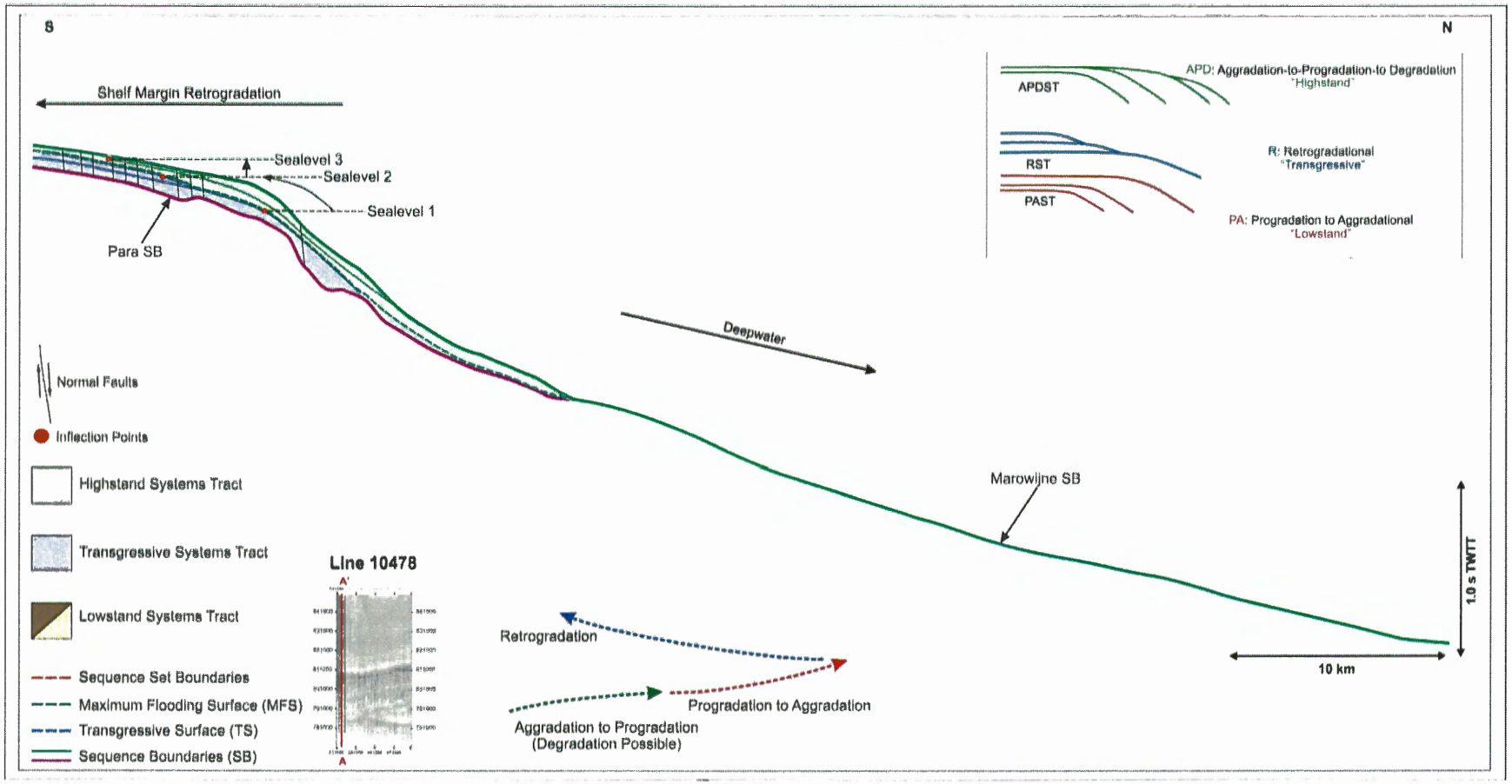

Figure 4.8 Detailed sequence stratigraphic interpretation of the seismic line shown in Figures 3.12 and 4.1, showing depositional sequences within the Para RSS (Retrogradation Sequence Set) of the Suriname margin's Cenozoic composite sequence. R, and APD systems tracts are identified within the sequence set.

4.2.5 Marowijne Sequence Set (AP(D)SS)

The Marowijne Sequence Set of the composite sequence (Figures 4.1 and 4.4) represents an APD (aggradational to progradational to degradational) Sequence Set (Figure 4.9). The sequence set is bound at its base by the Late Pliocene composite maximum flooding surface (Marowijne Sequence Boundary) (Figures 4.1 to 4.3). Overlying the composite maximum flooding surface, reflections indicate a rapid drop in sea level and the formation of a lowstand system tract (PAST). Interpretation of the Marowijne surface indicates a series of minor gullies that appear subdued as if buried, which presumably formed during the previous lowstand systems tract and were partially buried as the transgressive and highstand system tracts built over them (Figure 3.9). Within the lowstand system tract (PAST) of the Marowijne Sequence Set, reflections under the paleo-shelf and slope of the Saramacca Sequence Boundary indicate rapid aggradation then slow progradation as sea level began to rise and outer shelf deltas migrated basinward (Figure 4.9). In the lower slope, a series of stacked mass transport deposits within the lowstand systems tract (PAST) formed similar characteristics as the Wanica, Nickerie and Sipaliwini Sequence Sets. Under the upper paleo shelf of the Saramacca Sequence Boundary, a 30 ms TWTT (~ 33 m) thick, transgressive systems tract (RST) built landward as reflections began to backstep. The transgressive systems tract (RST) represents a healing phase of the underlying lowstand system tract (PAST) attributed to accelerated base level rise. The transgressive sequence is capped by the maximum flooding surface as sea level reached its maximum (Figure 4.9). The highstand system tract (AP(D)ST) then built over the underlying transgressive (RST) and lowstand system tracts (PAST) which formed a condensed section in the lower slope as base level rise

decreased. The development of a second lowstand system tract (PAST) is representative of a complete depositional cycle, in which extensive mass transport deposits dominate the lower slope region. Outer shelf deltas built basinward as incision and bypass processes dominated as a result of rapid base level lowering. A second transgressive systems tract (RST) within the sequence set is not identified. It is presumably too thin to be resolved seismically or there was limited sediment supply at the time (Figure 4.9). The lowstand system tract (PAST) is then capped by a 90 ms TWTT (~ 98 m) thick highstand system tract (AP(D)ST) as reflections indicate an aggradational phase. The Marowijne Sequence Set is then capped by the Early Pleistocene Saramacca Sequence Boundary.

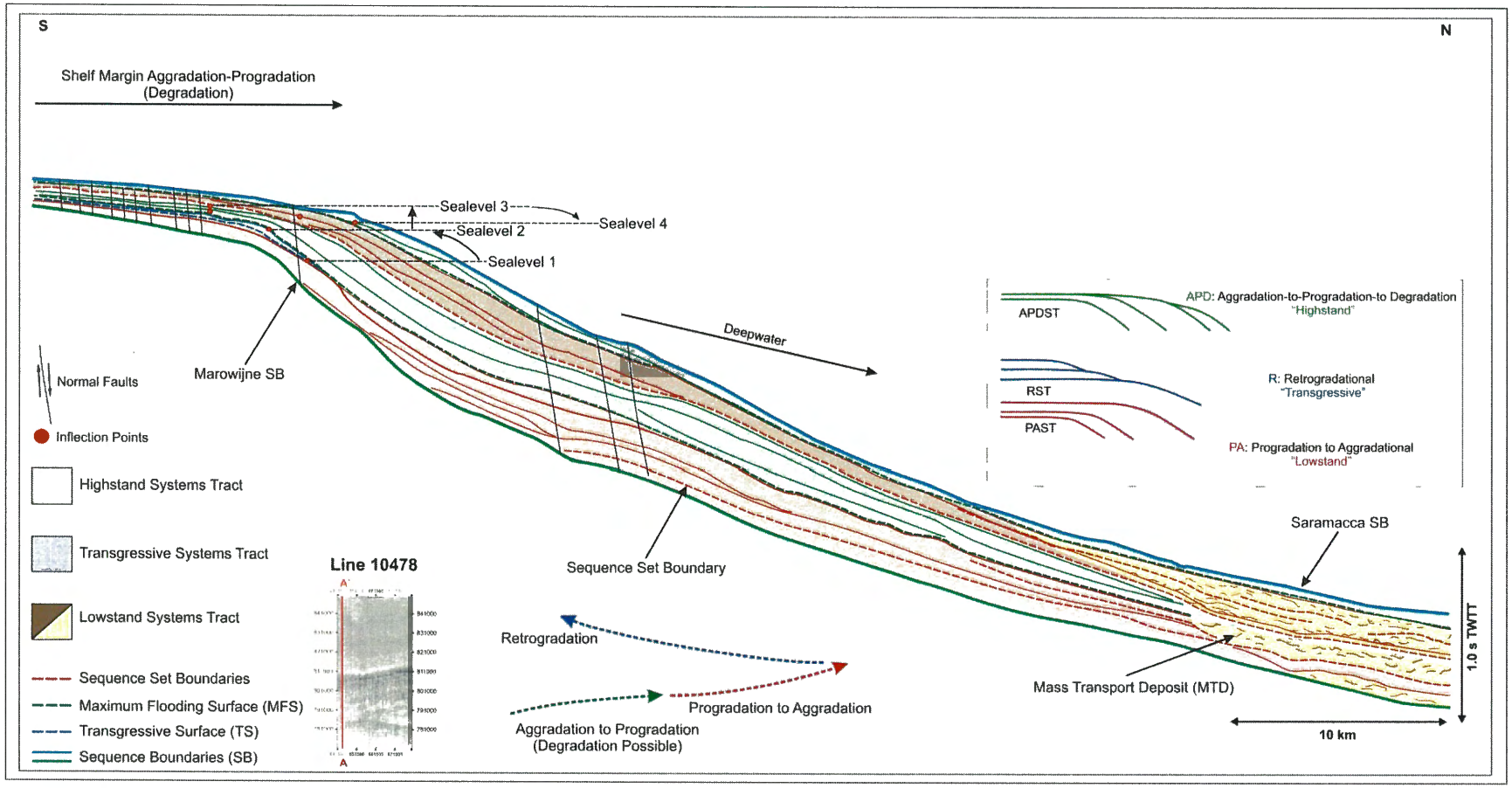

Figure 4.9 Detailed sequence stratigraphic interpretation of the seismic line shown in Figures 3.12 and 4.1, showing depositional sequences within the Marowijne APDSS (Aggradation to Progradation to Degradation Sequence Set) of the Suriname margin's Cenozoic composite sequence. PA, R, and APD systems tracts are identified within the sequence set.

4.2.6 Saramacca Sequence Set (PASS)

Within the Saramacca PA Sequence Set, four cycles of lowstand, transgressive and highstand systems tracts are interpreted. The Saramacca Sequence Set formed under highly variable sea level fluctuations from the late Pleistocene to present. The base of the sequence is bounded by the Early Pleistocene Saramacca Sequence Boundary. Reflection geometries above Saramacca Sequence Boundary define a lowstand system tract (PAST). Clinoforms indicate rapid progradation followed by aggradation as base level rise accelerated. In the lower slope of the lowstand systems tract (PAST) extensive packages of chaotic/incoherent internal reflections dominate. This characteristic indicates a period of major downslope sediment movement. Sediment delivery was presumably through conduits that overlie interpreted sequence set boundaries. Following the development of the lowstand system tract, a rapid rise in sea level resulted in brief deposition of a transgressive system tract (RST), capped by a maximum flooding surface (Figure 4.10). Overlying the maximum flooding surface, highstand systems tract (AP(D)ST) deposition is identified from the most southern extent of the profile to the middle slope region. Reflection geometries indicate rapid aggradation to slow progradation that formed a condensed interval below the shelf edge inflection points before terminating in the lower middle slope region. This depositional cycle repeated three more times with varying magnitude before the paleo shelf break reached its present position. This depositional pattern resulted in an overall basinward advance of outer shelf deltas of nearly 20 km (Figures 4.1 to 4.4).

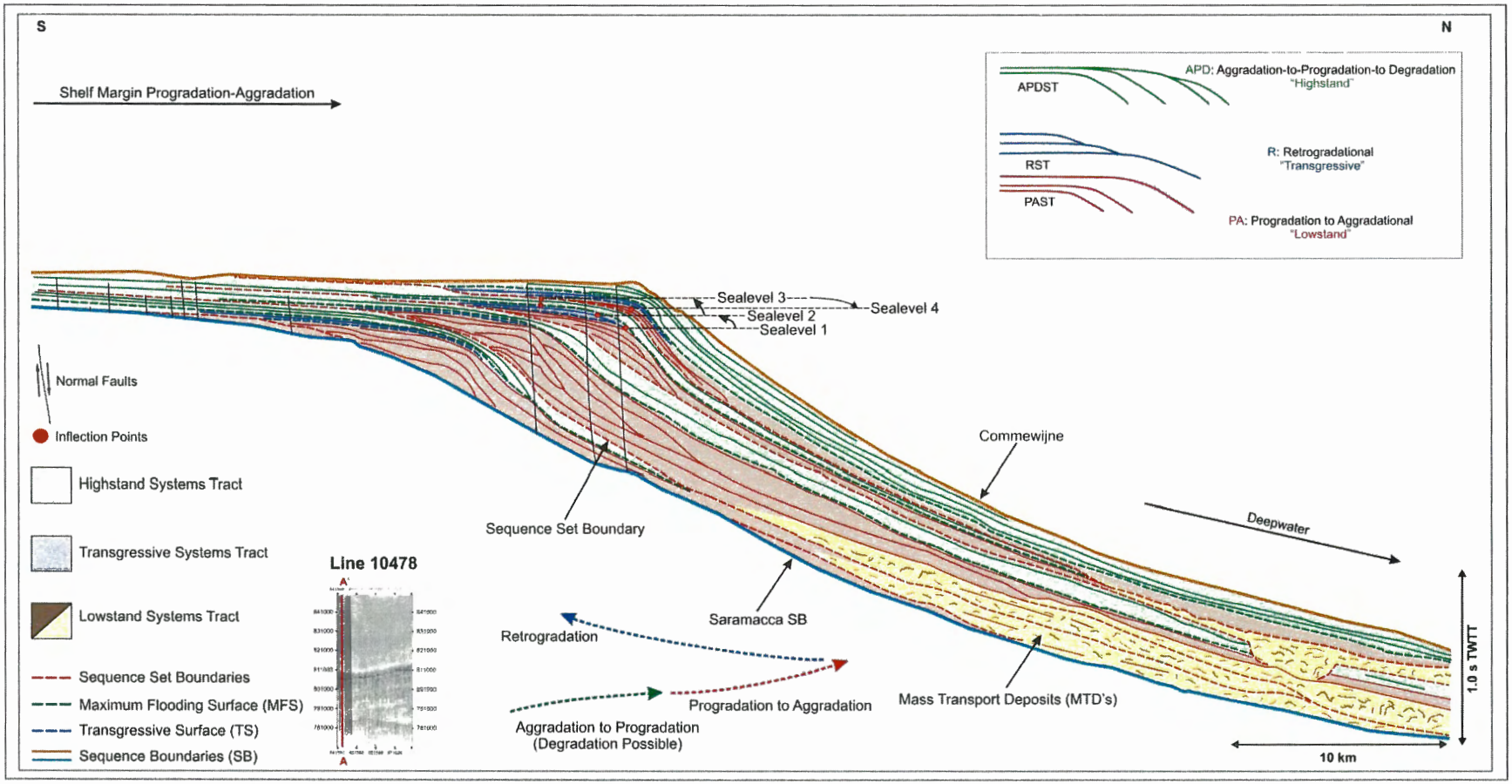

Figure 4.10 Detailed sequence stratigraphic interpretation of the seismic line shown in Figures 3.12 and 4.1, showing depositional sequences within the Saramacca PASS (Progradation to Aggradation Sequence Set) of the Suriname margin's Cenozoic composite sequence. PA, R, and APD systems tracts are identified within the sequence set.

4.3 Chronology of Sea-Level Variation and Associated Depositional Sequences

The effects of global sea-level change are recognized in the stratigraphic record of the Suriname margin. Numerous publications suggest that since the mid-Cretaceous, oscillations in sea-level are superimposed on a gradual sea level rise (Vail et al. 1977; Mitchum et al. 1977a; Haq et al. 1987; Miller et al. 1996; Christie-Blick et al. 1998; Zachos et al. 2001; Miller et al. 2005). Vail et al (1977) and Haq et al. (1998) suggested that sea-level variations, grouped into global eustatic cycles, are reflected in the seismic stratigraphic records of the World's continental shelf margins (Figures 4.11 and 4.12). The eustatic sea level curve of Haq et al. (1987) provides a proxy at a global scale. Subsequent to the establishment of the Haq et al. (1987) eustatic sea level curve, studies that have focused on Cenozoic sea-level fluctuations and its influence on the stratigraphic evolution have generally been skeptical of its accuracy (Miller et al. 1996; Christie-Blick et al. 1998; Zachos et al. 2001; and Miller et al., 2005).

$^{18}\delta O$ isotope data from benthic foraminifera in Cenozoic marine sediments provide a proxy for a suggested glacially-driven eustatic change (glacioeustasy) (Broecker and Van Donk 1970; Imbrie et al. 1984; Christie-Blick et al. 1998; Miller et al. 1998, Zachos et al. 2001, Miller et al. 2005). Since the early 1970's, $^{18}\delta O$ isotope data served as the principle means for reconstructing global and regional climate change variability (Zachos et al. 2001). Glacioeustasy is controlled by the ratio of global ice volume to free water through the formation of polar ice sheets since the Late Eocene (Bartek et al. 1991). Growth and decay in global ice volume causes changes in sea-level which are reflected in the oxygen isotope record (Miller et al., 1998). The formation of polar ice caps in the Eocene (Bartek et al. 1991, Miller et al. 1998) and Oligocene (Zachos et al. 2001) increased the amount

of $^{18}\delta O$ in the oceans, as lighter oxygen isotopes $^{16}\delta O$ are preferentially sequestered through evaporation and snowfall. In general, the higher ratios of $^{18}\delta O/^{16}\delta O$ correlate with sea-level falls; conversely the lower the ratios of $^{18}\delta O/^{16}\delta O$ can be attributed to ice melt, and global sea-level rise (Broecker and Van Donk 1970; Imbrie et al. 1984; Miller et al. 1998; Miller et al. 2005). Oxygen isotope records are multidimensional in that they provide a means to make both climate and stratigraphic predictions that are correlated to observations within this study.

The six key reflections (sequence boundaries) from this study were correlated to the eustatic curves of Haq et al. (1987), Miller et al. (1996), Zachos et al. (2001) and Miller et al. (2005) (Figure 4.12). Relative positions of the reflections are based on biostratigraphic age dates from the well ties (Figure 4.11). A relative sea-level curve was generated for the Suriname margin based on the sequence stratigraphic interpretation of this study (Figure 4.11).

4.3.1 Early Oligocene to end Late Early Miocene

The Early Oligocene (Rupelian?) to end late Early Miocene (Burdigalian?) is recognized in this study as the Wanica Sequence Set (RSS), in which higher frequency lowstand, transgressive, and highstand systems tracts are interpreted. The Wanica reflection, base of the Wanica Sequence Set, is recognized throughout the study area as an Early Oligocene erosional unconformity. It corresponds to an abrupt drop in sea-level during the Early Oligocene, recognized as a sharp inflection point on the oxygen isotope curves and the Haq et al. (1988) sea level curve of (Figure 4.12). The Middle Oligocene represents a

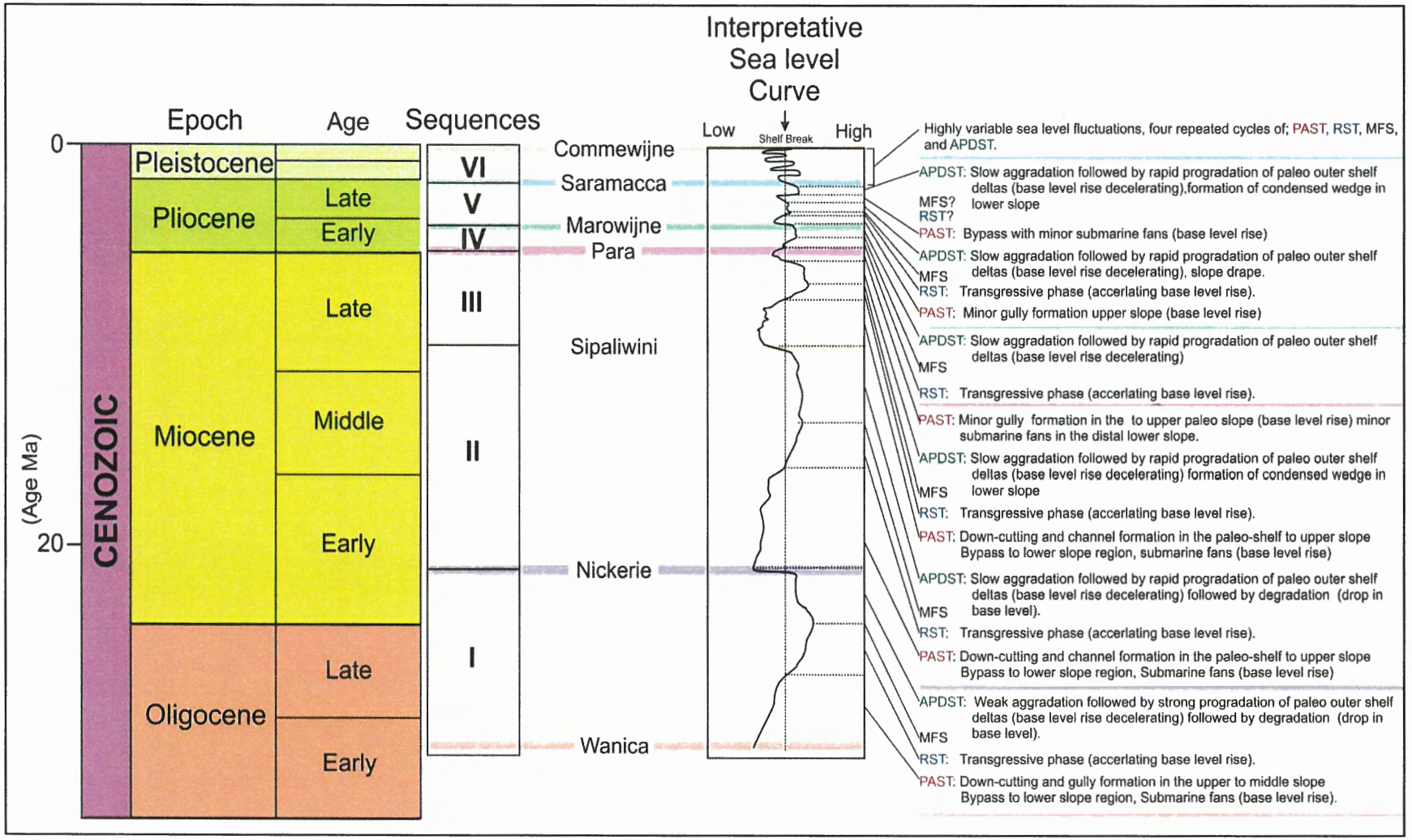

Figure 4.11 Interpretive relative sea level curve from this study. Sequence boundaries have been plotted across which indicate fluctuating trends in sea level.

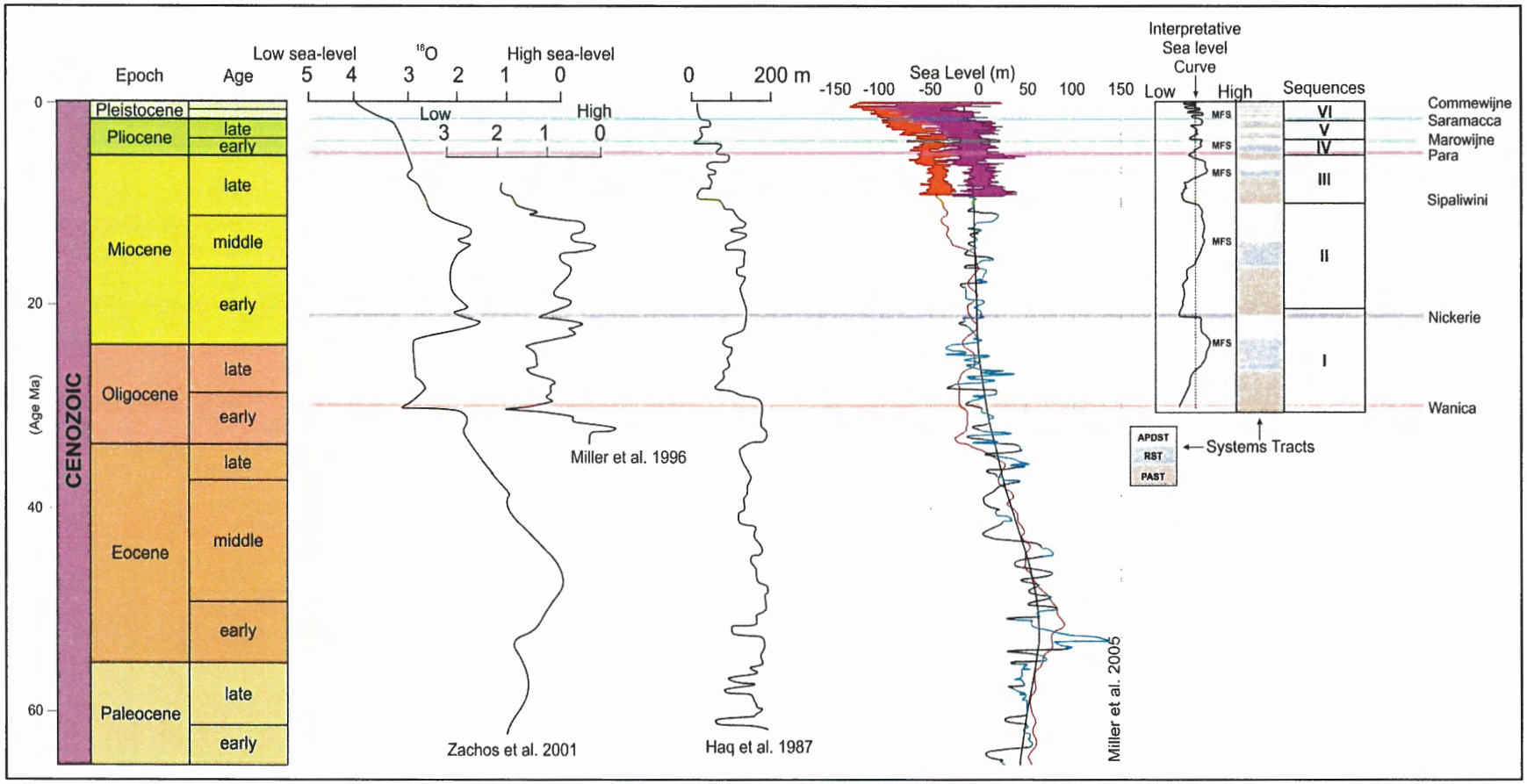

Figure 4.12 Three oxygen isotope curves derived from global data (Zachos et al. 2001) and the New Jersey margin (Miller et al. 1996, 2005) as well as, the global eustatic curve from Haq et al. (1988) derived on the basis of sequence stratigraphy. Reflections and sequence stratigraphic interpretations of relative sea-level from this study are correlated to the published curves.

eustatic lowstand period dominated by a lowstand system tract (Figure 4.4 and 4.5) of gully incision and bypass on the paleo-slope (Figure 4.5).

Nearing the Late Oligocene (Chattian?), a rise in eustatic sea-level is recognized in the oxygen isotope curves (Zachos et al. 2001) and shown in the Haq et al. (1988) sea level curve (Figure 4.12). This rise ended the lowstand deposition in the middle to lower paleo slope resulting in development of a transgressive surface as the shoreline presumably began to recede landward. A transgressive systems tract (RST) then built in the middle to upper paleo slope (Figure 4.4 and 4.5). Towards the Latest Oligocene (late Chattian?) to Earliest Miocene (Aquitian?), the maximum flooding surface developed when depositional trends changed from coastal transgressive (RST) deposition to highstand (AP(D)ST) deposition (Figure 4.11). As the rate of base level rise decreased, highstand (AP(D)ST) sediments infilled the remaining gullies in the upper paleo shelf and slope.

4.3.2 Late Early Miocene to Early Late Miocene

The late Early Miocene (Burdigalian?) to end early Late Miocene (Torontian?) is recognized in this study as the Nickerie Sequence Set (APDSS), in which higher frequency lowstand, transgressive and highstand systems tracts are interpreted. The Nickerie reflection, base of the Nickerie Sequence Set, is recognized throughout the study area as a late Early Miocene erosional unconformity (Figures 3.4, 3.5, 4.1 and 4.6). It corresponds to a rapid drop in eustatic sea level on oxygen isotope curves (Zachos et al. 2001) and the Haq et al. (1988) sea level curve (Figure 4.12). The rapid drop in base level resulted in significant erosion, channel incision and sediment bypass in the upper southeast region of the outer paleo-shelf and slope (Figure 3.6). As eustatic sea-level

began to rise, the incised channels acted as periodic feeder conduits to lower slope mass transport deposits until the latest Burdigalian? to earliest Langhian?. During this time, transgressive (RST) deposits began to backstep landward (Figure 4.6). Sea level reached its maximum landward position perhaps in the Serravillian, resulting in the development of a maximum flooding surface. The maximum flooding surface marked the change in deposition from transgressive to aggradational (Figure 4.6 and 4.11). As eustatic sea level continued to rise, a highstand systems tract (AP(D)ST) formed a thick clinoform package on the outer paleo shelf and slope. Highstand deposits draped the middle to lower slope, which formed a condensed interval in the distal lower slope region. As base level slowly dropped, degradational stacking produced offlap breaks that stepped down into the basin, as topsets onlapped the previously deposited highstand (AP(D)ST) sediments. Outer shelf deltas continued to migrate basinward to the latest Torontian? (Figure 4.6). Although transgressive and highstand sedimentation kept pace with sea level change, the channel systems that developed at the base of this interval in the south-eastern region of the paleo shelf and upper slope were not completely backfilled and were reoccupied in the Sipaliwini Sequence Set.

4.3.3 Early Late Miocene to Earliest Pliocene

The Early Late Miocene (Torontian?) to Earliest Pliocene (Zanclean?) is recognized in this study as the Sipaliwini Sequence Set (PASS), in which higher frequency lowstand, transgressive and highstand systems tracts were interpreted (Figures 4.1 and 4.7). The Sipaliwini reflection, base of the Sipaliwini Sequence Set, is recognized throughout the study area as a composite sequence boundary in which a rapid drop in eustatic sea level subsequently followed (Figure 4.1 and 4.12). This rapid drop in sea level resulted in a

lowstand systems tract that dominated the upper to lower paleo-slope. Channel incision reoccupied the earlier developed system in the south eastern region of the paleo-shelf. Reoccupation in this area provided a sediment conduit for periodic sediment bypass resulting in the development of mass transport deposits in the lower slope regions (Figure 3.15a). Lowstand deposition continued until the latest Miocene (earliest Messinian?) before eustatic sea level began to rise, resulting in the development of a transgressive surface. Transgressive deposition began to heal over the upper paleo-shelf and slope, as sediment supply kept pace with rising relative sea level (Figure 4.7). As transgressive packages built landward, the entire channel system on the outer paleo-shelf and slope completely backfilled (3.15a). As sea level reached its maximum landward position, the formation of the maximum flooding surface developed (middle Messinian?). At this time deposition shifted becoming aggradational with slow then rapid progradation (Figures 3.8 and 4.11). Highstand deposition was short lived as sediments draped the outer paleo shelf and slope, resulting in the formation of a condensed section pinching out in the distal extent of the profile. Sea-level then rapidly dropped (latest Messinian?) and short lived lowstand deposition built in the middle to lower slope regions with development of minor mass transport deposits (Figures 4.7. 4.11 and 4.12).

4.3.4 Earliest Pliocene to Middle Pliocene

The Earliest Pliocene (Zanclean?) to Middle Pliocene (Piacenzian?) is recognized in this study as Para Sequence Set (RSS), in which higher frequency lowstand, transgressive and highstand systems tracts were interpreted (4.1 and 4.4). Para reflection, base of Para Sequence Set, is recognized throughout the study area as the composite transgressive surface. As relative sea level rise shifted from lowstand deposition in the last phase of

Sipaliwini Sequence Set, transgressive deposition dominated as sediment supply kept pace with sea level rise (Figure 4.11). On the upper paleo-shelf, reflections backstepped landward until perhaps the earliest Piacenzian when the depositional trend changed from transgressive to mainly highstand, resulting in the development of the maximum flooding surface (Figures 4.8 and 4.11). This change in deposition resulted in a diminishing rate of base level rise, as highstand deposition built over the previously deposited transgressive sediments. Highstand deposition formed a 90 ms (~ 105 m, assuming an average velocity of 2342 m/s) aggradational blanket in the upper slope that became progradational and thickened over the paleo shelf inflection point. The remaining upper to middle slope gradually thinned, resulting in the formation of a condensed section where the lower Para reflection terminates in the distal extent of the profile (Figure 4.8).

4.3.5 Middle Pliocene to Early Pleistocene

The Middle Pliocene (Piacenzian?) to Early Pleistocene is recognized in this study as Marowijne Sequence Set (APDSS), in which higher frequency lowstand, transgressive and highstand systems tracts were interpreted (Figure 4.1 and 4.4). The Marowijne reflection, base of the Marowijne Sequence Set, is recognized throughout the study area as the composite maximum flooding surface. Following the development of this surface, sea level dropped rapidly marking a shift in depositional conditions to dominantly lowstand (Figure 4.9 and 4.12). A 50 ms (~ 54 m, assuming an average velocity of 2179 m/s) interval of lowstand deposits is located on the upper paleo shelf that formed a thickening wedge in the distal lower slope (Figure 4.9). As base level reached its lowest position, minor gully incision on the middle slope region resulted in the development of mass transport deposits (Figure 4.9). Sea level then began to rise and a transgressive

surface developed in the upper paleo shelf in which the maximum flooding surface subsequently developed (Gelasian?) and highstand deposition dominated. Highstand sediments formed extensive drapes that are very thin 20 - 30 ms (~ 22 - 33 m, assuming an average velocity of 2179 m/s) and aggrade on the upper paleo shelf that expanded seaward. Seaward the paleo shelf inflection point, sediments prograded basinward (Figure 4.9). In the distal lower slope, highstand deposition formed a condensed section, over which lowstand sediments later deposited. This lowstand deposition resulted from a rapid drop in sea level (latest Gelasian?). This rapid drop in sea level resulted in the development of stacked mass transport deposits in the distal lower slope. Sediments presumably bypassed the shelf during a period in which base level was slowly rising (Figures 4.9 and 4.11). During the earliest Pleistocene, sea level rise was rapid, and evidence for transgressive sedimentation and the development of a maximum flooding surface is apparent.

4.3.5 Early Pleistocene to Recent

The early Pleistocene to Recent interval is recognized in this study as Saramacca Sequence Set (PASS), in which higher frequency lowstand, transgressive and highstand systems tracts were interpreted. The Saramacca reflection, base of the Saramacca Sequence Set, is recognized throughout the study area as the second composite sequence boundary, completing the Cenozoic depositional cycle (Figures 4.1 and 4.4). Subsequent to the development of this boundary, sea level conditions were highly variable throughout the remainder of the Quaternary. Four cycles of high frequency lowstand, transgressive and highstand systems tracts were identified (Figure 4.10). In general these cycles formed basinward thickening lowstand intervals with evidence of erosion and bypass to the distal

lower slope. Transgressive intervals were short lived and constrained to the upper paleo shelf and slope, capped by a maximum flooding surface. Highstand deposits prograded basinward, which formed condensed sections that pinch out in the upper to lower paleo slopes, or thin distally to the most northern extents of the profile.

4.4 Overview of Sea-Level Variation and Depositional Sequences

In general, stratigraphic successions and stratal geometries on the Suriname margin indicate highly variable sea level conditions throughout the upper Paleogene and Neogene (Figures 4.11 and 4.12). On a broad scale, these stratal geometries include; basal lowering and Miocene flooding; Lower Miocene (Aquitanian - Burdigalian) aggradation, and lowstand deposits; Middle Miocene (Langhian and lowermost Serravallian) flooding, Middle Miocene (Serravallian) major progradation, end of Middle Miocene lowstand deposits; upper Miocene aggradation with lowstand deposits; lowermost Pliocene flooding, Pliocene- Lower Pleistocene aggradation with multiple lowstand deposits; and Upper Pleistocene high-frequency sequences. The stratigraphic pattern for the Suriname margin is similar to that of the Neogene from the Southeast Coast of Africa, Ross Sea, Northwest Java and Offshore Guyana (Bartek et al. 1991). These similar patterns suggest globally correlative sequences and systems tracts, presumably driven by Late Eocene/Early Oligocene glacioeustatic fluctuations of unstable Antarctic ice sheets (Haq et al. 1987). This waxing and waning of ice sheets caused globally synchronous shifts in coastal onlap and the manifestation of the global Neogene stratigraphic signature including the stratal succession of the Suriname margin.

4.5 Passive Margin Comparison: Nova Scotian

The Suriname margin's tectonic and sedimentary history is similar but younger than that of the Eastern Canadian Scotian margin. Both margins formed under comparable rifting conditions bound by significant transform faults creating translateral motions. Both margins exhibit prominent break-up unconformities as a result of rifting, followed by shallow epeiric seas with evaporate, then carbonate deposition and global ocean anoxic events. Both margins separated from present-day Africa in equatorial settings, and early post-rift sedimentation consists of mixed carbonate and clastic sediments. Following rifting and final separation both margins underwent rapid subsidence generating accommodation space that resulted in thick sequences of deep water continental margin sediments. In the case of Suriname because of its younger age, these sequences are still coherent in seismic profile. On the Scotian margin, many of these sequences have been subsequently subsided, compacted, faulted and disturbed by salt tectonism, erosion and margin collapse (mass transport deposition). The Suriname margin, therefore, may be viewed as an analogue to the Scotian margin, where the original stratigraphic architecture and depositional patterns are intact and may be imaged.

On the Scotian margin major transgressive sequences developed in response to a rise in relative sea level throughout the Late Cretaceous. These were punctuated by major sea level drops and regressive low stand sequences that were deposited through turbidity currents, mass sediment flows, and large slump deposits (Kidston et al. 2002). The result of such processes were significant volumes of sands and muds transported into deep water where they were deposited on the slope and abyssal plain (Kidston et al. 2002).

Later sediment loading on the shelf mobilized Jurassic salts that intruded vertically into the overlying strata forming positive relief features on the seafloor.

Clearly, similarities can be established for the Cenozoic Suriname and Jurassic Scotian margins. The relatively complete stratigraphy of the Suriname margin provides insights into passive margin development elsewhere in the Atlantic. Such processes can be extrapolated to help constrain Jurassic stratigraphy on the Atlantic Scotian margin that subsequently were modified by canyon incision and salt mobilization. Drilling on the Scotian shelf and upper slope has proven to be risky, with little success to date. This may in part be due to lack of reservoir preservation potential in the shelf and slope regions, as canyon and channel development transported sediments to deep water regions. This lack of preservation is also tied with the modification of strata as salt mobilization translated laterally and vertically. Depositional patterns from the Suriname margin indicate that significant volumes of sediments were likely deposited in the lower slope regions during periods of sea level lowstands. Lowstand deposits are presumably sand rich and may represent potential future exploration targets. Exploration potential is further supported as periods of sea level rise and highstands presumably provide conditions for deep marine sediments to bury such deposits. The repetition of such depositional cycles throughout the Cenozoic but devoid of salt mobilization and glacial influence may help predict depositional processes on the Jurassic Scotian margin prior to extensive incision and salt mobilization events.

CHAPTER 5: CONCLUSION

This study examined the Cenozoic stratigraphic evolution and sediment distribution of the Suriname margin, South America, through application of sequence stratigraphic concepts to understand varying influences of external forcing mechanism such as sediment input, sea level, tectonics, and paleoceanography.

A composite seismic stratigraphy for the Suriname margin was developed based on the Block30 3D seismic volume and regional 2D profiles. Seven key reflections are readily recognized throughout the study area on both 3D and 2D seismic reflection data and were correlated to biostratigraphic control at the North Coronie-1 industry well, and scientific well ODP Leg 207 Site 1257. The Wanica reflection is approximately Early Oligocene, the Nickerie reflection is approximately Early Miocene, the Sipaliwini reflection is approximately lower Middle to Late Miocene, The Para reflection is approximately Early Pliocene, The Marowijne reflection is approximately Late Pliocene, The Saramacca reflection is approximately Early Pleistocene, and the Commewijne reflection represents the present day sea-floor. These seven key reflections were placed into a sequence stratigraphic framework using the method of accommodation succession, proposed by Neal and Abreu (2009). Seismic reflection stacking geometries were interpreted into the context of lowstand, transgressive, and highstand, systems tracts (ST) with associated maximum flooding surfaces based on facies descriptions and reflection geometries. Clinoform geometries indicating progradation then aggradation, with reflections onlapping the inherited depositional profile are interpreted to represent a lowstand systems tract. Periods of lowstands are correlated to paleo-channel incision on the outer

shelf and slope, with interpreted mass transport and turbidite deposits. Interpretations suggest, lowstand and highstand systems tracts are presumably separated by an unconformable transgressive surface and packages of back stepping transgressive reflections that onlap and aggrade the depositional profile as the shoreline likely began to transgress. The interpreted transgressive systems tracts were then likely capped by the formation of the maximum flooding surface, presumably marking a change in deposition from transgressive and highstand systems tracts. Outer shelf and slope clinoform packages with reflection geometries indicating aggradation followed by slow then rapid basinward progradation are interpreted to represent highstand systems tracts. Degradational reflection stacking are interpreted to occur during a drop in base level, recognized as clinoforms that likely prograded basinward with interpreted offlap breaks that stepped down into the basin.

During the Middle Oligocene, Early-Middle Miocene, and Early-Late Miocene, significant erosion likely resulted from several sea level lowstands and presumably the development of interpreted outer shelf and slope channels and minor gully incision. Channel flow presumably bypassed the upper to middle slope region, resulting in interpreted mass transport and turbidite deposits which appear to accumulate in lowstand wedges. During periods of rising sea level, presumably during the Late Oligocene, Middle Miocene and the middle Late Miocene transgressive reflections presumably backfilled channel and gully incisions associated with high sedimentation rates, culminating in the likely formation of the a maximum flooding surface. Periods of high sea slevel most likely during the Latest Oligocene-Earliest Miocene, Middle to Late Miocene, and Latest Miocene resulted in outer shelf deltas aggrading, as sediments are

interpreted to drape the outer shelf and upper slope, that typically formed condensed sections in the lower slope regions.

This study was characterized by sea level rises and falls from the Late Miocene to the end of the Pliocene, followed by higher frequency shifts from the Late Pliocene to Recent. This time period was marked by high sedimentation rates, minor gully incision events, lower slope infilling and rapid progradation of the shelf break nearly 20 km to its present day location. Sea level fluctuations were related to the waxing and waning of glaciers in Antarctica, Greenland, Europe, and North America.

In summary the Suriname margin provides an excellent site to test new sequence stratigraphic concepts, using the method of accommodation succession, proposed by Neal and Abreu (2009). The Suriname margin's framework is constrained within six sequences which are age controlled by biostratigraphic data correlated to paleooceanographic sea-level changes. Within each sequence, high frequency systems tracts are identified. Overall the stratigraphic architecture of the Suriname margin is recognized as having; 1) stratigraphic development influenced by sea level changes, 2) minimal effects of tectonic activity since the Late Cretaceous, and 3) high sedimentation rates resulting in the overall progradation of the margin.

In terms of an exploration model, lower slope fans, shelf edge deltas and turbidite deposits may provide significant amounts of clean reservoir sands, with potential for being charged by late Cretaceous source rocks. These deposits are the result of sea level

lowering and channel and gully incision in the outer shelf providing sediment conduits to the deep water.

REFERENCES

Allen, P.A, and Allen, J.R. 1990. Basin Atlas. Blackwell, Oxford.

Bartek, L.R., Vail, P.R., Anderson, J.B., Emmet, P.A., and Wu, S. 1991. Effect of Cenozoic ice sheet fluctuations in Antarctica on the stratigraphic signature of the Neogene. Journal of Geophysical Reseach. v. 96. p. 6753-6778.

Benkhelil, J., Mascle, J., and Tricart, P. 1995. The Guinea continental margin; an example of a structurally complex transform margin. Tectonophysics 248: 117-137.

Broecker, W., and Van Donk, J. 1970 Isolation changes, ice volumes and 180 record in deep-sea cores: Reviews of Geophysics and Space Physics. v. 8 p. 169-198.

Brown, A.R. 1999. Interpretation of three-dimensional seismic data, 5th edition. AAPG Memoir 42, Tulsa, Ok. pp.514

Brown, A.R. 1996. Seismic attributes and there classification. The Leading Edge, 15: 1090.

Brown, A.R. 2003. Interpretation of three-dimensional seismic data. AAPG Memoir 42, SEG Investigations in Geophysics, No, 9: pp. 20-42.

Brown, L.F., and Fisher W.L. 1980. Seismic stratigraphic interpretation and petroleum exploration: Continuing education. v.16: Austin, AAPG.

Catuneanu, O. 2002. Sequence stratigraphy of clastic systems: concepts, merits, and pitfalls. Journal of African Earth Sciences. v. 35. Issue 1. p. 1-43.

Christie-Blick, N. 1991. Onlap, offlap, and the origin of unconformity-bounded depositional sequences. Marine Geology, 97: 35-56.

Christie-Blick, N., Austin, J.A., Jr., and Shipboard Scientific Party. 1998. Introduction: Oligocene to Pliocene eustatic change at the New Jersey continental Margin- a test of sequence stratigraphy, Proceedings of the Ocean Drilling Program, Intitial Reports, ODP, p. 5-16.

Erbacher, J., Mosher, D.C., Malone, M.J. and shipboard scientific party. 2004a. Proc. ODP, initial reports., 207 [CD-ROM]. Ocean Drilling Program, Texas A&M University, College Station, TX. 77845-9547, USA

Erbacher, J., Mosher, D.C., Malone, M.J. and shipboard scientific party. 2004b. Drilling probes past carbon cycle perturbations on the Demerara Rise. EOS, v. 85, p. 57.

Flicoteaux, R., Latil-Brun, M.V., and Michaud, L. 1988. Histoire de la subsidence post-rift du bassin cotier mauritano-senegalo-guineen, relation avec l'amincissement crustal pendant la periode jurassique a Cretace inferieur; comparaison avec l'evolution des marges peri-atlantiques au niveau de l'Atlantique central et equatorial (cote est des U.S.A., Sud-Sahara, Cote d'Ivoire et Plateau du Demerara) In: The West African connection; evolution of the central Atlantic Ocean and its continental margins. Sougy J, Rodgers, J. (eds) Journal of African Earth Sciences 7: 345-359.

Flynn, R.F.J. 2000. Tunnel valleys under the southeastern Scotian shelf. BSc thesis. Saint Mary's University, Halifax, NS.

Forester, A., Sturt, H., Meyers, P.A., and the LEg 207 Shipboard Scientific Party. 2004. Molecular biogeochemistry of Cretaceous black shales from the Demerara Rise: preliminary shipboard results from Sites 1257 and 1258, ODP Leg 207. *In*: Erbacher, J., Mosher, D.C., Malone, M.J. et al., Proc. ODP Init. Repts., 207: College Station TX (Ocean Drilling Program)

Galloway, W.E. 1989. Genetic stratigraphic sequences in basin analysis, I. Architecture and genesis of flooding-surface bounded depositional units. AAPG Bulletin, 73: 125-142.

Gouyet, S., Unternehr, P., and Mascle., A. 1994. The French Guyana margin and the Demerara Plateau; geological history and petroleum plays. *In*: Mascle A (ed), Hydrocarbon and petroleum geology of France. Special Publication of the European Association of Petroleum Geoscientists 4: 411-422.

Haq, B.U., Hardenbol, J., and Vail, P.R. 1988. Response: Sea Level History. *In*: Wilgus, C.K., Hastings, B.J., Posamentier, H., van Wagoner, J.C., Ross, C.A. and Kendall, C.G. St. C. (*eds.*) Sea-level Change: an Integrated Approach. SEPM Spec. Pub, 42: 71-108

Haq, B.U., Hardenbol, J., and Vail, P.R. 1987. Chronology of fluctuating sea levels since the Triassic. Science, v. 235, p. 1156-1166.

Hart, B.S. 1999. Definition of subsurface stratigraphy, structure, and rock properties from 3-D seismic data. Earth Reviews. Vol. 47. p.189-218.

Imbrie,J., Hays, J.D., Martinson, D.G., McIntyre, A., Mix, A., Morely, J., Pisias, N.G., Prell, W., and Shackleton, N. 1984. The orbital theory of pleistocene climate: support from a revised chronology of the marine 18O record. *In:* Berger, A., Imbrie, J., Hays, J.D., Kulka, G., and Saltzman, B., eds., Dordrecht. Milankovitch and Climate, The Netherlands, Riedel. p. 269-305.

Jervey, M.T. 1988. Quantitative geological modeling of siliciclastic rock sequences and their seismic expression. *In*: Wilgus, C.K., Hastings, B.S., Kendall, C.G.St.C., Posamentier, H.W., Ross, C.A., Van Wagoner, J.C. (eds.), Sea Level Changes - An Integrated Approach. . Special Publication, vol. 42. Society of Economic Paleontologists and Mineralogists (SEPM), pp. 47–69.

Keary, P., and Brooks, M. 1991. An introduction to geophysical exploration: Blackwell Scientific Publications, p. 254.

Kidston, A., Brown, D., Altheim,B., Smith, B. 2002. Hydrocarbon potential of the deep-water Scotian Slope. Canada Nova Scotia Offshore Petroleum Board. Halifax, Nova Scotia, 111 p.

Mascle J, Marinho, M. and Wannesson J. 1986. The structure of the Guinean continental margin: implications for the connection between the central and South Atlantic Oceans. Geol. Rundsch. 75: 57-70.

Miller, K.G., Liu, C., and Feigenson, M. 1996 Oligocene to middle Miocene Sr-isotope stratigraphy of the New Jersey continental slope: Proceedings of the Ocean Drilling Program, Scientific Results. v. 150, p. 97-114.

Miller, K.G., Mountain, G.S., Browning, J.V., Kominz, M.A., Sugarman, P.J., Christie-Blick, N., Katz, M.E., and Wright, J.D. 1998. Cenozoic global sea level, sequences, and the New Jersey transect: Results from coastal plain and continental slope drilling: Reviews of Geeophysics, v. 36, p. 569-601.

Miller, K.G., Kominz, M.A., Browning, J.V., Wright, J.D., Mountain, G.S., Katz, M.E., Sugarman, P.J., Cramer, B.S., Christie-Blick, N and Pekar, S.F. 2005. The Phanerozic record of global sea-level change. Science, 310: 1293-1298.

Mitchum, R.M., Vail, P.R. and Sangree, J.B. 1977a. Seismic stratigraphy and global changes of sea level; Part 2, The depositional sequence as a basic unit for stratigraphic analysis. *In:* C.E. Payton (ed). Seismic stratigraphy; applications to hydrocarbon exploration.. AAPG Memoir no. 26, Tulsa, OK, pp 53-62.

Mitchum, R.M., Vail, P.R. and Sangree, J.B. 1977b. Seismic stratigraphy and global changes of sea level; Part 6, Stratigraphic interpretation of seismic reflection patters and depositional sequences. *In*: C.E. Payton (ed). Seismic stratigraphy; applications to hydrocarbon exploration.. AAPG Memoir no. 26, Tulsa, OK, pp 117-133.

Mitchum, R.M., 1977. Seismic stratigraphy and global changes of sea level; Part 11, Glossary of terms used in seismic stratigraphy. AAPG Memoir no. 26, Tulsa, OK, pp 205-212.

Mitchum, R.M. and Van Wagoner, J.C. 1991. High frequency sequences and their stacking patterns: sequence stratigraphic evidence of high-frequency eustatic cycles. *In:* K.T. Biddle and W. Schlager (eds). The record of sea-level fluctuations. Sedimentary Geology., 70: 131-160.

Mosher, D.C., Erbacher, J., Zuelsdorff, L., Meyer, H., ODP Leg 207 Shipboard Scientific Party. 2005. Stratigraphy of the Demerara Rise, Suriname, South America: a rifted margin, shallow stratigraphic source rock analogue. *In*, Exploring energy systems: 2005 Canadian Association of Petroleum Geologists-American Association of Petroleum Geologists Joint Annual Convention: abstracts; 2005; 8 pages (ESS Cont.# 2004341)

Neal, J., and Abreu, A. 2009. Sequence stratigraphy hierarchy and the accommodation succession method. Geology. v. 37. p. 779-782.

Pindell, J., and Kennan, L. 2005. Mapping and Basin History along the western flank of the Demerara Rise, Suriname. Tectonic Analysis Ltd. For RepsolYPF, Suriname. 1-34

Plint, A.G., Nummedal, D. 2000. The falling stage systems tract: recognition and importance in sequence stratigraphic analysis. *In*: Hunt, D., Gawthorpe, R.L. (eds.). Sedimentary Response to Forced Regression, v. 172. Geol. Soc. London Speci. Publ. p. 1–17.

Posamentier, H.W., and Allen, G.P. 1999. Fundamental concepts of sequence stratigraphy. *In* R.W. Dalrymple (ed). Siliclastic sequence stratigraphy - concepts and applications. SEPM special publications, Tulsa OK. p. 9-51.

Posamentier, H.W., and Kolla, V. 2003. Seismic geomorphology and stratigraphy of depositional elements in deep water settings. Journal of Sedimentary Research. v. 73. p. 367-388.

Posamentier, H.W., and Vail, P.R. 1988. Eustatic controls on clastic deposition II-Sequence and system tract models, sea level changes- An intergrated approach. SEPM special publications. p. 125-154.

Rock Solid Attribute User Guide. Produced by Seismic-Micro-Technology, Inc (2006)

Sangree, J.B., and Widmier, J.M. 1977. Seismic stratigraphy and global changes of sea level; Part 9, Seismic interpretation of clastic depositional facies. *In* C.E. Payton (ed). Seismic stratigraphy; applications to hydrocarbon exploration. AAPG Memoir no. 26, Tulsa, OK, pp165-184.

Sangree, J.B., and Widmier, J.M. 1979. Interpretation of depositional facies from seismic data. Geophysics, 44: 131-160.

Schumm, S.A. 1993. River response to baselevel change: implications for sequence stratigraphy. Journal of Geology 101, 279-294.

Sheriff, R.E., and Geldart, L.P. 1995. Exploration Seismology. Cambridge University Press. Cambridge

Sheriff, R.E. 2002. Encyclopedic dictionary of applied geophysics, 4th edition, Society of Exploration Geophysics, Tulsa, OK.

Sloss, L.L. 1963. Sequences in the cratonic interior of North America. Geologic Society of America Bulletin. 74: 93-113.

Staatsolie Annual Report, 2005. http://www.staatsolie.com/petroleum_inv/browser.html

Staatsolie, 1976, North Coronie (NCO-1) Well Completion Report C-103. Record RDP-W-041

Vail, P.R., 1987. Seismic stratigraphic interpretation using sequence stratigraphy. Part 1. *In:* Bally, A.W. (ed). Atlas of seismic stratigraphy. vol. 1.AAPG Stud. Geology., 27 1-10.

Vail, P.R., Audemard, F., Bowman, S.A., Eisner, P.N., and Perez-Cruz, G. 1991. The stratigraphic signatures of tectonics, eustacy and sedimentation— an overview. *In*: G. Einsele, W. Ricken and A. Seilacher, Editors, Cyclic Stratigraphy, Springer-Verlag, New York (1991), pp. 617–659.

Vail, P.R., Hardenbol, J. and Todd, R.G. 1984. Jurassic unconformities, chronostratigraphy and sea level changes from seismic and biostratigraphy. *In:*J.S. Schlee (ed). Interregional unconformities and hydrocarbon accumulation, AAPG Memoir 36: 347-363

Vail, P.R., Mitchum, R.M., Todd, Jr., R.G., Widmier, J.M., Thompson, S., III, and Sangree, J.B. 1977. Seismic stratigraphy and global changes of sea level. *In*: C.E. Payton (ed). Seismic stratigraphy—applications to hydrocarbon exploration, American Association of Petroleum Geologist Memoir vol. 26. pp. 49–212 Tulsa.

Van Wagoner, J.C., Posamentier, H.W., Mitchum, R.M., Vail, P.R., Sarg, J.F., Loutit, T.S., Hardenbol, J. 1988. An overview of sequence stratigraphy and key definitions. *In:* Wilgus, C.K., Hastings, B.S., Kendall, C.G., St.C., Posamentier, H.W., Ross, C.A., Van Wagoner, J.C. (eds.), Sea Level Changes—An Integrated Approach, v. 42. SEPM Special Publication. p. 39–45.

Veeken, P.C.H. 2007.Seismic stratigraphy, basin analysis and reservoir characterization. K. Helbig and S. Treitel (eds). Handbook of Geophysical exploration, seismic exploration. Oxford: Elsevier Press. 37: pp. 78-92.

Wong, T.E., 1992. Quaternary stratigraphy of Suriname. *In*: Prost, M.T. & Charron, C., editors. Évolution des littoraux de Guyane et de la zone caraïbe méridionale pendant le Quaternaire - Symp. PICG 274/ORSTOM - ORSTOM, Paris: 559-578.

Wong, T.E., Krook, L., Zonneveld, J.I.S., 1998. Investigations in the Suriname coastal plain and offshore area. *In*: Wong, TE, de Vletter, DR, Krook, L, Zonneveld, JIS, van Loon, AJ (eds). The history of the earth sciences in Suriname. Royal Netherlands Academy of Arts and Sciences, Netherlands Institute of Applied Geoscience TNO; 1998. p. 3–100. Amsterdam, Netherlands.

Workman, W. 2000. Guyana basin: A new exploration focus. World Oil Magazine. P. 55-60

Yilmaz, O. 1987. Seismic Data Processing. Society of Exploration Geophysics, Tulsa, OK.

Zachos, J.C., Pagani, M., Sloan, L., Thomas, E., and Billups, K. 2001. Trends, rhythms, and abbreviations in global climate 65 Ma to present. Science. 292: 686-693.

APPENDIX I: DATA

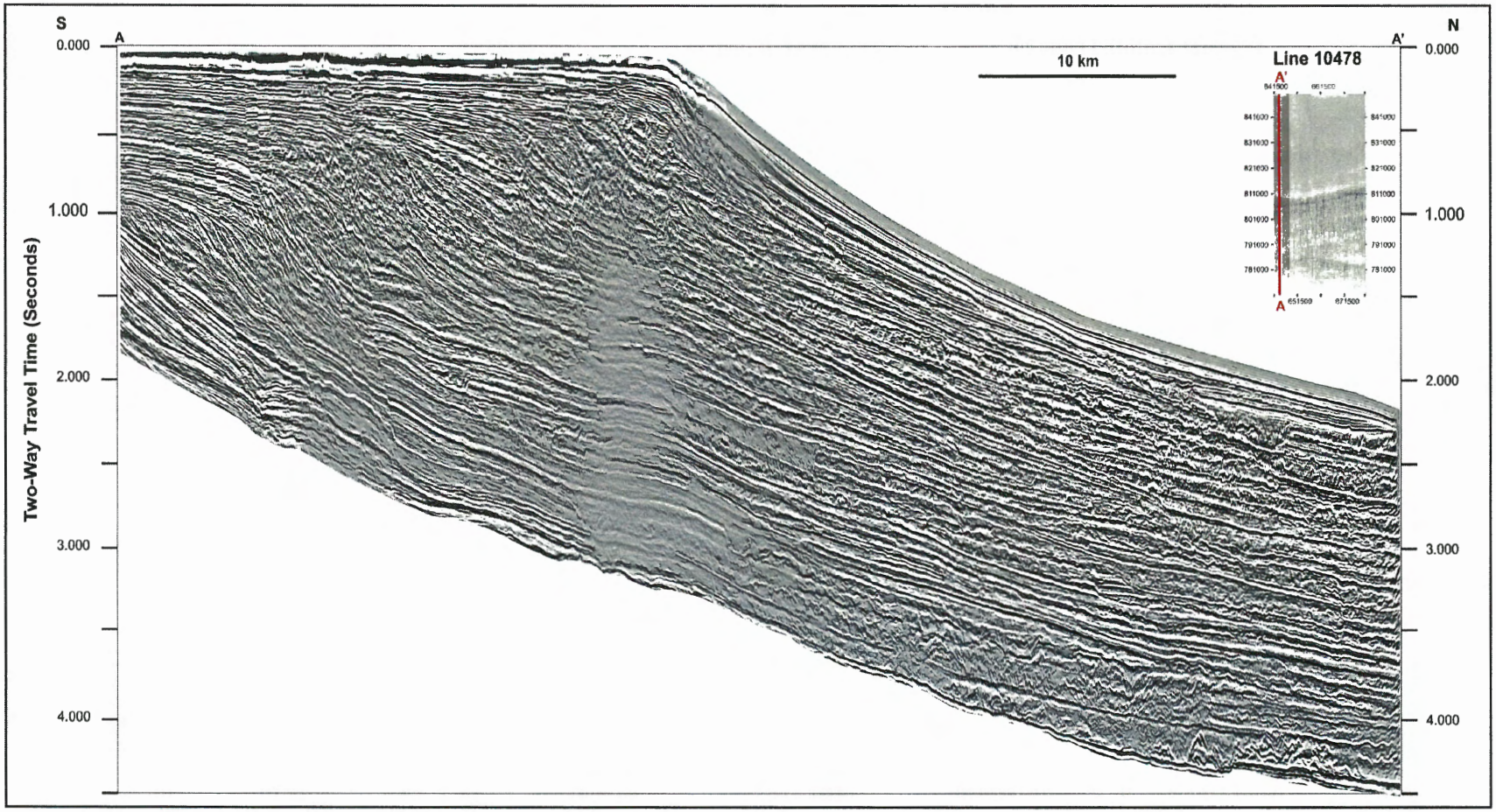

Data used for: Figure 3.2, Figure 3.12, Figure 4.1, and Figures 4.4 to 4.10.

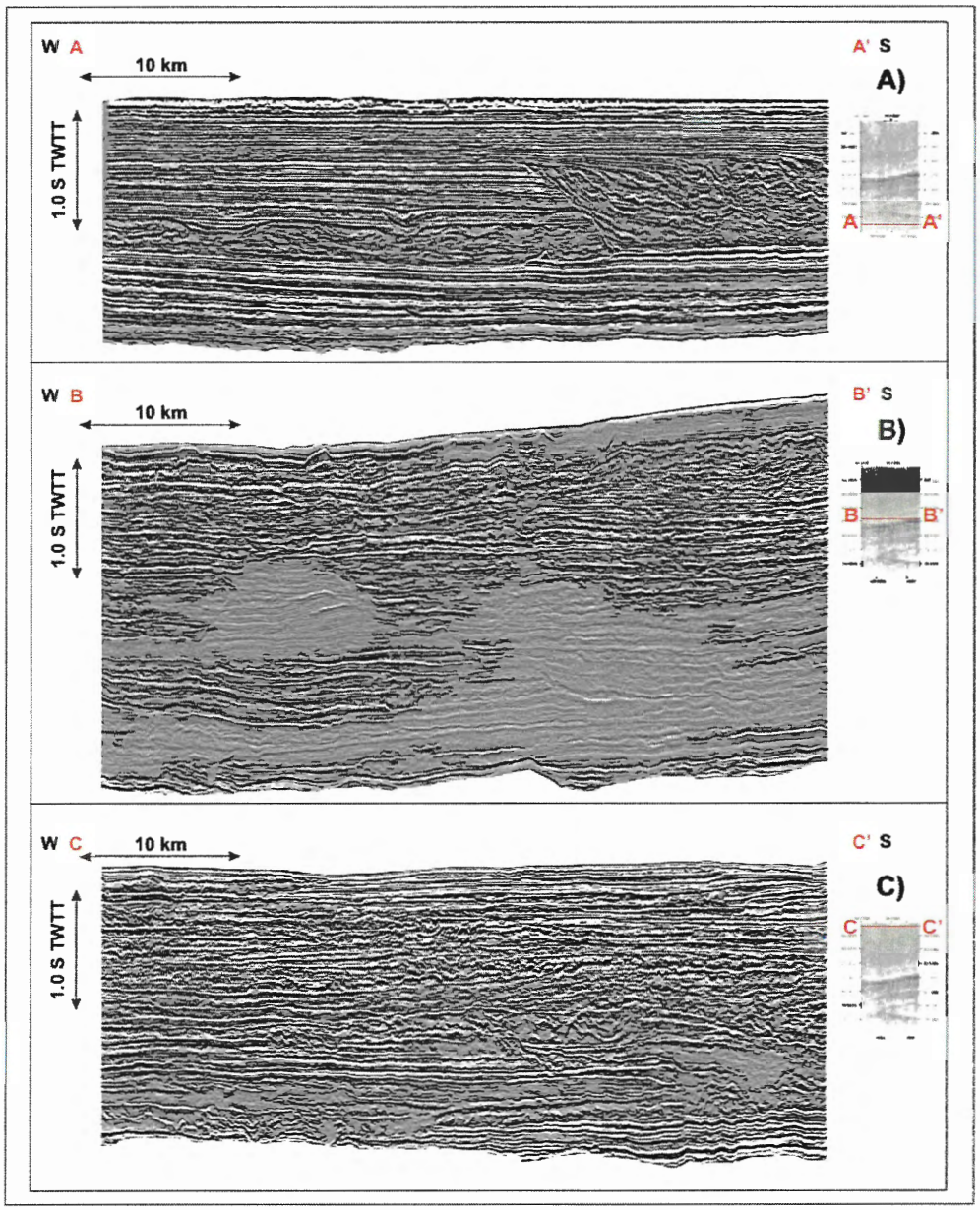

Data used for: Figures 3.3 and 3.15

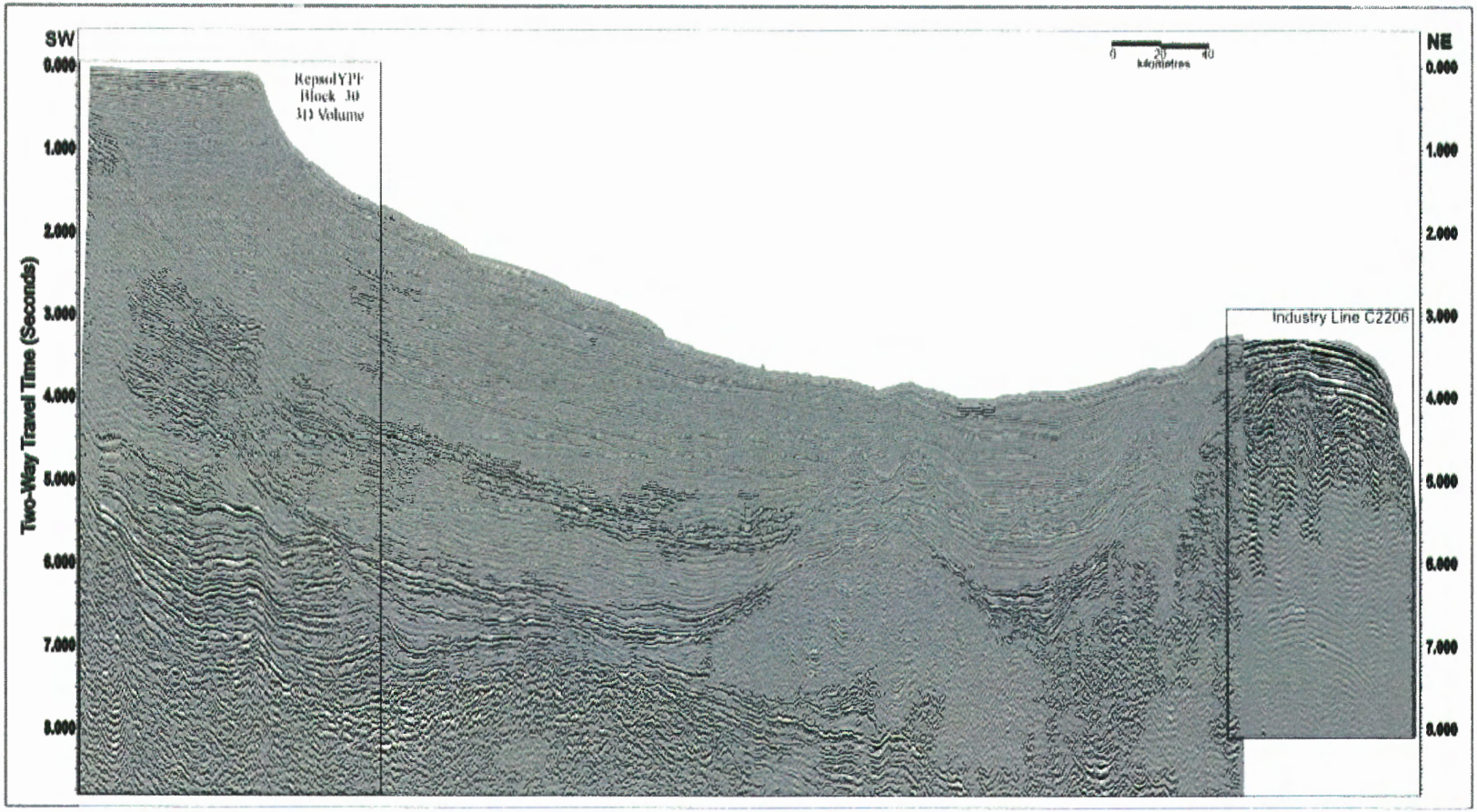

Data used for: Figure 3.4

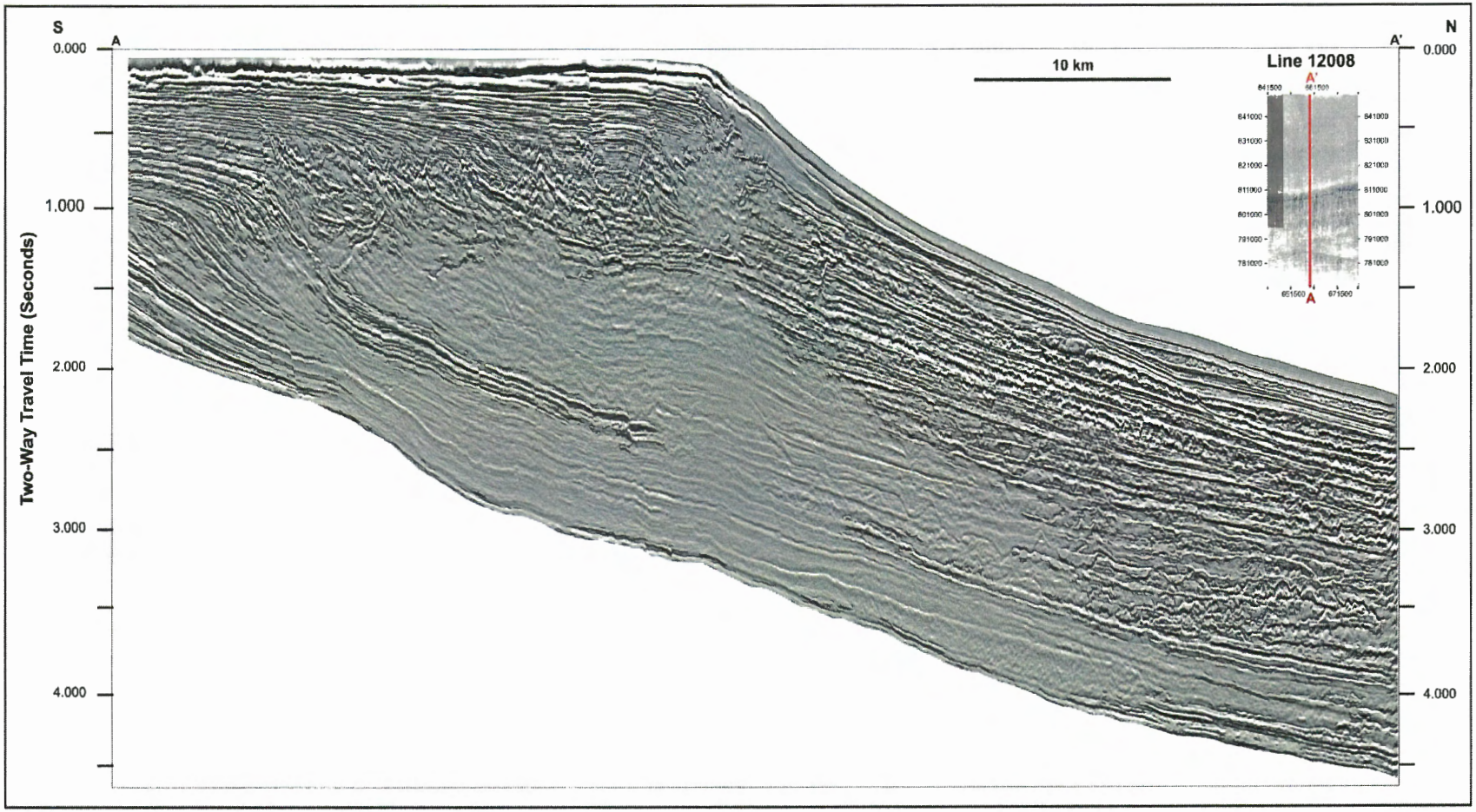

Data used for: Figures 3.13 and 4.2.

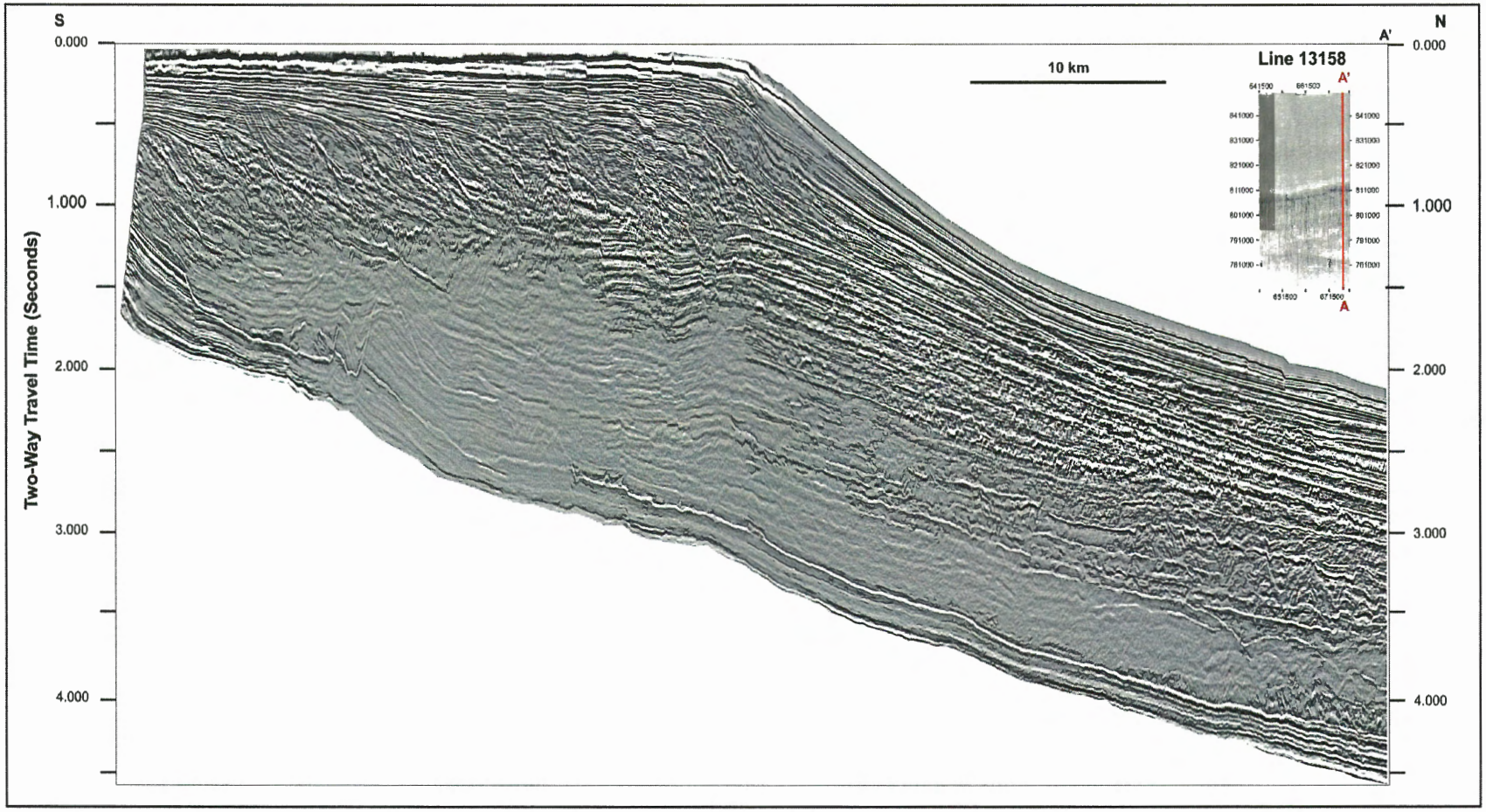

Data used for: Figures 3.14 and 4.3.

APPENDIX II: SHALLOW GEOHAZARD ASSESMENT

Shallow Geohazard Assessment, RepsolYPF Block30, Demerara Rise, offshore Suriname, South America

Shawn J. Goss and David C. Mosher,
Depts. Earth Sciences and Oceanography,
Dalhousie University,
Halifax, NS
Canada

DALHOUSIE UNIVERSITY

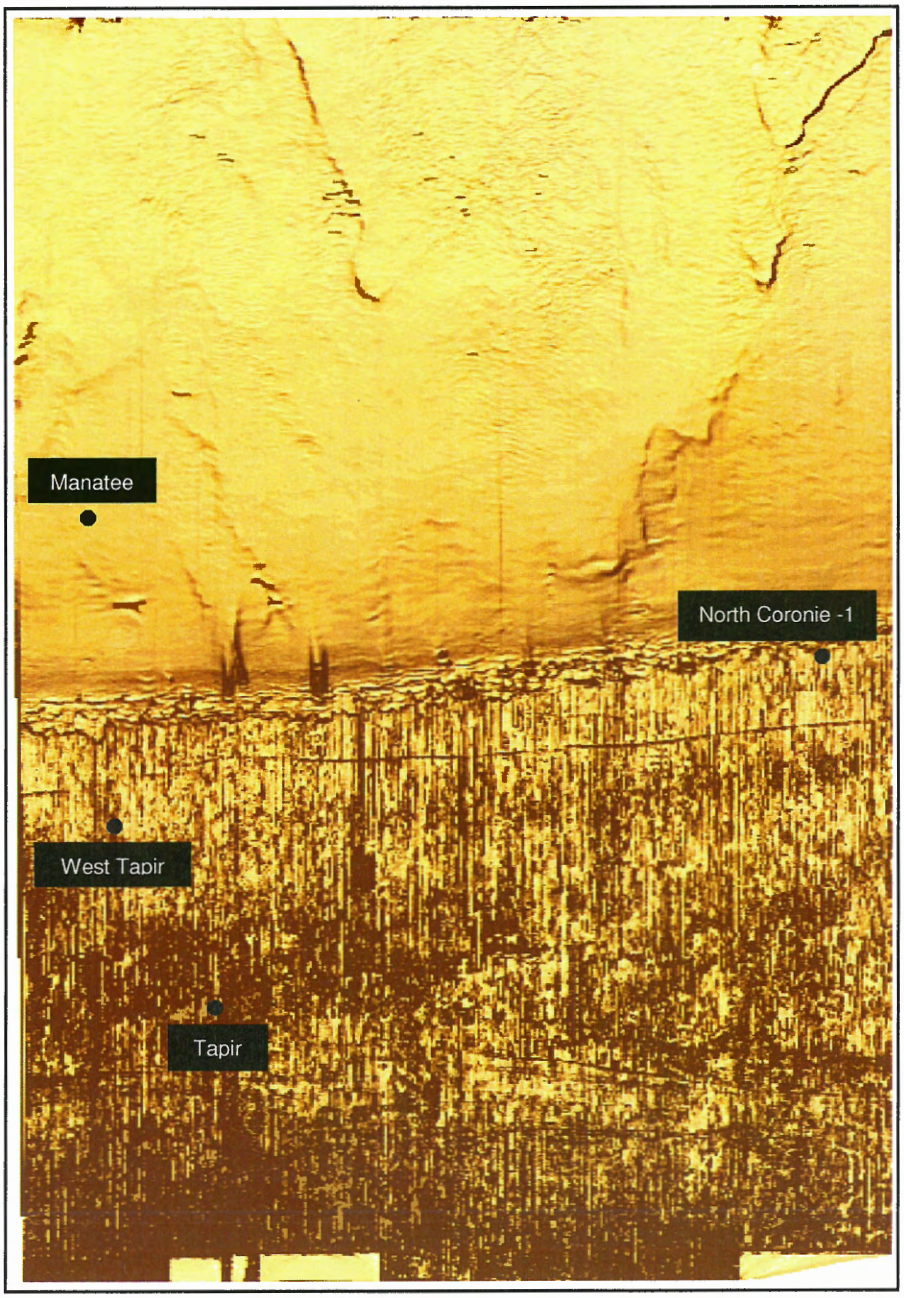

EXECUTIVE SUMMARY

The 3D seismic volume from Repsol YPF Block 30 of the Suriname continental margin transits from the shelf to slope environments. The region is a passive continental margin and seismicity is rare. A number of features are identified from the shallow, near surface section that represent potential geohazards or constraints to offshore hydrocarbon development.

1) **Shallow faults** break the seafloor producing clear offsets that correlate across the width of the survey area. Faults provide conduits for overpressured gas and fluids and provide planes of weakness for initiation of mass failures. Faults parallel the shelf break and extend laterally for significant distances, suggesting they are related to sediment loading and subsidence, further increasing their potential role in sediment mass failure. A major fault that offsets the seafloor breaks within 2 km of the West Tapir drill site.
2) **Hard substrate:** Variable and high amplitude reflections occur on the shelf. Combined with outcropping reflectors, these features suggest an erosional environment with a hard substrate. Strong currents, therefore, may be present.
3) **Bright spots** (high amplitude anomalies) are common beneath the uppermost slope. These anomalies possibly represent shallow gas or sand bodies (channels). The may be indicative of shallow overpressure, which in turn may pre-condition the sediments to mass failure. In this region also, seafloor slope angles are steepest (~3°) and there is evidence of buried headscarps suggesting mass-failures have occurred.
4) A possible **BSR** (bottom simulating reflector), indicative of the base of gas hydrate, was noted in the upperslope region. Gas hydrate dissociation can lead to formation overpressures and lead to slope failure.
5) **Mass transport deposits** are indicated by bodies of incoherent reflections with irregular contacts and surface renders showing 0.1 s high head scarps, lateral escarpments, and rugose surface patterns fanning out downslope. Although the low angles of the slope in this region suggest static stability, these deposits indicate mass failures have occurred in the past. Trigger mechanisms are unknown, but possibly relate to ground motions due to rare earthquakes. Shallow gas, gas hydrate dissociation and periods of high sediment input may be contributing factors. Recurrence intervals are unknown but presumably are rare because of the combination of events required to initiate failure. The shallowest mass transport deposit is buried by ~0.2 s of parallel, coherent reflections forming the present seafloor. Shallow mass transport deposits can consist of a variety of lithologies of varying strength properties and states of consolidation. They can; therefore, pose drilling difficulties.

.

TABLE OF CONTENTS

1.0 INTRODUCTION

1.1 Purpose:

This preliminary report summarizes results obtained from initial study of 3D seismic data from the Western Demerara Rise in the Repsol YPF block 30. The purpose of this study was to investigate these data for evidence of shallow geohazards and geologic constraints to offshore exploratory drilling and potential hydrocarbon development.

1.2 Location

The study area lies on the shelf and upper slope in ~ 100 to ~1750 m of water depth just west of the Demerara Rise, between latitudes of approximately 7°N and 9°N and longitudes 54° and 56°W (Figs. 1 and 2). The shelf break is indicated by a change in slope gradient from essentially zero (<0.5°) to almost 5°, which corresponds with approximately the 175 m contour (Fig. 2). In gross scale, the region encompasses a generally expressionless seafloor and gently dipping platform without significant regional or large-scale morphological features.

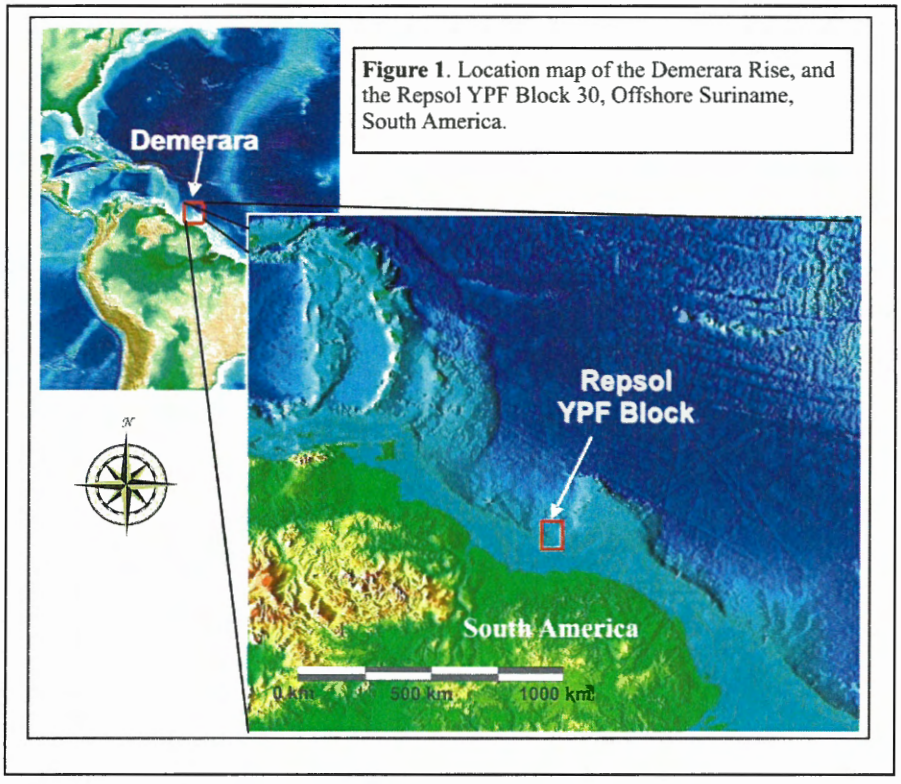

Figure 1. Location map of the Demerara Rise, and the Repsol YPF Block 30, Offshore Suriname, South America.

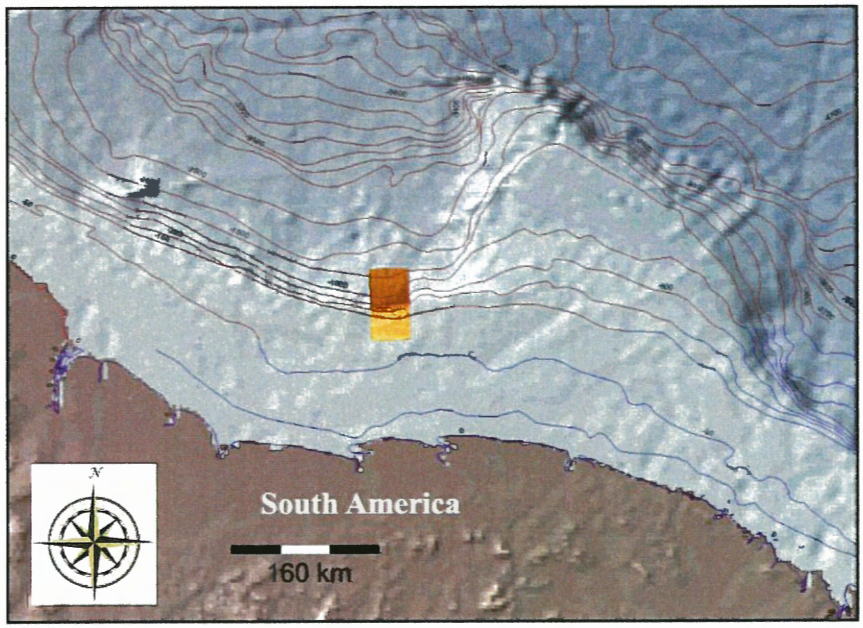

Figure 2. Location diagram of Repsol YPF Block 30 with depth contours.

1.3 Tectonic Setting

The Demerara Rise is built on Precambrian and early Mesozoic aged continental crust. It is believed that the Guinea Plateau (Western Africa) and the Demerara Rise are conjugate margins (Figs. 3 and 4) that formed the southern border of the central Atlantic margin during Jurassic times prior to rifting (Benkhelil et al., 1995; Mosher et al., 2007). At the onset of Middle Jurassic rifting, the Demerara Rise was contiguous with the Guinea Plateau of West Africa, and its composite terrain was contiguous with the SE limit of the continental crust beneath the Grand Banks of the Bahamas. In the central Atlantic, north-south rifting causing east-west extension with a large component of dextral shearing initiated about 180 Ma (Mascle et al., 1988; Mosher et al., 2007). This rifting initiated synsedimentary normal and strike-slip faulting (Mosher et al., 2005, 2007). Complexities caused by plate rotation resulted in a late compressional phase before final rifting. This compression led to en échelon folding and flower structures within the Demerara Rise.

Beneath the Demerara Rise, a Late Aptian and Late Albian double unconformity is reported within the sedimentary section (Benkhelil et at., 1995; Erbacher et al., 2004; Mosher et al., 2005, 2007). The first unconformity may be correlated with the formation of en échelon folds. While the late Albian event resulted from the main compression phase and is recorded by a strikingly prominent unconformity easily distinguishable temporally and spatially across the Demerara and Guinea Plateaus (Benkhelil et at., 1995; Erbacher et al., 2004; Mosher et al., 2005, 2007).

Following the minor recurrence of compressive tectonics, an extensional regime ensued during the Late Cretaceous. This regime is characterized by a general collapse of

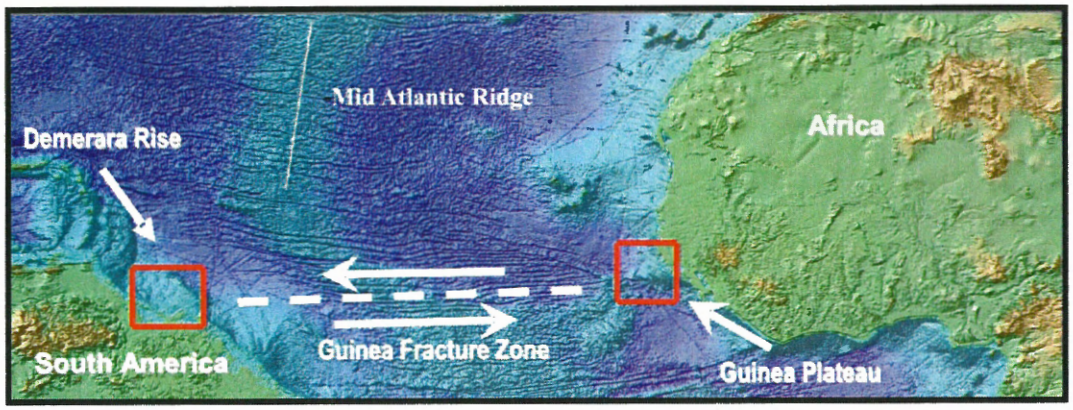

Figure 3. Location of the Demerara Rise and Guinea Plateau conjugate margins separated along the Guinea Fracture Zone (Modifed after Mosher et al, 2007)

the margin, resulting in the final parting between the African and South American continental plates and creation of oceanic crust (Benkhelil et al., 1995). Subsidence was presumably rapid, along with continental synrift sedimentation filling the accommodation space provided by this subsidence (Flicotaux et al., 1988; Mosher et al., 2007). Global sea level continued to rise throughout this period, and reached its highest levels in the Turonina (Haq et al., 1988; Mosher et al., 2007). Tectonic deformation ceased in the Late Cretaceous, followed by normal cooling subsidence as a largely clastic cover was deposited over the previous rift graben on the Demerara Rise (Gouyet et al., 1994).

Today the Suriname margin is a classic "Atlantic Type" passive continental margin. Present equatorial Atlantic spreading rates between South America and West Africa are 28.74 mm/year, thus about half that is accommodated by westward drift of South America. Regional reports for Suriname and French Guyana show little evidence of historical seismicity. The USGS Global Seismic Hazard Assessment Program reports a moderate to severe earthquake generated at 10 km depth, with magnitude 5.2 occurred NNE of Cayenne, French Guiana (1471 miles NE of Paramaribo, Suriname) on March 21, 2007. This event is unique for the Suriname margin in the USGS database. The National Geophysical Data Center lacks historical of seismicity data for Suriname, but Guyana reported a severe earthquake in August, 1774 of unknown magnitude. No further seismological hazard data has been reported for the offshore regions of French Guyana, Guyana, or Suriname. Additionally, gravity data show the region to be in isostatic equilibrium (Lithgow-Bertelloni and Gurnis, 1997).

1.4 Bathymetry

The modern bathymetry offshore Suriname resulted from its tectonic framework overprinted by subsequent Paleogene and Neogene sedimentation and subsidence. The continental shelf lies between the coast and 200 m water depth and is on average 160 km wide (Fig. 2). The continental slope lies between the 200 and 3000 m isobath and is about 130 km wide near the study area. Its average slope angle is 1.2°. The Demerara Rise is an anomaly along the margin, protruding some 220 km northward from the shelf into the

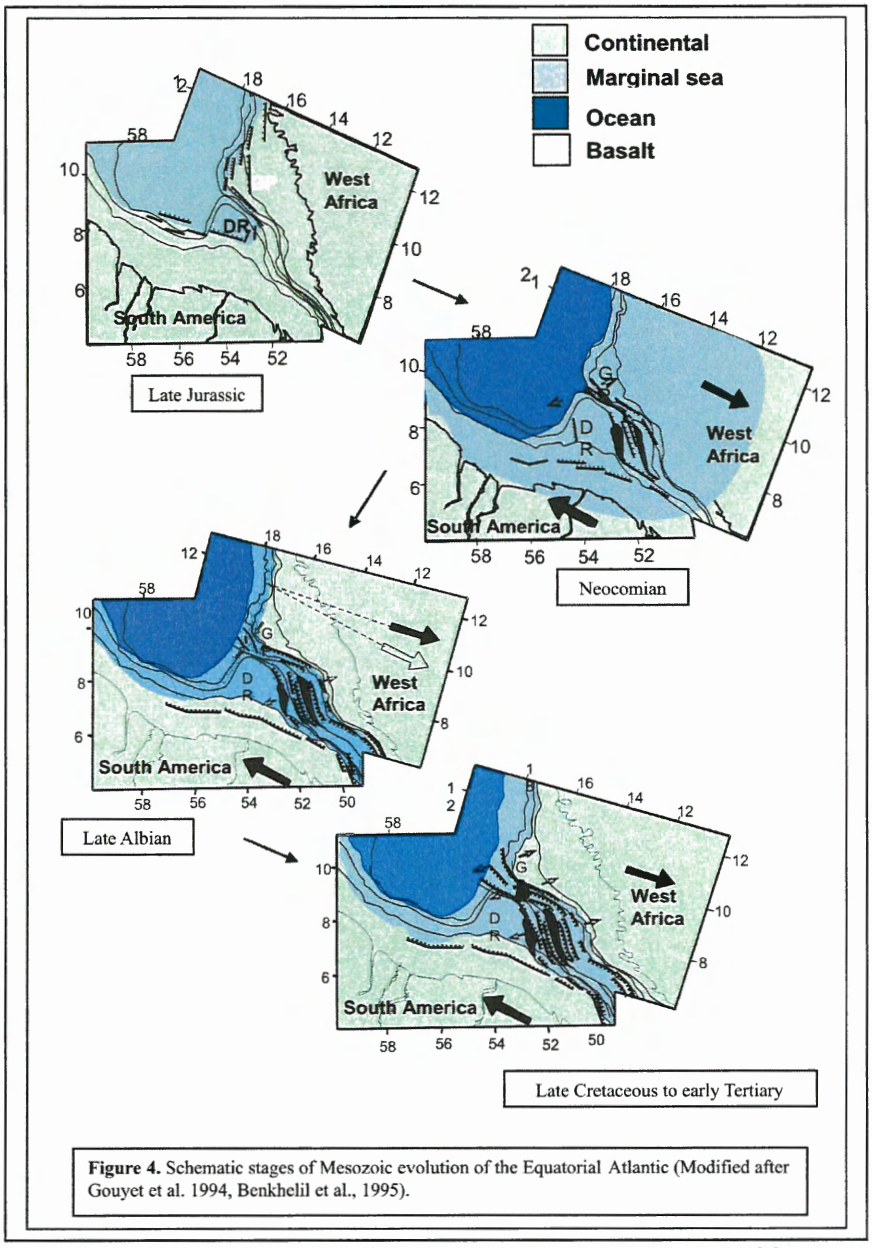

Figure 4. Schematic stages of Mesozoic evolution of the Equatorial Atlantic (Modified after Gouyet et al. 1994, Benkhelil et al., 1995).

equatorial Atlantic (Fig. 2). It is a gently dipping ramp to about 1500 m water depth before dropping rapidly to abyssal depths at its easternmost flank. This flank is a remnant transform margin. The Rise forms a plateau that is about 56,000 km^2 in area. The study area is located at the innermost edge of this plateau, just as the contours turn northward along its western flank (Fig. 2).

Bathymetry for the study area derived from the 3D seismic volume is shown in Figure 5. The area encompasses the outer shelf, lying in less than 200 m water depth, and the continental slope down to 3000 m. The focus of the study is the area surrounding the West Tapir drill site, for which there is a reprocessed 3D seismic subset volume. This volume is on the shelf in water depths of 100 to 175 m (Fig. 6).

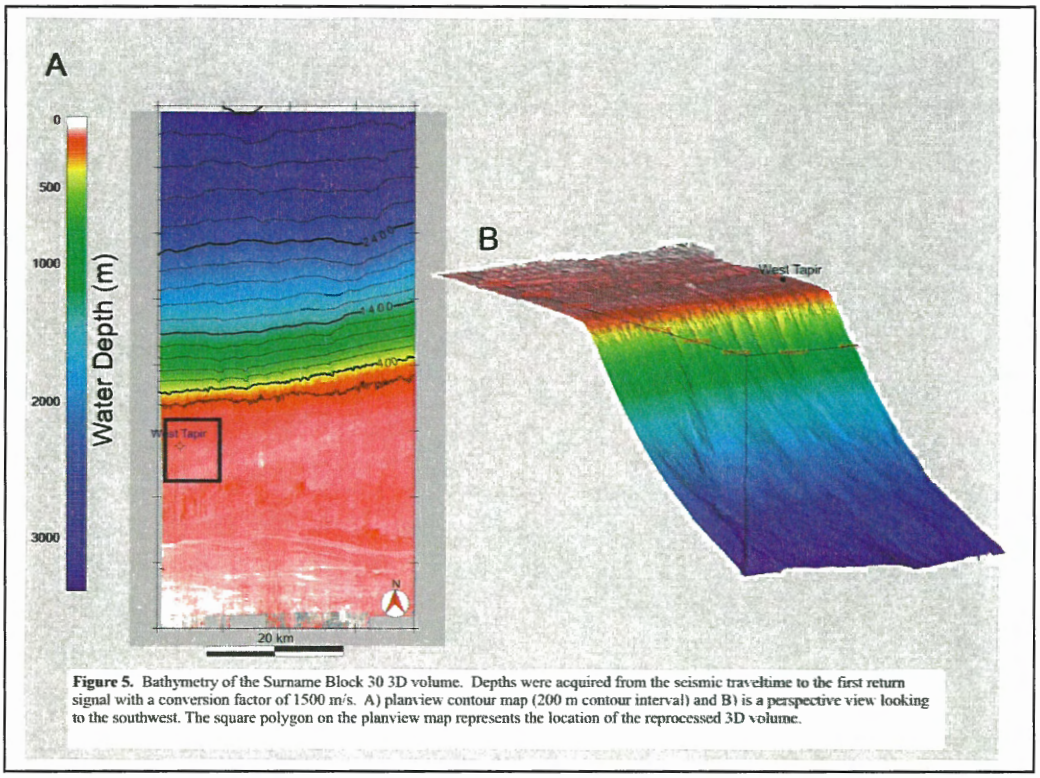

Figure 5. Bathymetry of the Surname Block 30 3D volume. Depths were acquired from the seismic traveltime to the first return signal with a conversion factor of 1500 m/s. A) planview contour map (200 m contour interval) and B) is a perspective view looking to the southwest. The square polygon on the planview map represents the location of the reprocessed 3D volume.

2.0 METHODS

Regional bathymetric data were derived from the ETOPO2 grid, downloaded from the National Geophysical Data Centre and gridded and imaged with ArcMAP. The sole data source for this investigation were 3D seismic data from the RepsolYPF Block 30 survey (Repsol_sur_blk30_final_mig_2x2_grid_final_migration.sgy). Bathymetry data for the survey area were derived from the seafloor first return pick; traveltime converted to water depth assuming a water column velocity of 1500 m/s (Fig. 5). Slope angle data were generated from these surface picked surfaces. The 3D seismic data form a 79.5 x 38.5 km grid of 25 x 25 m bin space (Fig. 5). Maximum horizontal resolution, therefore, is not better than 50 m (assuming Nyquist sampling theorem). Seismic frequencies span from 5 to 70 Hz, with peak energy about 15 Hz. At 70 Hz and assuming a velocity of 1500 m/s (water velocity), the maximum vertical resolution is about 5 m (1/4λ (wavelength) according to the Rayleigh criteria). Resolution deteriorates with depth as velocities increase and higher frequencies attenuate.

Data were loaded into Seismic-Micro Technologies™ Kingdom Suite interpretation software. Seismic stratigraphic horizons, defined by key high amplitude reflectors or noticeable changes in acoustic character, were digitally correlated throughout the data volume. Horizon data were exported to ArcMAP™ for surface rendering and deriving slope angles as well as to integrate with other geographic data.

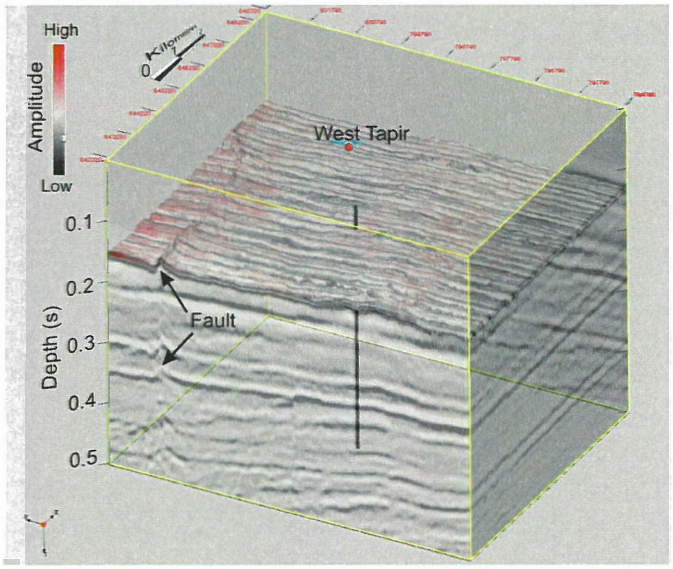

Figure 6. Block diagram of the reprocessed West Tapir 3D seismic subset. The *top is* the seafloor. The seafloor (top surface) is draped with reflection amplitude, showing amplitude variations across the volume. North-trending lineations are survey artefacts. In profile, subsurface faults are readily apparent, the northernmost one clearly offsets the seafloor.

3.0 RESULTS

3.1 Seismic Stratigraphy

3.1.1 Shelf

Shallow seismic data on the continental shelf from the full 3D seismic volume are of poor quality. This result is likely due to poor static correction, poor data stacking velocity models, multiple interference and high amplitude returns from the seafloor geology. Data quality improves considerable in the reprocessed 50 km^2 volume on the shelf, but survey artefacts in the form of strong linear data trends in the survey inline direction are apparent (Fig. 6). These are possibly related to poor static corrections in the array. The first high amplitude seismic return signal of these data represents the seafloor. A morphological render of this return within the reprocessed volume shows a generally expressionless seafloor (aside from the linear artefacts) (Fig. 7). An amplitude map of this surface shows amplitude variations across the volume, trending in general from high amplitude in the inboard portion to lower amplitudes outboard, despite little change in water depth (Fig. 6). High amplitude variations appear to be real and may indicate the intermittent presence of carbonate hardground or carbonate concretions. The West Tapir well site lies in one of these high amplitude areas.

Numerous listric-normal faults are present beneath the shelf to the southernmost extent of the study area (Figs. 6 to 8). These faults have a general trend of E-W or ESE-WNW, except one major fault that trends ENE-WSW. Seafloor expressions of some of these faults are noted (Figs. 6 to 8) and one of the main faults trends just north of the West Tapir drill site (Fig. 6). The nature of the fault surfaces is concave upward, with dips decreasing with depth (Fig. 8). These faults are responsible for minor offset (<0.03 s) of reflections from the sediment sea-floor interface to depths of 2.75 s twtt.

Below the seafloor of the shelf, reflection amplitudes are generally high with strong lateral coherency (Fig. 9). In dip section, these reflections offlap with dips on the shelf of less than 0.1° and the section thickens northwards (offshore) (Fig. 9 top). Along strike, reflections are largely parallel and laterally extensive (Fig. 9 bottom). Below a strong reflector at 0.6 to 0.8 s, reflections become nearly incoherent with apparent folds and contortion of reflection events. Despite this lateral incoherency along strike, in dip profile the offlap reflection pattern continues. Clearly this seismic facies change

represents a lithologic/structural change with probable strong lateral variability in the deeper incoherent section.

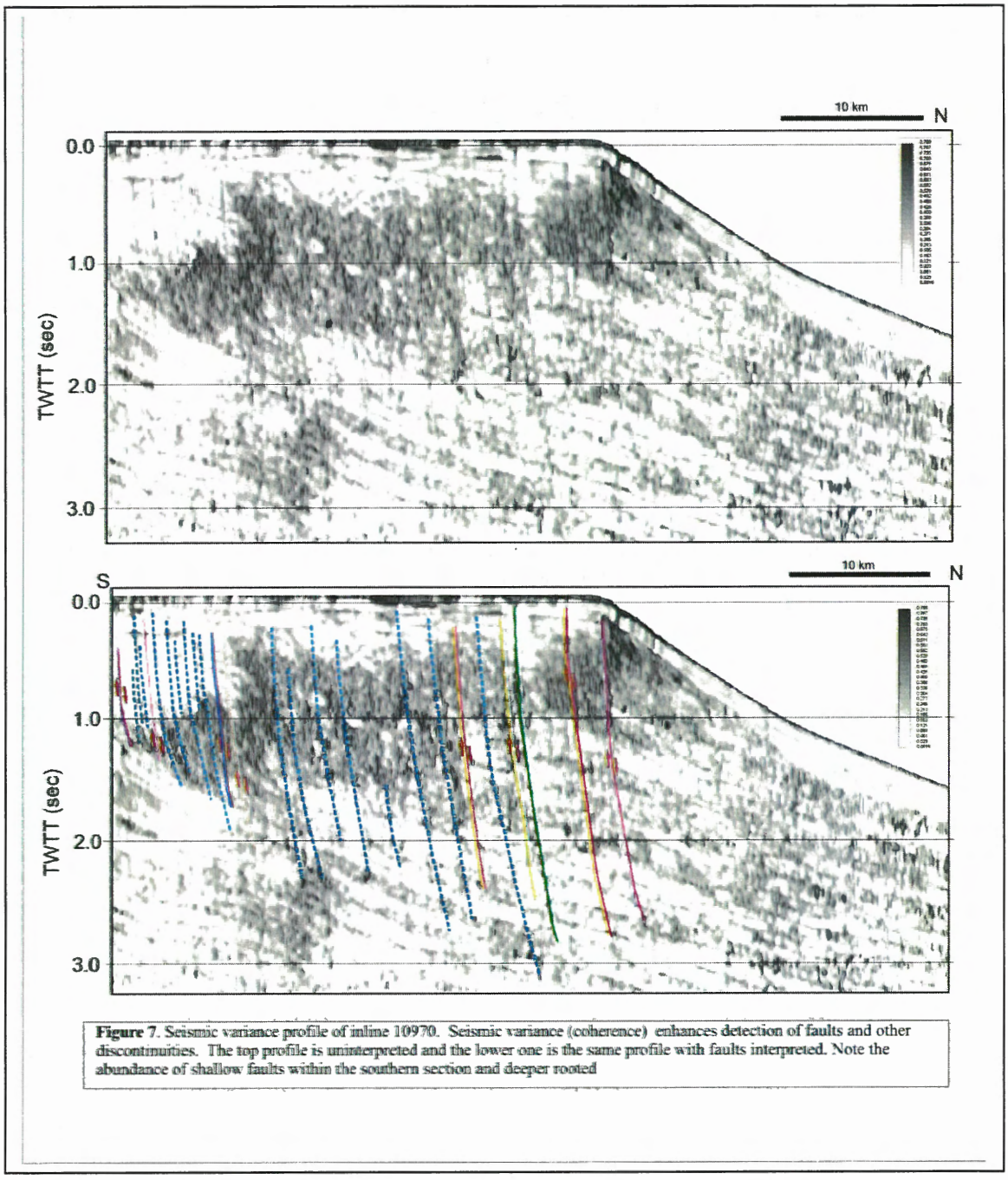

Figure 7. Seismic variance profile of inline 10970. Seismic variance (coherence) enhances detection of faults and other discontinuities. The top profile is uninterpreted and the lower one is the same profile with faults interpreted. Note the abundance of shallow faults within the southern section and deeper rooted

3.1.2 Shelf break

The shelf break occurs in about 200 m water depth (Fig. 5), marking a change from <0.5° to 3.0° in slope angle (Figs. 10 and 11). Shallow reflection data under the position of the shelf break are of low amplitude (Fig. 10). The section beneath the shelf break and uppermost slope becomes incoherent below 0.2 to 0.4 s subbottom. Generally,

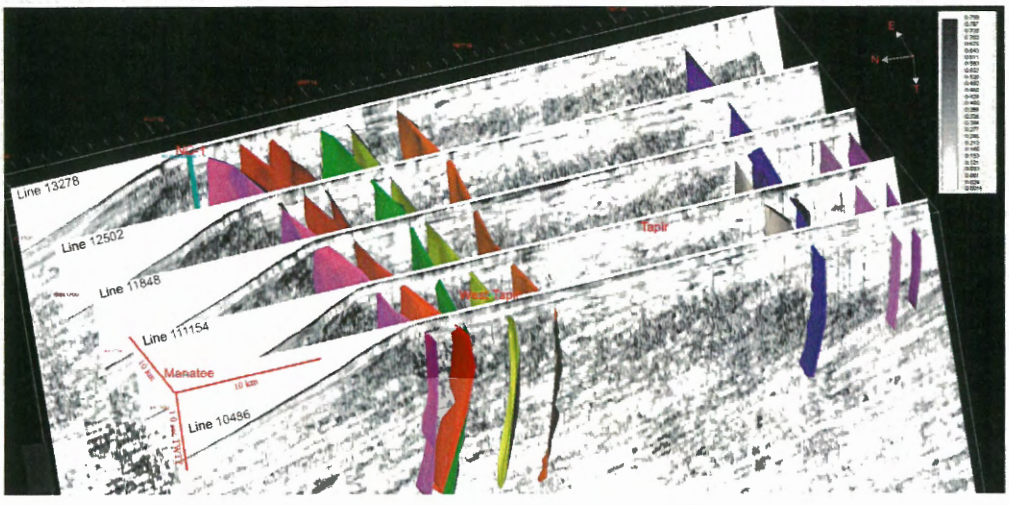

Figure 8. Selected fault planes interpreted from the 3D seismic volume and superimposed within selected variance profiles. This figure illustrates the steep listric nature of the faults parallelling the margin, as well as their lateral continuity. The West Tapir well location is indicated.

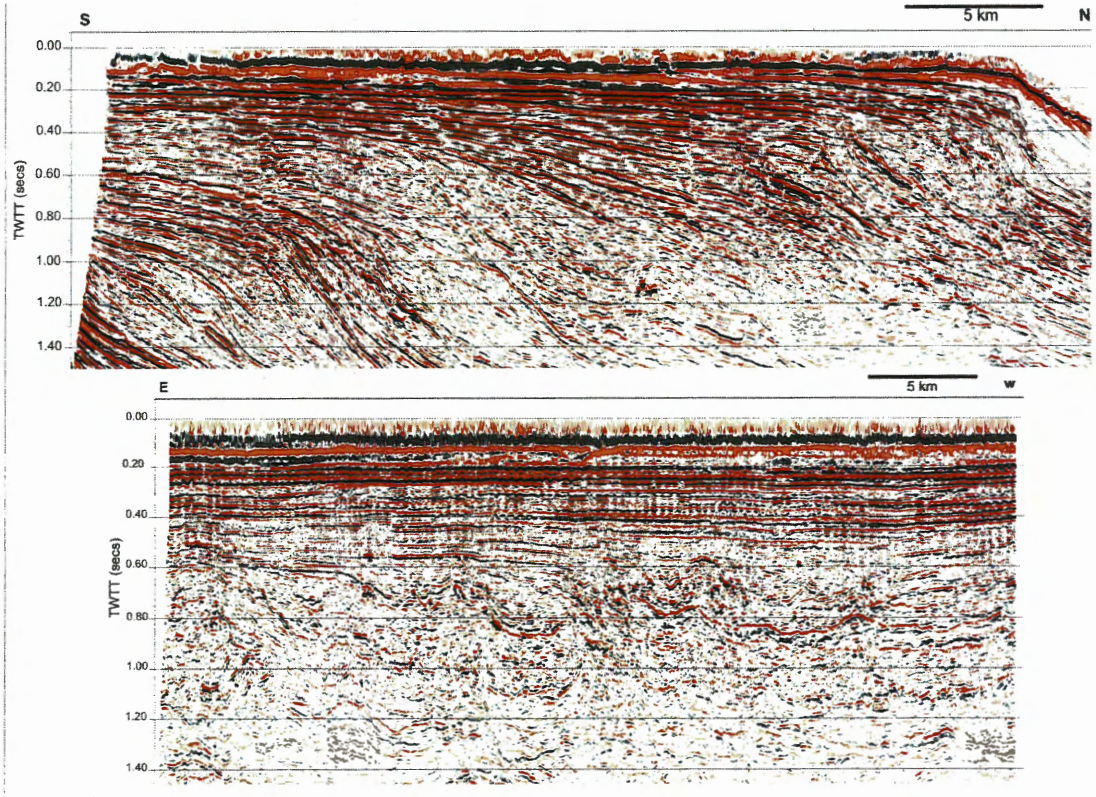

Figure 9. Top: Dip oriented seismic profile across the shelf (inline 10970), illustrating off-lapping reflections underlying the shelf. **Bottom:** Seismic profile (crossline 6084) at the 100 m isobath illustrating high amplitude and strong lateral coherency of reflections in the top 0.5 s of the section under the shelf. It also clearly demonstrates the seismic facies change at about 0.6 s TWTT.

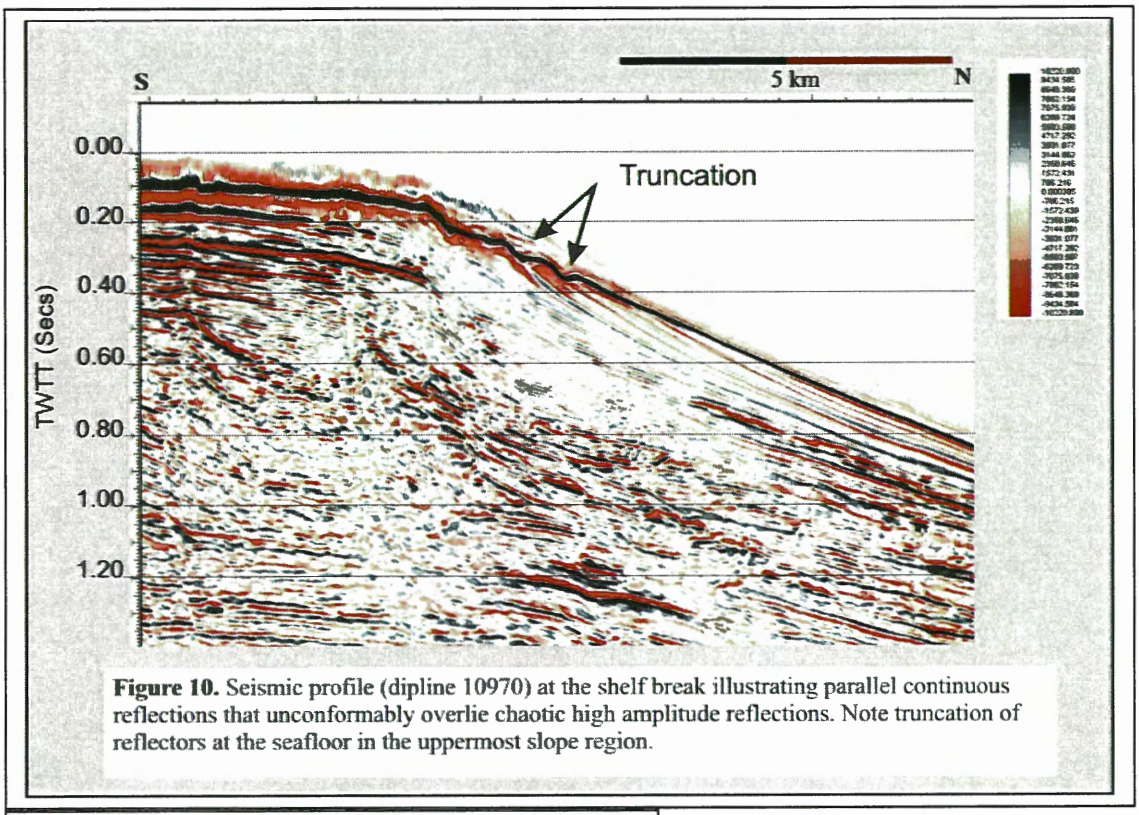

Figure 10. Seismic profile (dipline 10970) at the shelf break illustrating parallel continuous reflections that unconformably overlie chaotic high amplitude reflections. Note truncation of reflectors at the seafloor in the uppermost slope region.

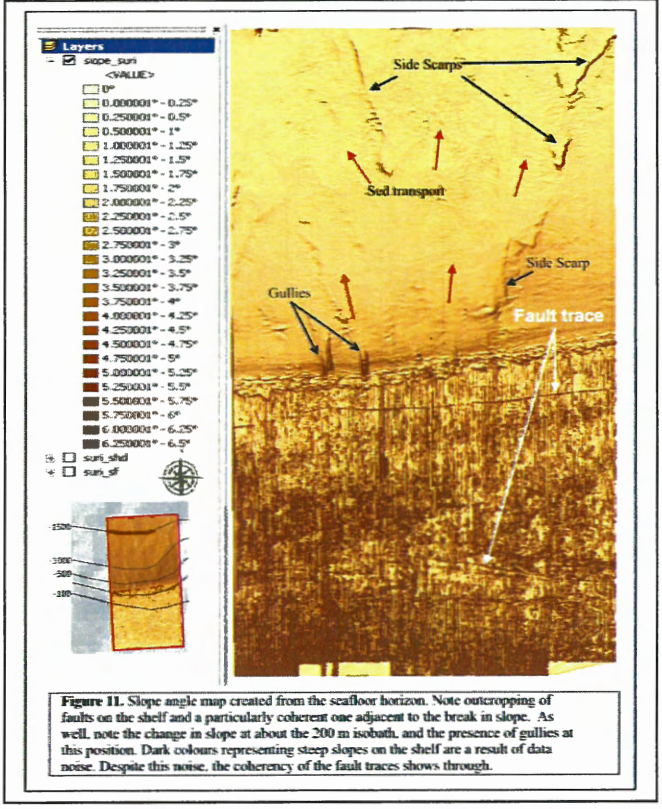

Figure 11. Slope angle map created from the seafloor horizon. Note outcropping of faults on the shelf and a particularly coherent one adjacent to the break in slope. As well, note the change in slope at about the 200 m isobath, and the presence of gullies at this position. Dark colours representing steep slopes on the shelf are a result of data noise. Despite this noise, the coherency of the fault traces shows through.

reflections offlap the shelf edge, leading to a progradational wedge of nearly parallel reflections on the slope. The seafloor in this region is marked by many small indentations giving a ridge and gully morphology (Figs. 10 and 11). In addition, the shallowest reflections from the slope clearly truncate against the seafloor in this uppermost slope region (Fig. 10). This truncation and gully morphology suggests erosive off-shelf flow and possible sediment transport is occurring in the modern environment.

3.1.3 Slope

The low amplitude reflections beneath the shelf break increase in amplitude downslope and in general there is a thinning of the sediment section distal from the margin (i.e. basinwards) (Fig. 12). A morphologic render of the seafloor horizon shows a relatively

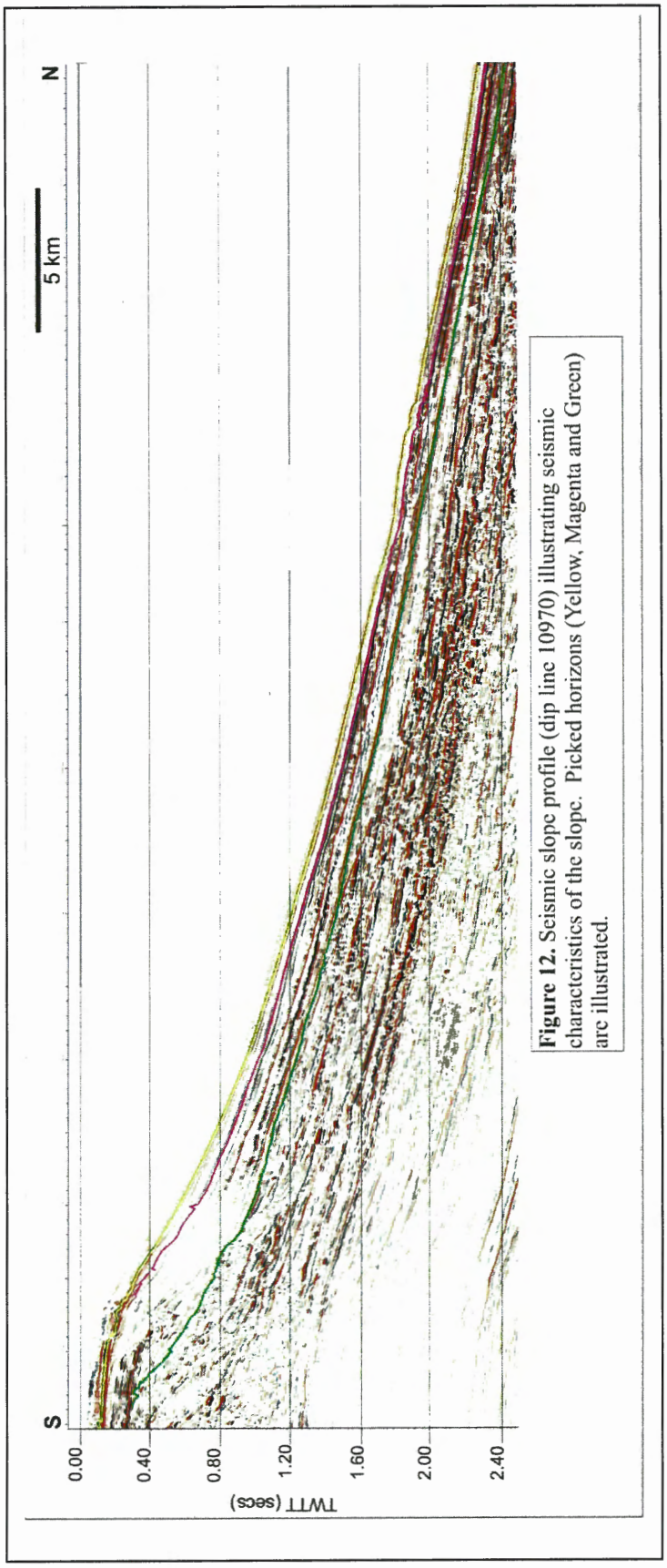

Figure 12. Seismic slope profile (dip line 10970) illustrating seismic characteristics of the slope. Picked horizons (Yellow, Magenta and Green) are illustrated.

featureless slope, with the exception of the aforementioned gullies at the break in slope and a single channel that extends the length of the slope within the limits of the study area (Fig. 13). Below 1200 m water depth, the seafloor is overprinted with escarpments and a rugose morphology that is somewhat subdued, suggesting it is draped with sediment. Slope angles are low, ranging from about 3° in the uppermost slope/shelf break region to 1.5° on the lower slope (Fig. 11). Steep slope angles occur only locally on the edges of gully's and escarpments.

In the seismic section of the slope, there are discrete seismic facies including largely strong amplitude and coherent events that dip to the north at approximately 1.7° and pinch out in the downslope direction (Fig. 14). These are intercalated with packages of incoherent reflections that form wedge-shaped units within this succession (Fig. 14). These patterns of reflections are interpreted as probable mass transport deposits (MTD) interbedded with turbidites and probable hemipelagic material (Fig. 14). Morphologic renders of some the subsurface

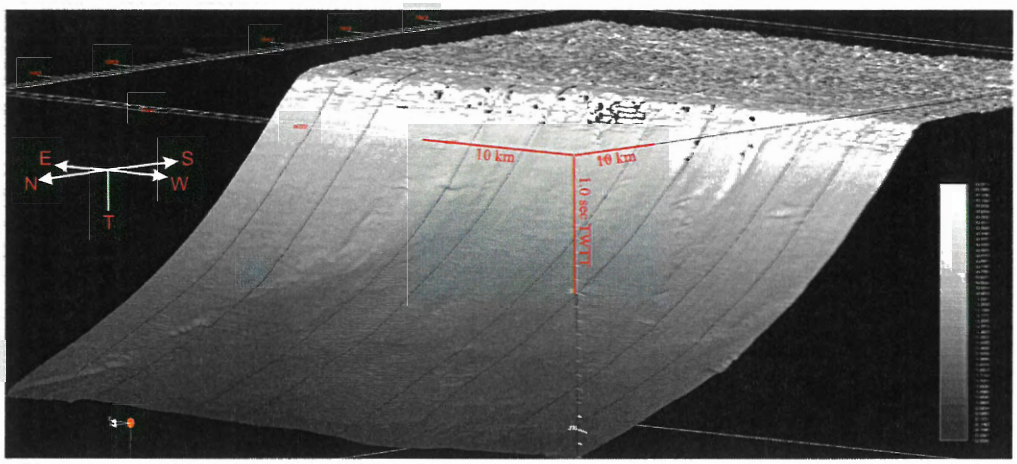

Figure 13. Perspective view of a rendering of the seafloor in the study area looking SE and showing the morphology of the slope.

reflection horizons reveal the complexity of these MTD's and erosional sediment transport processes (Fig. 15). These data clearly reveal a history of at least minor slope failure.

Beneath the slope, particularly in the upper slope region, are patches of high amplitude, phase reversed reflections, or bright spots (Fig. 16). Phase reversal infers a velocity inversion (although possibly density) and the strong amplitude infers a significant velocity contrast. Strong velocity reversals are most typically caused by free gas in formation, so in all likelihood these bright spots reflect pockets of shallow gas.

A potential bottom simulating reflector (BSR) was identified in the lower slope region of the study area (Fig 17). It is located between strike lines 8646 and 10636, and dip lines 11728 and 10636. This anomalous seismic reflection event covers an area of 258 km^2 and dips at ~0.018°. It is identified by its relatively high-amplitude and phase reversed nature and it parallels the seafloor, cross-cutting other reflections. A BSR represents the base of the gas hydrate stability field, where free gas is trapped beneath solid hydrate. It parallels the seafloor because the hydrate stability field is temperature and pressure dependent. Beneath the seafloor, the temperature gradient is typically relatively stable, thus temperature is the dominant controlling factor governing the base of the stability field and explains why the BSR parallels the seafloor. The depth of this BSR is about 0.4 s below seafloor.

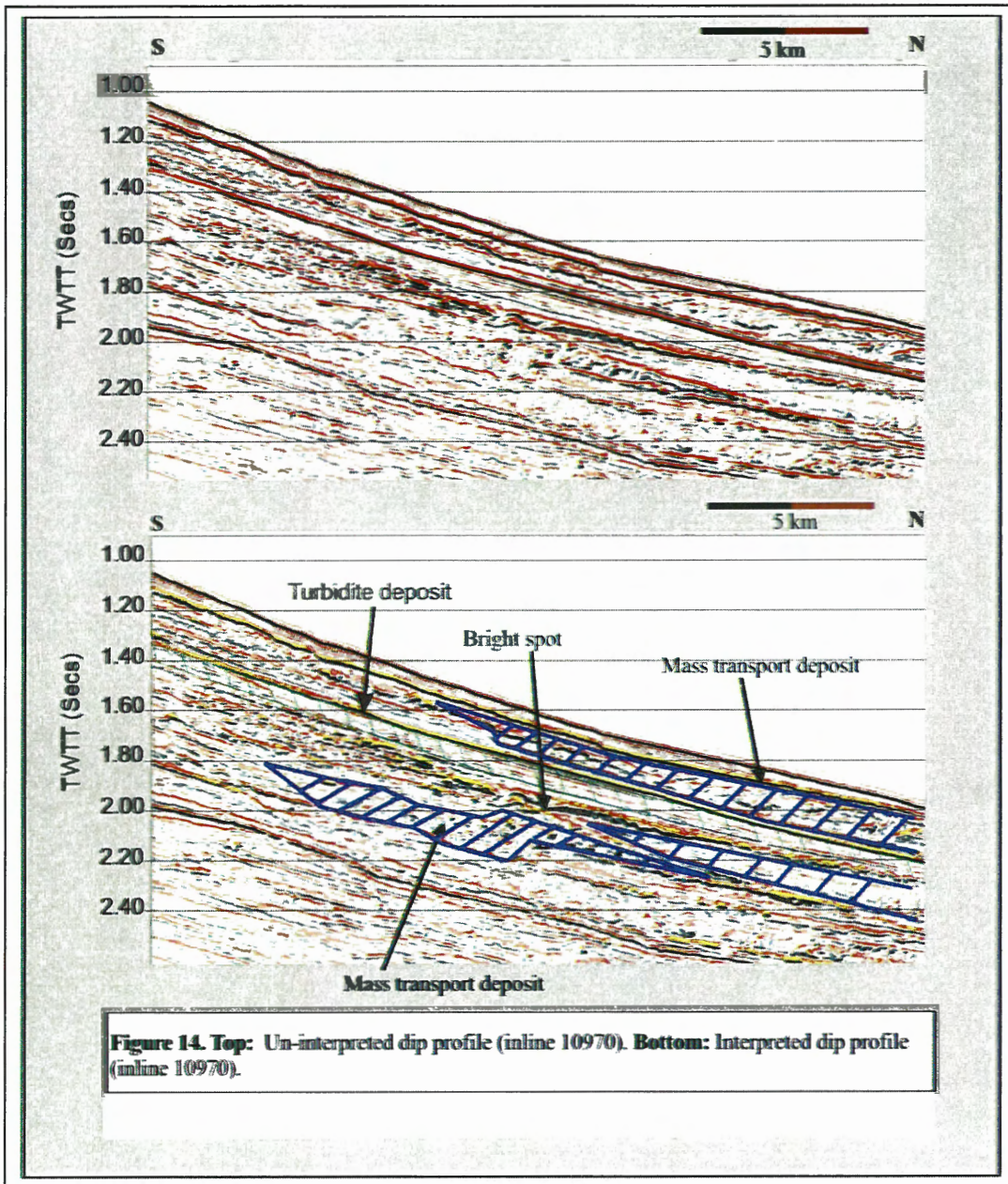

Figure 14. Top: Un-interpreted dip profile (inline 10970). **Bottom:** Interpreted dip profile (inline 10970).

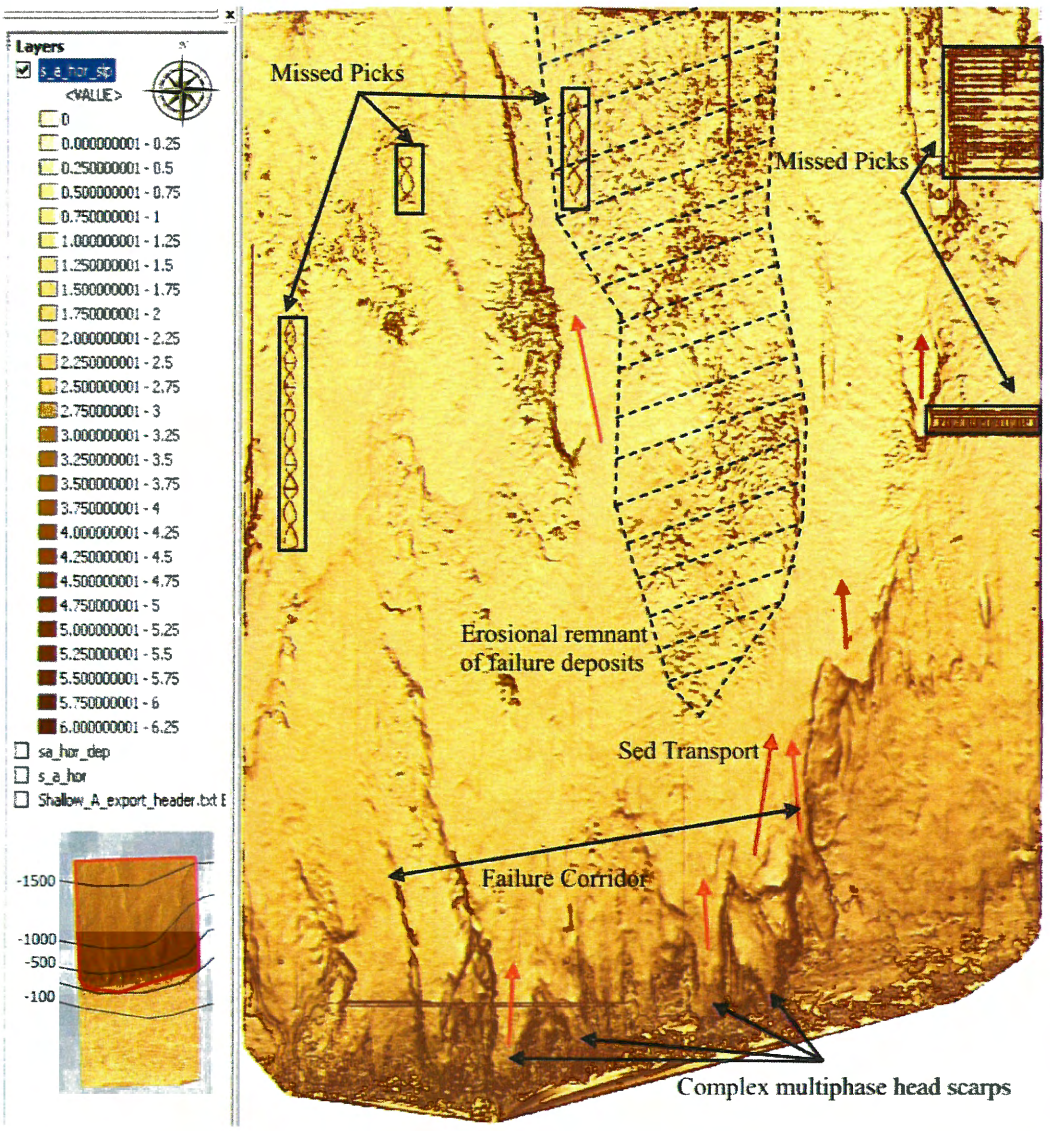

Figure 15. Slope angle map created from rendered magenta horizon on the slope. The lower left corner indicates location of rendered area (red) within the block. Not the complexity of the surface with mass transport deposits and erosional gullies and scars.

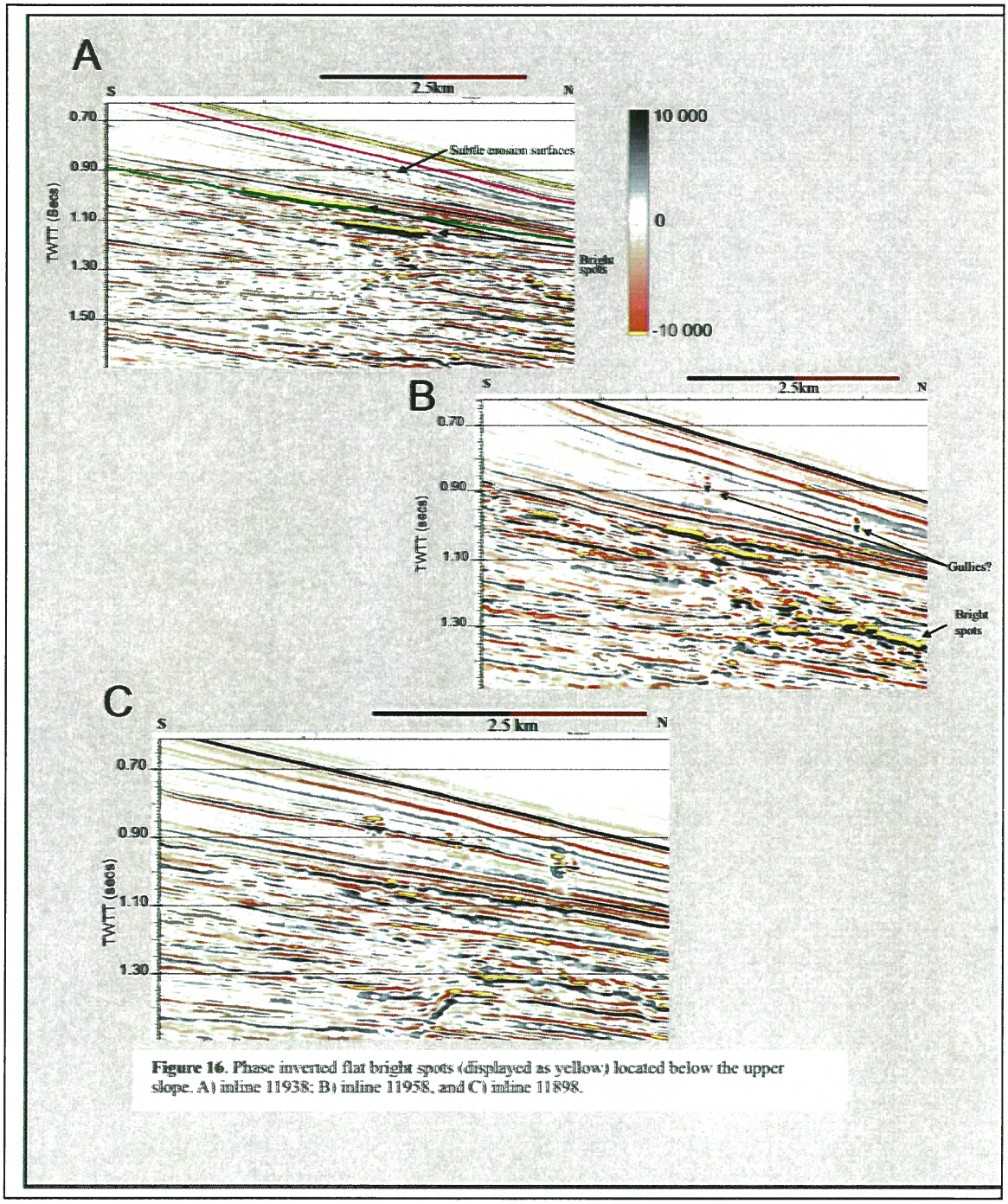

Figure 16. Phase inverted flat bright spots (displayed as yellow) located below the upper slope. A) inline 11938; B) inline 11958, and C) inline 11898.

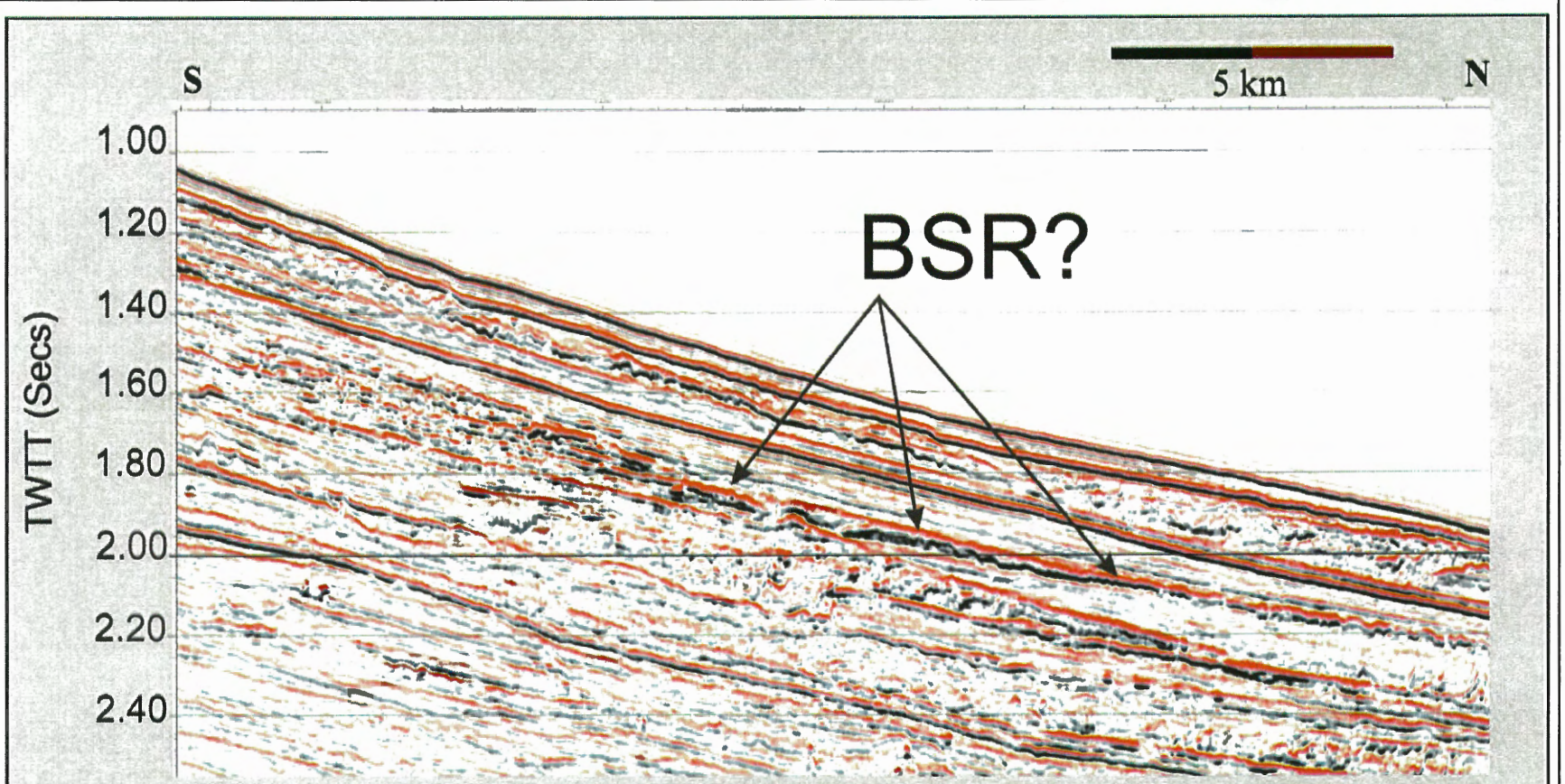

Figure 17. Inline 10970 showing a possible bottom simulating reflector (BSR), recognized by its strong negative phase that does not conform to stratigraphic relationships but rather parallels the seafloor.

4.0 POTENTIAL GEOHAZARDS

For the purposes of this investigation, features identified as representing potential geohazards or constraints to exploratory drilling and hydrocarbon development are presented. Specifically, such features within this data set include 1) shallow faults, 2) hard substrate, erosional scour and seafloor slopes, 3) mass transport processes, and 4) suspicious amplitude anomalies and BSR's.

4.1 Shallow Faults

It is considered that the most significant geohazard identified from the Surinamme Block 30, including within the immediate area of the West Tapir well site, is the presence of abundant shallow faults (Fig. 6 to 8). These faults are largely listric-normal and are responsible for offsetting reflections on the order of tens of metres. They are restricted to areas beneath the shelf and shelf break. Some are constrained within the near-surface but others clearly extend to depth. One particular fault trace, with a seafloor expression demonstrated in Figures 6 to 8 and 13, parallels the shelf break for the full extent of the survey and comes within two kilometres of the West Tapir well site. It is not known whether these faults represent splays of a master fault system or represent gravitational extension of the shallow margin due to subsidence and gravitational collapse. Faults such as this represent hazards in several senses: 1) they may act as conduits for overpressure fluids or gas from depth, and 2) they form a plane of weakness, which in this particular case is adjacent to a free slope and subsequently there is a risk of detachment and mass failure.

4.2 Seafloor and Seafloor Slope

Acoustic characteristics of the seafloor on the shelf, indicated by varying high amplitude first return reflections (Fig. 6), suggest a hard substrate (carbonate), which may have engineering implications for rig and well head foundation conditions. Increased amplitudes toward the shelf break and truncated reflections at the shelf edge and uppermost slope along with prominent gully formation suggest an erosive environment, probably due to off-shelf flow and possible sediment transport. If they indicate bottom water flow, then these currents may well exist near the West Tapir well site.

Slope angles within Block 30 are generally low, being about 3° at the shelf break and less than 2° over the remainder of the slope. In most marine environments with such low slopes, the risk of static failure (no external trigger mechanisms) is low. In other words, the internal shear strength of surficial sediment is great enough to withstand the gravitational force acting on the sediment column on a slope. External factors, such as seismic ground-shaking or generation of elevated pore pressures by gas or fluid is required to initiate failure. Generation of high pore pressures reduces the shear strength of the sediment. The West Tapir well site is on the shelf and no significant slope angles exist within the immediate area.

4.3 Mass Transport Deposits

Although slope angles are low and subsequently risk of landsliding is low, as indicated above, there is abundant evidence on the slope of mass transport deposits that demonstrate a history of sediment mass-failure on this margin. Packages of incoherent

reflections on the slope are interpreted to represent mass transport deposits, such as debris flows or rotational failure. They form approximately 30% of the upper sediment column (upper 2 s below seafloor) (Fig. 14). As shown on seafloor morphologic renders, the slope shows escarpments and a rugose pattern suggestive of near-surface mass transport deposits (Posamentier, 2004). Close inspection shows that these features are buried by a sequence of parallel reflections several 10's of ms thick, but their expression still is visible at the seafloor. Two subsurface horizons, representing shallow mass transport deposit surfaces were picked.

A shallow reflection horizon (within 0.1 s of the seafloor), named Magenta, was picked from the shelf break to the most northern extent of the block (Fig. 15). The morphologic render and associated slope angle map show numerous gullies and headscarps. A failure corridor is lined with steep walls and side scarps from 400 to 1000 m water depth, the inter-corridor ridges are commonly less sharp. In deeper water, corridors coalesce and the inter-corridor ridges are much flatter, with various low scarps. The mid-slope (1000 m) to the north extent of the study area presents a rugose hummocky morphology, with minor sediment lobes (Fig. 15), typical of mass-transport deposit surface morphologies (Posamentier, 2004, Posamentier and Kolla, 2003). The nature of these areas tends to fan and broaden with depth away from the corridor head scarps.

Although not a specific geohazard, mass-transport deposits substantiate a history of submarine landsliding. It is a common process on most continental margins, although trigger mechanisms are not well understood. With age control, estimates of recurrence rates can be derived. In general, risk of landsliding during exploratory drilling is low due to the infrequent occurrence of such events. The risk to development infrastructure is slightly higher because of the longer duration of the facility on the seafloor. Steps to mitigate initiation of landsliding by drilling or development disturbance should be considered. For the West Tapir drill site, mass failure is not an issue because of low slope and dip angles. Significant slope failure retrogression (> 10 km) would have to occur in order to impact the drill site area.

4.4 Subsurface Amplitude Anomalies

High seismic reflection amplitude anomalies (bright spots) represent potential free gas within a rock formation. In many cases, these anomalies are clearly phase-reversed, as expected from a free gas anomaly where velocities are inverted. Typically, theses features are seen north of the shelf break in ~350 m water depth, between 0.8 and 1.2 s twtt (Fig. 16). No evidence of pockmarks or gas escape features (chimneys, vents) within seismic profile or morphologic surface render are apparent, however. Free gas represents a hazard in that it may cause an overpressured zone leading to reduced sediment shear strength or higher than expected formation pressures.

A possible bottom simulating reflector (BSR) was noted spanning cross lines 5000 to 6500 and 1.45-2.25 s twtt (Figs. 31, and 32). BSR's are believed to represent the base of the gas hydrate stability zone, where free gas is trapped beneath solid-phase hydrate, causing a velocity inversion. Because the stability field for hydrates is dictated by pressure and temperature conditions, the lower surface may simulate the seafloor and not necessarily correspond with geological structure. In fact, BSR's are most easily recognized if they cross stratigraphy.

Gas hydrate represents a possible geohazard in that dissociation of the hydrate to free gas can cause formation overpressures; volume expansion during dissociation is significant (164:1). Formation overpressure leads to weakening of sediment shear strength and thus a higher susceptibility to landsliding. Dissociation may be caused by drilling activity and resource extraction (formation heating). Hydrate formation can also be a significant drilling constraint by blocking pipes and other conduits. Within the immediate area of the West Tapir drill site, no BSR's were detected.

5.0 CONCLUSIONS

The 3D seismic volume from the RepsolYPF Block 30 of the Suriname continental margin transits from the shelf to slope environments. The region is a passive continental margin and earthquake seismicity is rare. In large scale, these 3D reflection data show a classic progradational margin down to several seconds travel time below the seafloor. A number of features were identified from the shallow, near surface geologic section that represent potential geohazards or constraints to offshore hydrocarbon development.

The shelf section encompassed by the volume ranges from 60 to 230 m water depth, with shallow dipping (<0.5°), high amplitude reflectors underlying a rather rugose seafloor. Shallow data are of poor quality in this area but high amplitudes and rugose morphology, combined with outcropping reflectors suggest an erosional environment with a hard substrate. Strong currents, therefore, may be present, such as the northward flowing Guyana Current. Shallow faults which break the seafloor are the predominate geohazard in this environment. These fault traces produce clear seafloor offsets that correlate for the width of the survey. Faults can provide conduits for overpressured gas and fluids and provide planes of weakness for initiation of mass failures.

Faults extend to the shelf break as well. The shelf break appears to be the most dynamic environment. The seafloor over the entire width of the survey is dominated by gully cutting, potentially the result of off-shelf transport. Beneath the shelf break, amplitude anomalies are common, possibly representing shallow gas or sand bodies (channels). In this region also, seafloor slope angles are steepest (~3°). Infinite slope stability analysis indicate that these angles are still statically stable for most sediment types but evidence of buried headscarps suggest mass-failures have occurred in the past.

The top several seconds of the continental slope is a progradational wedge created by shelf edge deltas, with sediment offlapping the shelf and thinning in the downslope direction. Seismic characteristics indicate that probable turbidites intercalated with mass transport deposits dominate the sedimentary succession. Surface renders of these features show head scarps, lateral escarpments, and rugose surface patterns fanning out in the downslope direction; typical characteristics recognized of mass transport deposits. Although the low angles of the slope in this region suggest static stability, these deposits indicate mass failures have occurred in the past. Trigger mechanisms are unknown, but possibly relate to ground motions due to rare earthquakes. Shallow gas, gas hydrate dissociation and periods of high sediment input may be contributing factors. Recurrence intervals of these mass transport events are unknown due to present poor age control. Probably these events are rare because of the combination of events required to initiate

failure. The shallowest mass transport deposit is buried by ~0.2 s of parallel, coherent reflections forming the present seafloor.

6.0 RECOMMENDATIONS

The following recommendations are provided to enable a more thorough assessment of shallow geohazards and drilling conditions in the Repsol YPF Block 30.

1) Reprocessing of the 3D seismic cube with near-offset traces and modified processing flow to improve vertical and lateral resolution for the shallow sediment section. Attribute analysis of these cubes may assist interpretations.
2) Conduct ultra-high resolution geophysical surveys of proposed drill areas. These techniques include multibeam bathymetry, sidescan sonar and ultra high resolution seismic reflection, as examples.
3) Acquire sediment piston cores, with physical property measurements, and assess well logs from previously drilled sites in the area to provide data for a quantitative geotechnical assessment (foundation conditions and slope stability analysis), age control and seismic-lithologic groundtruth.

7.0 REFERENCES

Benkhelil, J., Mascle, J. and Tricart, P. (1995) The Guinea continental margin; an example of a structurally complex transform margin. Tectonphysics, 248: 117-137.

Erbacher, J., Mosher, D.C., Malone, M. and shipboard scientific party. 2004. Initial Results, ODP Leg 207, Demerara Rise. Initial Results V. 207, Ocean Drilling Program, Texas A&M University, 89 pp. + CDRom.

Flicoteaux R, Latil-Brun MV, and Michaud L (1988) Histoire de la subsidence post-rift du bassin cotier mauritano-senegalo-guineen, relation avec l'amincissement crustal pendant la periode jurassique a Cretace inferieur; comparaison avec l'evolution des marges peri-atlantiques au niveau de l'Atlantique central et equatorial (cote est des U.S.A., Sud-Sahara, Cote d'Ivoire et Plateau du Demerara) *In*: The West African connection; evolution of the central Atlantic Ocean and its continental margins. Sougy J, Rodgers, J. (eds) Journal of African Earth Sciences 7: 345-359.

Gouyet, S., Unternehr, P., and Mascle, A. (1994) The French Guyana Margin and the Demerara Plateau; Geologic History and Petroleum Plays. In: Mascle A (ed) Hydrogen and petroleum geology of France. Special Publication of the European Association of Petroleum Geoscientists 4: 411-422.

Lithgow-Bertelloni, C., and Gurnis., M. 1997. Cenozoic subsidence and uplift of continents from time-varying dynamic topography. Geology, 25: 735-738.

Mascle, J., Marinho, M., and Wannesson, J. (1986) The structure of the Guinean continental margin: implications for the connection between the central and South Atlantic Oceans. Geik. Rundsch, 75: 57-70.

Mienert, J., Berndt, C., Laberg, J.S. and Owen, T.O. (2001). Slope Instability of Continental Margins. In: Ocean Margin Systems. G. Wefer., D, Billet., D. Hebbeln, B.B., Jorgensen, M. Schlueter and T.C.E., van Weering (eds.) Springer-Verlag Berlin Heidelberg. NY. p. 179-193

Mosher, D.C.. Erbacher, J. and Malone, M. 2007. Synthesis: Extreme warmth, organicrich sediments and an active deep biosphere: Cretaceous to Paleogene paleoceanographic depth transect at Demerara Rise, western tropical Atlantic, ODP Leg 207. Ocean Drilling Program, Scientific Results, 207.

Mosher, D.C., Erbacher, J., Zuelsdorff, L., Meyer, H., 2005. Stratigraphy of the Demerara Rise, Surname, South America: a rifted margin, shallow stratigraphic source rock analogue. Extended Abstract, American Association of Petroleum Geologists annual meeting, Calgary, Alberta, June 19-22.

Pindell, J. and Kennan, L. (2005) Mapping and Basin History along the western flank of the Demerara Rise, Suriname. Tectonic Analysis Ltd. For Repsol (Confidential), Suriname. 1-34.

Posamentier, H., 2004, Stratigraphy and Geomorphology of Deep-Water Mass Transport Complexes Based on 3D Seismic Data, in Offshore Technology Conference, Houston, TX.

Posamentier, H. W., and Kolla, V., 2003, Seismic geomorphology and stratigraphy of depositional elements in deep-water settings: Journal of Sedimentary Research, 73: 367- 388.

Workman, W. (2000) Guyana Basin, a new exploration focus. World Oil Magazine, May, 2000: 55-60.